



# KAHRAMANMARAŞ SÜTÇÜ İMAM ÜNİVERSİTESİ

e-ISSN 1309-1751

## Mühendislik Bilimleri Dergisi Journal of Engineering Sciences

**2020** | SAYI / NUMBER : 4  
CILT / VOLUME : 23



# Kahramanmaraş Sütçü İmam University

## Journal of Engineering Sciences



### Yazışma Adresi / Corresponding Address

**Kahramanmaraş Sütçü İmam Üniversitesi**  
**Mühendislik Bilimleri Dergisi**  
**46050, Onikişubat/Kahramanmaraş**  
**TÜRKİYE**

### E - Posta

**jes@ksu.edu.tr**

### Web

**<http://jes.ksu.edu.tr/>**

**Bu dergi hakemli olup yılda 4 kez yayınlanır.**

**This journal is peer - reviewed and published 4 issues per year.**



### Sahibi / Owner

**Prof.Dr. Niyazi CAN**  
KSU Rector

### Baş Editör / Editor in Chief

**Prof. Dr. Hüseyin TEMİZ**  
htemiz@ksu.edu.tr

### Baş Editör Yardımcısı / Vice Editor in Chief

**Assist. Prof. Dr. Zeynep Banu ÖZGER**  
zeynepozger@ksu.edu.tr

### Editörler / Editors

**Prof. Dr. Ahmet Serdar YILMAZ**  
Electrical and Electronics Eng.  
KSU Univ. TURKEY  
asyilmaz@ksu.edu.tr

**Prof. Dr. Ahmet ALKAN**  
Electrical and Electronics Eng.  
KSU Univ. TURKEY  
aalkan@ksu.edu.tr

**Prof. Dr. Mehmet ÜNSAL**  
Civil Eng.  
KSU Univ. TURKEY  
munsal@ksu.edu.tr

**Prof. Dr. Ahmet KAYA**  
Mechanical Eng.  
KSU Univ. TURKEY  
kaya38@ksu.edu.tr

**Prof. Dr. Remzi ŞAHİN**  
Civil Eng.  
Atatürk Univ.,TURKEY  
rsahin@atauni.edu.tr

**Prof Dr. Yücel ÖZMEN**  
Mechanical Eng.  
Karadeniz Teknik Univ.,TURKEY  
yozmen@ktu.edu.tr

**Prof.Dr. Özlem TURGAY**  
Food Eng.  
KSU Univ. TURKEY  
ozlem@ksu.edu.tr

**Prof. Dr. Fatih MENGELOĞLU**  
Landscape Arc.  
KSU Univ. TURKEY  
fmengelo@ksu.edu.tr

**Assoc.Prof.Dr. Suat ÇETİNER**  
Textile Eng.  
KSU Univ. TURKEY  
suatcetiner@ksu.edu.tr

**Assoc. Prof.Dr.Tamer RIZAOĞLU**  
Geological Eng.  
KSU Univ.  
TURKEY  
tamer@ksu.edu.tr

**Assoc. Prof. Dr. Çetin AKINCI**  
Electrical Eng.  
İstanbul Teknik Univ,  
TURKEY  
akincitc@itu.edu.tr

**Assist. Prof. Dr. Toni NIKOLIC**  
Civil Eng.  
Univ. Dzemal Bijedic,  
BOSNIA AND HERZEGOVINA  
nikolic\_t@yahoo.com

**Assist.Prof.Dr. Yakup CUCİ**  
Environmental Eng.  
KSU Univ. TURKEY  
cuci@ksu.edu.tr

**Assist. Prof. Dr. Beril ÖZÇELİK**  
Mechanical Eng.  
KSU Univ. TURKEY  
bozcelik@ksu.edu.tr

**Assist. Prof. Dr. Hasan BADEM**  
Computer Eng.  
KSU Univ. TURKEY  
hbadem@ksu.edu.tr

**Research Assist. Fahriye GEMCİ**  
Technical Editor  
KSU Univ. TURKEY  
fahriyegemci@ksu.edu.tr

**Research Assist. Elif ÇELİK**  
Technical Editor  
KSU Univ. TURKEY  
elifcelik@ksu.edu.tr

## Danışma Kurulu / Advisory Board

**Prof. Dr. Cetin Kaya KOC**

Dep. of Computer Eng.  
Univ Of Cal.  
Santa Barbara. USA  
[koc@cs.ucsb.edu](mailto:koc@cs.ucsb.edu)

**Prof. Dr. Ayhan ÖZDEMİR**

Dep. of Elect. & Elcn Eng.  
Sakarya Univ. Sakarya,  
TURKEY  
[aozdemir@sakarya.edu.tr](mailto:aozdemir@sakarya.edu.tr)

**Prof. Dr. Hüseyin AKILLI**

Dep. of Mechanical Eng.  
ÇU Univ.  
Adana, TURKEY  
[hakilli@cu.edu.tr](mailto:hakilli@cu.edu.tr)

**Prof. Dr. Mehmet KORÜREK**

Dep. Of Elcn & Comm Eng.  
İTU Univ.  
İstanbul. TURKEY  
[korurek@itu.edu.tr](mailto:korurek@itu.edu.tr)

**Prof. Dr. Yasemin KORKMAZ**

Dep. of Textile Eng.  
KSU Univ.  
TURKEY  
[ykorkmaz@ksu.edu.tr](mailto:ykorkmaz@ksu.edu.tr)

**Prof. Dr. Ahmet PINARBAŞI**

Dep. of Mechanical Eng.  
Alanya Alaaddin Keykubat  
Univ. Antalya, TURKEY  
[apinarbasi@alanya.edu.tr](mailto:apinarbasi@alanya.edu.tr)

**Prof. Dr. S. Serhat ŞEKER**

Dep. Of Elect. Eng.  
İTU Univ. İstanbul.  
TURKEY  
[sekers@itu.edu.tr](mailto:sekers@itu.edu.tr)

**Prof. Dr. Şerafettin EREL**

Dep. of Elect. & Elcn Eng.  
YBU Univ.  
Ankara, TURKEY  
[serel@ybu.edu.tr](mailto:serel@ybu.edu.tr)

**Assoc. Prof. Dr. Mustafa ONAT**

Dep. of Computer Eng.  
Marmara Univ.  
İstanbul. TURKEY  
[monat@marmara.edu.tr](mailto:monat@marmara.edu.tr)

**Prof. Dr. Eyüp DEBİK**

Dep. of Environmental Eng.  
Yıldız Technical Univ.  
İstanbul. TURKEY  
[debik@yildiz.edu.tr](mailto:debik@yildiz.edu.tr)

**Prof. Dr. Fan MIZI**

Dep. of Civil Eng.  
Brunel Univ.  
Uxbridge,UK  
[mizi.fan@brunel.ac.uk](mailto:mizi.fan@brunel.ac.uk)

**Prof. Dr. A. Fevzi BABA**

Dep. of Elect. & Elcn. Eng.  
Marmara Univ. İst.,  
TURKEY  
[fbaba@marmara.edu.tr](mailto:fbaba@marmara.edu.tr)

**Dr. Amit CHAUDHRY**

Dep. of Microelectronics  
Panjab Univ,  
Chandigarh, India  
[amit\\_chaudhry01@yahoo.com](mailto:amit_chaudhry01@yahoo.com)

**Assoc. Prof. Dr. Nazmi EKREN**

Dep. of Elect. & Elcn. Eng.  
Marmara Univ.  
İstanbul, TURKEY  
[nekren@marmara.edu.tr](mailto:nekren@marmara.edu.tr)

**Prof. Dr. Mustafa YAZICI**

Dep. of Physics Education.  
KSU Univ.  
K.Maras. TURKEY  
[yazici@ksu.edu.tr](mailto:yazici@ksu.edu.tr)

**Prof. Dr. Selim AY**

Dep. Of Elect. Eng.  
YTU Univ.  
İstanbul. TURKEY  
[selimay@yildiz.edu.tr](mailto:selimay@yildiz.edu.tr)

**Prof. Dr. Musa GÖĞEBAKAN**

Dep. of Physics  
KSU Univ.  
K.Maras, TURKEY  
[gogebakan@ksu.edu.tr](mailto:gogebakan@ksu.edu.tr)

**Prof. Dr. Murat PALA**

Dep. of Civil Eng.  
Adiyaman Univ.  
Adiyaman. TURKEY  
[pala@adiyaman.edu.tr](mailto:pala@adiyaman.edu.tr)

**Prof. Dr. İ.Taner OKUMUŞ**

Dep. of Computer Eng  
KSU Univ.  
K.Maras. TURKEY  
[iokumus@ksu.edu.tr](mailto:iokumus@ksu.edu.tr)



## İÇİNDEKİLER

### **ARAŞTIRMA MAKALESİ – RESEARCH ARTICLE**

- Design Of Ammonium Stripping Tower And Optimization Of Ammonium Removal From Landfill Leachate  
**Amonyum Sıyırma Kulesi Dizaynı ve Çöp Sızıntı Suyundan Amonyum Giderimi Optimizasyonu** 188-196  
Melike ÖZTEKİN, Vildan AKGÜL, Ahmet DUYAR, Serdar GÖÇER, Kevser CIRIK
- Bitkilerde Duraylı Civa İzotoplarının Ayrımlılaşması  
**Stable Mercury Isotope Fractionation Behaviours Of Plants** 197-208  
Ayça DOĞRUL SELVER
- Kurutulmuş Nar (Punica granatum) Kabuğu Tozunun Glütensiz Bisküvilerin Tekstürel Duyusal ve Bazı Fizyokimyasal Özellikleri Üzerine Etkisi  
**Effect Of Dried Pomegranate (Punica Granatum) Peel Powder On Textural, Sensory And Some Physicochemical Characteristics Of Gluten-Free Biscuits** 209-218  
Sibel BÖLEK
- Titanyum Dioksit Sentezi  
**Synthesis Of Titanium Dioxide** 219-226  
Serdar GÖÇER, Zeynep ZAIMOĞLU, Kevser CIRIK
- Tel Çekme İşleminde Kalıp Kalibrasyon Bölgesi Uzunluğunun 1045 Çelik Tel Mukavemeti Üzerine Olan Etkisinin İncelenmesi  
**Investigating Effect Of Bearing Length On Tensile Strength Of 1045 Steel In Wire Drawing Operation** 227-235  
Ekrem ÇELİK, Fatih ÖZEN, Erdiç İLHAN, Salim ASLANLAR
- Karaçam Odununun Fiziksel Özellikleri Üzerine Farklı Atmosferlerde Uygulanan Isıl İşlemin Etkisi  
**The Effect Of Heat Treatment Applied Under Different Atmospheres On Physical Properties Of Blackpine Wood** 236-244  
Bekir Cihad BAL
- ### **DERLEME MAKALESİ – REVIEW ARTICLE**
- Advanced Technologies For Fiber Reinforced Polymer Composite Manufacturing: A Review  
**Elyaf Takviyeli Polimer Kompozit Üretimi İçin İleri Teknolojiler: Derleme** 245-257  
Çağrı UZAY, Necdet GEREN



# Kahramanmaraş Sutcu Imam University

## Journal of Engineering Sciences



Geliş Tarihi :25.06.2020  
Kabul Tarihi :15.09.2020

Received Date : 25.06.2020  
Accepted Date : 15.09.2020

### DESIGN OF AMMONIUM STRIPPING TOWER AND OPTIMIZATION OF AMMONIUM REMOVAL FROM LANDFILL LEACHATE

### AMONYUM SIYIRMA KULESİ DİZAYNI VE ÇÖP SIZINTI SUYUNDAN AMONYUM GİDERİMİ OPTİMİZASYONU

*Melike OZTEKİN<sup>1</sup>* (ORCID: 0000-0001-8850-8308)

*Vildan AKGUL<sup>2</sup>* (ORCID: 0000-0001-5507-2886)

*Ahmet DUYAR<sup>3</sup>* (ORCID: 0000-0001-8850-8308)

*Serdar GOCER<sup>4</sup>* (ORCID: 0000-0003-0443-8045)

*Kevser CIRIK<sup>1\*</sup>* (ORCID: 0000-0002-1756-553X)

<sup>1</sup> Department of Environmental Engineering, Kahramanmaraş Sutcu Imam University, Kahramanmaraş, Turkey

<sup>2</sup> Department of Bioengineering, Kahramanmaraş Sutcu Imam University, Kahramanmaraş, Turkey

<sup>3</sup> Department of Environmental Engineering, Suleyman Demirel University, Isparta, Turkey

<sup>4</sup> Department of Environmental Engineering, Cukurova University, Adana, Turkey

\*Sorumlu Yazar / Corresponding Author:Kevser CIRIK, kcirik@ksu.edu.tr

#### ABSTRACT

Landfill leachates are complex wastewater which has high pollution and their biological degradability is also difficult. Landfill leachate with high concentrations of contaminants must be pretreated. For this reason, the ammonium stripping process is an effective method for ammonium removal, especially for landfill leachate. With the ammonium stripping process, the ammonium and organic matter removal increases. This study aimed to investigate the applicability of the ammonium stripping process as remove ammonium (NH<sub>4</sub><sup>+</sup>) and chemical oxygen demand (COD) from raw leachate. A new system has been designed which is called ammonium stripping tower. During this study, the ammonium stripping process was operated temperature (30-40-60°C), aeration rate (HH, HL, LL m<sup>3</sup>air/min), and hydraulic retention times (6-12-24-48 h). System performance was evaluated by ammonium, and COD parameters. The optimum conditions of the ammonium stripping process were determined at 60°C temperature, HH(1m<sup>3</sup>air/min aeration rate), and hydraulic retention time (48h). The corresponding ammonium and COD removal efficiencies were about 88% and 79% respectively. The results of this study suggest that the use of an ammonium stripping process is an effective way to remove ammonium and COD concentration from raw landfill leachate.

**Keywords:** Physicochemical treatment, landfill leachate, ammonia removal, ammonia stripping proces

#### ÖZET

Düzenli depolama sahalarındaki sızıntı suları, yüksek kirliliğe sahip karmaşık atık sulardır ve biyolojik olarak parçalanabilirlikleri de zordur. Yüksek konsantrasyonlarda kirletici madde içeren deponi sahası sızıntı suyuna ön arıtma yapılmalıdır. Bu nedenle, amonyum sıyırma işlemi, özellikle sızıntı suyunun amonyum giderimi için etkili bir yöntemdir. Amonyum sıyırma işlemi ile amonyum ve organik maddelerin giderimi artar. Bu çalışmada, amonyum sıyırma işleminin ham sızıntı sularından amonyum (NH<sub>4</sub><sup>+</sup>) ve kimyasal oksijen ihtiyacı (KOİ) giderilmesinin uygulanabilirliği araştırıldı. Amonyum sıyırma kulesi adı verilen yeni bir sistem tasarlanmıştır. Bu çalışma sırasında amonyum sıyırma işlemi, sıcaklık (30-40-60°C), havalandırma oranı (HH, HL, LL m<sup>3</sup>air / dak) ve hidrolik bekletme süreleri (6-12-24-48 saat) olarak gerçekleştirildi. Sistem performansı amonyum ve KOİ parametreleri ile değerlendirildi. Amonyum sıyırma işleminin optimum koşulları 60°C sıcaklık, HH (1m<sup>3</sup>hava/dakika) havalandırma hızı ve (48 saat) hidrolik bekletme süresi belirlenmiştir. Karşılık gelen amonyum ve KOİgiderim verimleri sırasıyla yaklaşık% 88 ve % 79'dur. Bu çalışmanın sonuçları, bir amonyum sıyırma işleminin kullanılmasının, ham depolama sahası sızıntı sularından amonyum ve KOİ konsantrasyonunu gidermek için etkili bir yöntem olduğunu göstermektedir.

**Anahtar Kelimeler:** Fizikokimyasal arıtım, çöp sızıntı suyu, amonyum giderimi, amonyum sıyırma prosesi

\*Sorumlu Yazar / Corresponding Author: Kevser CIRIK, kcirik@ksu.edu.tr

**ToCite:** OZTEKIN, M., AKGUL, V., DUYAR, A., GOCER, S., CIRIK, K., (2020). DESIGN OF AMMONIUM STRIPPING TOWER AND OPTIMIZATION OF AMMONIUM REMOVAL FROM LANDFILL LEACHATE. *Kahramanmaraş Sütçü İmam Üniversitesi Mühendislik Bilimleri Dergisi*, 23(4), 188-196.

## INTRODUCTION

The regular storage method is cheaper and easier to maintain than other technologies. Therefore, it is generally used for garbage treatment and disposal. However, the major environmental concern of this method is the generation of large quantities of liquid leachate, which may cause serious pollution to groundwater aquifers as well as adjacent surface waters (Calace, N., et al., 2001). Because the landfill leachates treatment is very complex and expensive, it often needs a variety of applications in terms of high COD, ammonium concentrations and color. Various aerobic and anaerobic treatment systems have been applied to the treatment of leachate and high treatment efficiency has been achieved. However, with these systems, various problems have occurred depending on the age of the landfill leachate (Ledakowicz S., & Kaczorek, K., 2001). Landfill leachate contaminant contents depend upon the landfill age, the quality. Since the wastes coming to the storage area may contain many types of pollutants, if these wastes are not properly collected, treated and disposed of safely, they can cause serious environmental hazards. Biological treatment systems are no longer available alone and refractory organic materials are not sufficient to go through, so additional purification is needed. Physico-chemical systems are widely used as pretreatment and these systems; ammonium stripping, ion exchange, chemical precipitation, coagulation-flocculation, flotation and adsorption. Ammonium stripping is the most common purification system used to remove ammonia from landfill leachate (Collivignarelli, C., et al., 1998); (Martinen, S., et al., 2002). In the ammonium stripping process, the transition from the liquid phase to the gas phase depends on a mass transfer. That is, the ammonium ions ( $\text{NH}_4^+$ ) in the liquid phase are in equilibrium with ammonia ( $\text{NH}_3$ ) in the gas phase and hydrogen ions ( $\text{H}^+$ ). Briefly, ammonium stripping can be expressed by the following equation (Hossini, H., et al., 2016):



When the pH of the wastewater rises above 7, the balance shifts to the right. When the pH rises above 10, the ammonium ions turn into ammonia gas under the influence of air and separate from leachate. In the ammonium stripping process, volatile organic compounds are separated from the aqueous solution by maximum specific contact between liquid and air in a specially designed column (Hossini, H., et al., 2016). The landfill leachate must have a pH above 10 to achieve maximum ammonium removal efficiency. Here,  $\text{Ca}(\text{OH})_2$  is preferred because it is an alkali that is both economical and effective in increasing pH. Advantages of using  $\text{Ca}(\text{OH})_2$  include the removal of heavy metals and colors caused by co-precipitation of organic macromolecules, such as humic acids in the leachate (Renou, S., et al., 2009). It can also be said that high temperatures are used as an alternative method of providing high ammonium removal in the ammonium stripping process.

The objective of this paper was to investigate the pretreatment of landfill leachate physicochemical stage. Four experimental parameters have been tested during the study: (i) the reactor design and supply of the necessary consumables have been provided. (ii) the effect of different temperature parameters (30,40,60°C), (iii) the effect of high((HH)1m<sup>3</sup>air/min), medium((HL)0,85m<sup>3</sup>air/min) and low((LL)0,75 m<sup>3</sup>air/min) aeration rate and (iv) different hydraulic retention times(HRT) (6, 12, 24 and 48 h) on ammonium stripping. As a result of these studies, optimum conditions have been obtained by examining the ammonium and COD removal efficiencies and this study will help the projects on the future ammonium stripping processes.

## MATERIALS AND METHODS

### *Characterization of Landfill Leachate*

The landfill leachate from the municipal sanitary landfill of Kahramanmaraş that has an average 1.127.623 inhabitants and productions 2,23 kg/person of municipal solid waste per day. Samples were monthly taken from

aeration lagoon all samples were instantly stored at 4°C before applying ammonium stripping. The landfill leachate characterization shown in Table 1.

**Table I.** Characterization of Landfill Leachate

Parameter	Concentration (mg/L)
pH	8,87
COD	7500
Color (Pt-Co)	8380
Color (436)	297
Color (525)	88
Color (620)	37
Ammonium	2215
Nitrate	410
TOC	4432
TN	2506
SS	800

### Experimental Plan

Ammonium stripping processes were performed using ammonium stripping towers. This ammonium stripping tower has been designed by choosing Plexiglass material for its resistance to temperature, impacts and various adverse conditions. The dimensions of the ammonium stripping tower with 3 L internal volume are designed as 10x8x40 cm. The interior design of the reactor consists of three compartments. The sieves consisting of two plexiglass materials at a certain distance between each other were placed and filled with 400 K3 sized caldnesses which were determined as filling materials. Air ports, one of the operating parameters, are installed in each chamber of the three chambers, which play a role in determining the airflow. Ammonium stripping experiments were carried out under various temperature (30, 40 ve 60°C), aeration rate (1m<sup>3</sup>air/min(HH(high)-0.85m<sup>3</sup>air/min(HL)-0.75m<sup>3</sup>air/min(LL)) and hydraulic retention time (6,12,24,48 h) values in order to determine optimum temperature conditions. In the first period, the effect of temperature was evaluated on ammonium stripping. Then, the performance of aeration rate was investigated during period II and determined to hydraulic retention time. The operational conditions of ammonium stripping tower were given in Table II. The most appropriate methods have been established in the direction of the operational optimum condition.

**Table II.** Experimental Plan

PHASE	PERIODS	TEMPERATURE (°C)	AERATION RATE (m <sup>3</sup> air/min)	HRT(h)
I. Phase Reactor design	-	-	-	-
II. Phase Optimization of different temperature values	I	30	H H	48
	II	40		
	III	60		
III. Phase Optimization of different aeration rates	IV	Opt.	H H	48
	V		H L	
	VI		L L	
IV. Phase Optimization of Different Leachate	VII	Opt.	Opt.	48
	VIII			24
	IX			12
	X			6



The reactor has been placed on the kaldnesses worked with 1.65L landfill leachate. High, medium and low flow rates are provided between each chamber with the help of oxygen pumps. The ammonium stripping tower used in the study is shown in Figure I.

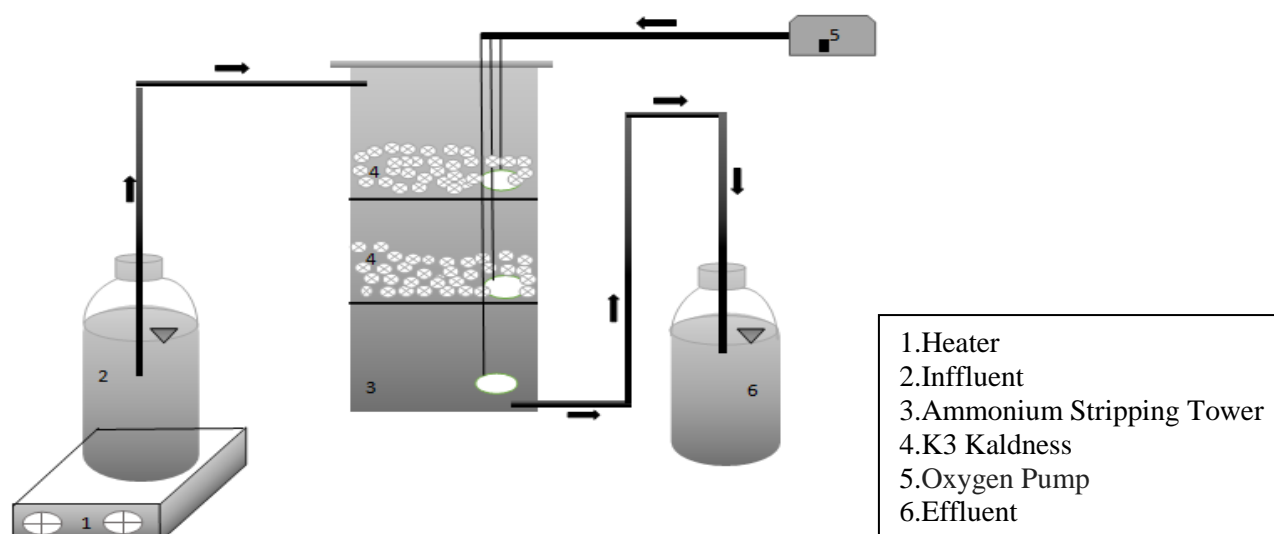


Fig. I. Schematic diagram of Lab-scale ammonia stripping tower

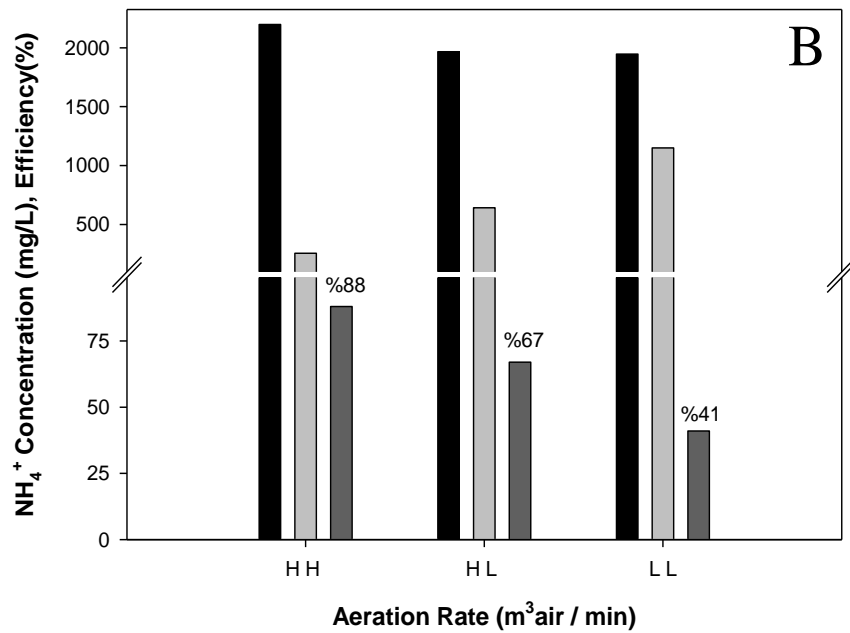
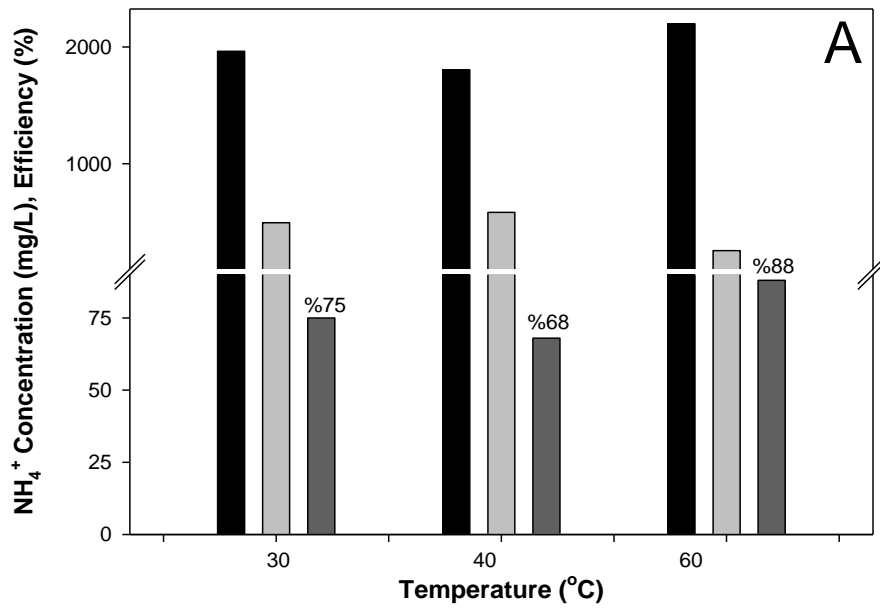
### Analyses

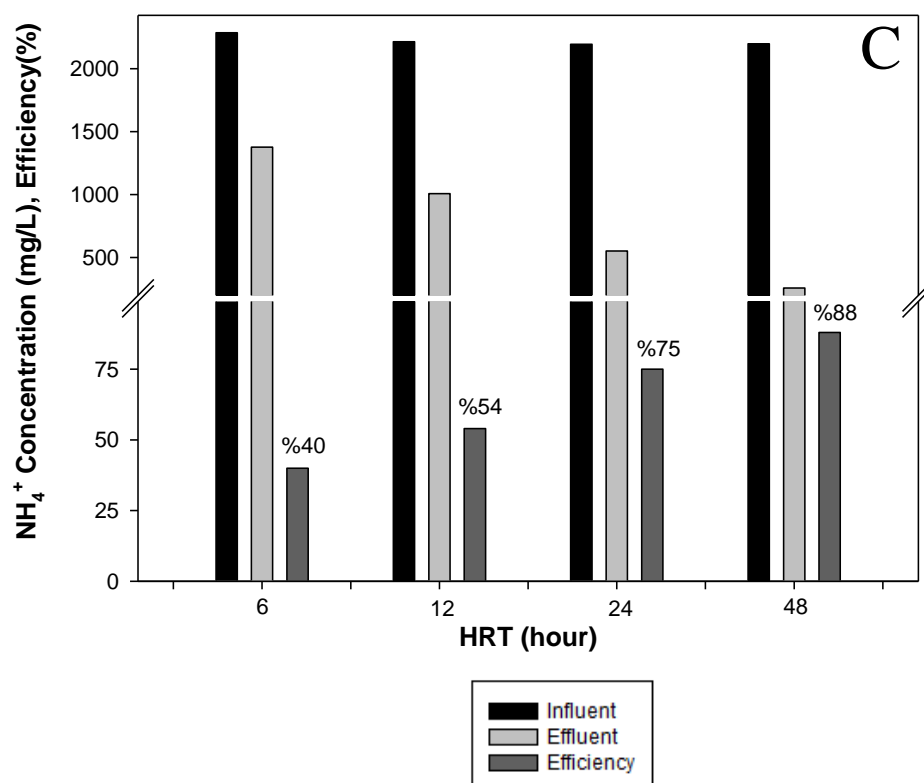
Before all analysis, liquid samples were centrifuged (Eppendorf Centrifuge 5415R, Hamburg, Germany) at 4000 rpm for 5 min and then supernatant was filtered through a 0.45- $\mu$ m pore size syringe filter. The COD analysis were performed by the dichromate closed reflux method in accordance with Standard Methods 5220D. pH was measured with a multimeter (340i, WTW, Oslo, Norway). The concentrations of ammonium, nitrate ions were determined by an ion chromatography (Dionex ICS-3000, Sunnyvale, CA, Japan) with IonPac AS19 analytical and Ion-Pac AG19 guard columns. Eluent was prepared from 9 mM sodium carbonate and 20 mM methane sulfonic acid and was pumped at flow rate of 1 ml/min.

## RESULTS AND DISCUSSION

### Ammonium Removal Performance

Ammonia stripping is the most common process for eliminating  $\text{NH}_4^+$  involved in leachate wastewater treatment technologies. The process involves the passage of large quantities of air over the exposed surface area of leachate, thus causing the partial pressure of the ammonia gas within the water to drive the ammonia from the liquid to the gas phase. The value of temperature, retention time and aeration rate are the main parameters effected on the  $\text{NH}_4^+$  removal ratio in this process. The effect of these parameters on ammonium removal during pre-treatment of LFL is demonstrated in Figure II.



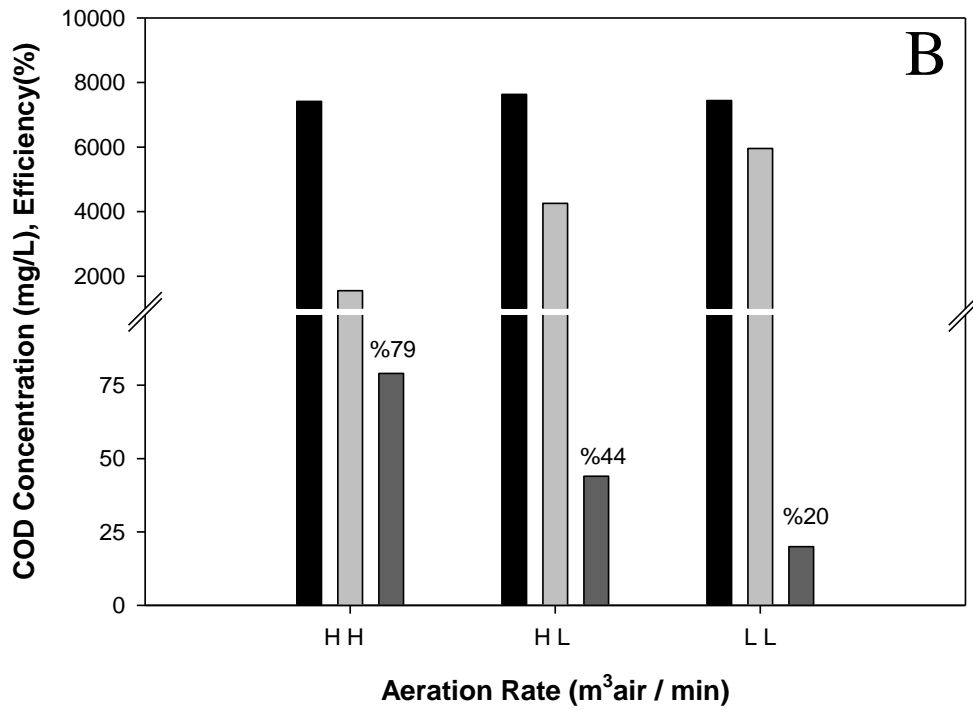
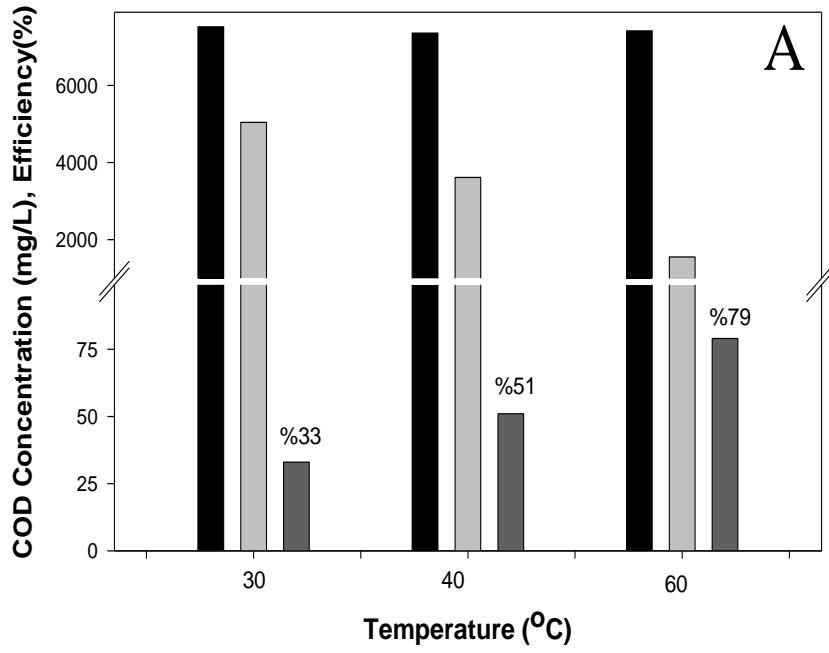


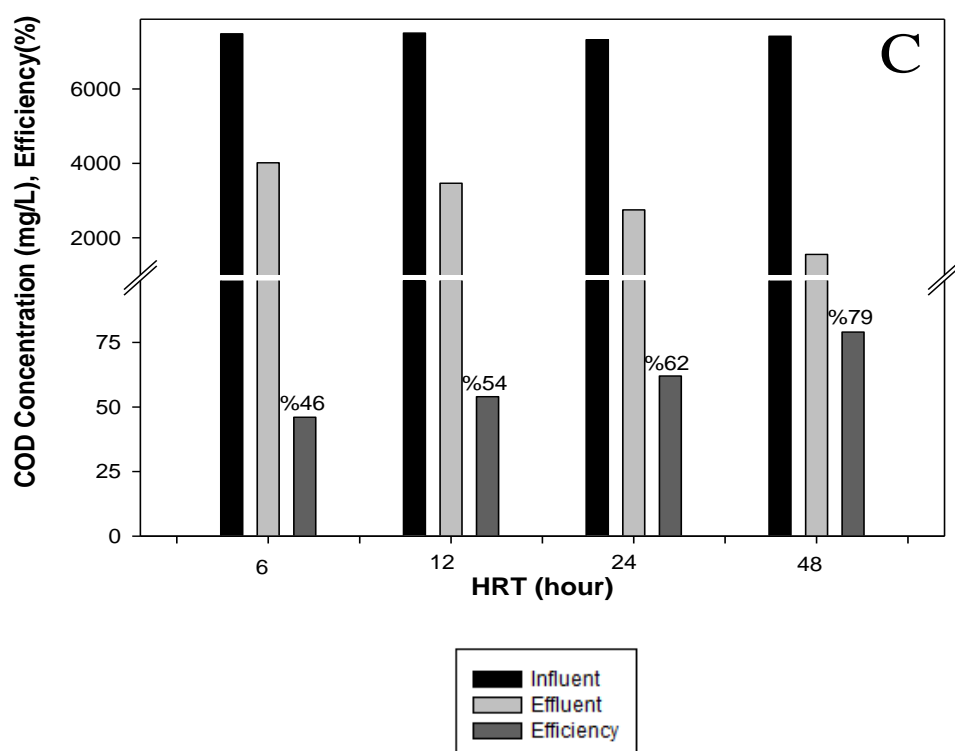
**Fig. II.** The effect of  $\text{NH}_4^+$  concentration removal by ammonium stripping: (A) Temperature, (B) Aeration rates and (C) Hydraulic retention times

Figure IIA shows the effect of temperature on  $\text{NH}_4^+$  removal efficiency. The removal ratio increased significantly with increases in the temperature.  $\text{NH}_4^+$  removal was about 75, 68 and 88 % at 30, 40 and 60 °C, respectively (Göçer, S., et al., 2018). reported the removal efficiency of  $\text{NH}_4^+$  at 60°C as 80%. Higher removal efficiency has been achieved in the study conducted with the ammonium stripping tower. As a result, the temperature of 60 °C should be the optimum because the removal efficiency is significantly increased. Figure IIB shows the effect of high, medium, and low aeration rates on  $\text{NH}_4^+$  removal efficiency. The highest  $\text{NH}_4^+$  removal efficiency was obtained at the high air rate corresponding to 88% (Cheung, K., et al., 1997). investigated airflow rate and pH as critical parameters for the optimization of ammonia stripping in a stirred tank. After one day, they achieved significant ammonia removal efficiency between 86 and 93% at the aeration rate of 5ml/min and pH greater than 11. Figure IIC shows the effect of hydraulic retention time on  $\text{NH}_4^+$  removal efficiency. Under optimum conditions, 6, 12, 24 and 48 h retention times have been tested and  $\text{NH}_4^+$  removal efficiencies have been respectively 40%, 54%, 75%, and 88%. Optimum retention time has been determined as 48 h.

### **COD Removal Performance**

The value of temperature, aeration rate and retention time are the main parameters affected on the COD removal efficiency in the ammonium stripping process (Figure III). The effect of temperature (30-40-60 °C) on the efficiency of COD removal was investigated (Fig IIIA). The removal efficiency has increased considerably with increasing temperature. An increase in temperature to 30-40-60 °C, had a positive effect on COD removal efficiency which was approached to 33%, 55% and 79% respectively. Therefore, the optimum temperature was 60°C. Figure IIIB shows the removal of COD by different aeration rates at ammonia stripping process. The COD removal efficiency increased significantly with increases in the aeration rate. The increasing aeration rate from LL to HL and HH ( $\text{m}^3\text{air}/\text{min}$ ) increased COD removal which approached to 79%, 44% and 20% respectively. The maximum COD removal efficiency of 79% was obtained in the aeration rate HH ( $\text{m}^3\text{air}/\text{min}$ ). Fig. IIIC shows the effect of COD removal by ammonium stripping processes at different HRT (6-12-24-48 h). The effect of hydraulic retention time on COD removal efficiency is shown in Figure IIIC. The highest COD removal efficiency has been reached in 48 hours and the removal efficiency has been 79%. Increased hydraulic retention time has decreased COD concentration (Hanira, N., et al., 2017).





**Fig. III.** The Effect Of COD Concentration By Ammonium Stripping: Temperature(A), Aeration Rates(B) And Hydraulic Retention Times(C)

## CONCLUSION

Ammonium stripping process in terms of physicochemical treatment of LFL performance was investigated. The following conclusions are drawn based on the results of the study:

- A new system (ammonium stripping tower) has been designed under laboratory conditions.
- The optimum conditions for the ammonia stripping process are determined as temperature (60°C), hydraulic retention time (48 h) and high aeration rate (1 m<sup>3</sup> air/min).
- In optimum conditions, the highest removal efficiencies have been 88% for NH<sub>4</sub><sup>+</sup> and 79% for COD.
- This study presents an alternative treatment technique for physicochemical treatment.

## KAYNAKLAR

Calace, N., Liberatori, A., Petronio, B., & Pietroletti, M. (2001). Characteristics of different molecular weight fractions of organic matter in landfill leachate and their role in soil sorption of heavy metals. *Environ Pollut*, 113:331–339.

Cheung, K. C., Chu, L. M., & Wong, M. H. (1997). Ammonia stripping as a pre-treatment for landfill leachate. *Water Air Soil Pollut.*, 94:209–221.

Collivignarelli, C., Bertanza, G., Baldi, M., & Avezzu, F. (1998). Ammonia stripping from MSW landfill leachate in bubble reactors: process modeling and optimization. *Waste Manage Res*, 16:455–466.

Göcer, S., Kozak, M., Duyar, A., Akgül, V., Zaimoğlu, Z., & Cırık, K. (2018). Synthesis Of Nanoscale Zero-Valent Iron (Nzvi). *International Symposium on Advanced Engineering Technologies*, 1526, 837-842.

Hanira, N., Hasfalina, C., Rashid, M., Luqman, C., & Abdullah, A. (2017). Effect of dilution and operating parameters on ammonia removal from scheduled waste landfill leachate in a lab-scale ammonia stripping reactor. *Materials Science and Engineering*.

Hossini, H., Rezaee, A., Ayati, B., & Mahvi, A. H. (2016). Health Scope 5 (1) e26479 doi: 10.17795/jhealthscope-26479.

Ledakowicz, S., & Kaczorek, K. (2001). Biodegradation of leachate from municipal landfill in Lodz enhanced by advanced oxidation processes. *8th International Waste Management and Landfill Symposium Proceedings*, Cagliari, Sardinia, Italy.

Martinen, S., Kettunen, R., Sormunen, K., & Soimasuo, R. (2002). Screening of physical-chemical methods for removal of organic material, nitrogen and toxicity from low strength landfill leachates. *Chemosphere*, 46:851-858.

Renou, S., Poulain, S., Givaudan, J. G., & Moulin, P. (2009). Amelioration of ultrafiltration process by lime treatment: case of landfill leachate. *Desalination*, 249:72-82.



# Kahramanmaraş Sutcu Imam University Journal of Engineering Sciences



Geliş Tarihi :25.06.2020  
Kabul Tarihi :25.09.2020

Received Date : 25.06.2020  
Accepted Date : 25.09.2020

## BİTKİLERDE DURAYLI CİVA İZOTOPLARININ AYRIMLILAŞMASI

## STABLE MERCURY ISOTOPE FRACTIONATION BEHAVIOURS OF PLANTS

Ayça DOĞRUL SELVER <sup>1</sup> (ORCID: 0000-0002-9003-5439)

<sup>1</sup> Kahramanmaraş Sütçü İmam Üniversitesi, Jeoloji Mühendisliği Bölümü, Kahramanmaraş, Türkiye

\*Sorumlu Yazar / Corresponding Author: Ayça DOĞRUL SELVER, aycaselver@ksu.edu.tr

### ÖZET

Bu çalışmanın ana amacı farklı fotosentez tiplerine sahip bitkilerde (C3, C4 ve CAM) civa (Hg) izotop davranışlarının belirlenmesi ve bitkilerin farklı kısımlarının Hg izotopları açısından farklılık gösterip göstermediğinin incelenmesidir. Bu amaçla, bitkilerin karbon izotopları analiz edilmiş ve böylece fotosentetik tipleri belirlenmiştir. Daha sonra bitkiler yaprak, sap ve kök olarak farklı kısımlara ayrılmış ve bu kısımların Hg izotopları analiz edilmiştir.

C3 ve C4 bitkilerinde çift kütle numaralı civa izotopları kütleyle bağımlı (MDF), tek kütle numaralı izotoplar ise kütlede bağımsız ayrımlaşma (MIF) göstermiştir. Hem C3 hem de C4 bitkilerinin hafif Hg izotoplarınca zenginleştiği fakat kütleyle bağımlı ayrımlaşmanın C3 bitkilerinde C4 bitkilerinden yaklaşık 3 kat fazla olduğu belirlenmiştir. Hem C3 hem C4 bitkileri negative MIF göstermiştir. Çalışmada sadece 1 adet CAM bitkisi analiz edilmiş ve bu CAM bitkisinin ağır Hg izotoplarınca az miktarda zenginleşme gösterdiği ve belirgin bir negative MIF göstermediği belirlenmiştir. Bu bulgular, Hg izotop bileşimi ve bitkilerin fotosentez tipi arasında bir ilişki olduğuna işaret etmektedir.

Ek olarak, bitkilerin yapraklarının köklerine kıyasla biraz daha fazla ayrımlaşmış bulunmuş ve bu farkın yaprak ve köklerin Hg kaynaklarının farklı olmasından kaynaklandığı öne sürülmüştür.

**Anahtar Kelimeler:** Civa izotopları, kütlede bağımsız ayrımlaşma, fotosentez tipleri, izotop ayrımlaşması

### ABSTRACT

The overarching aim of this study is to define mercury (Hg) isotopic features of plants which have different photosynthetic pathways (C3, C4 and CAM) and to understand if different parts of the plants have different Hg isotopic fractionation behavior. For this, carbon isotopic values of terrestrial plants were analyzed which were used to determine the photosynthetic pathways of plants. Plants were sub-sampled into leaves, stems and roots and their Hg isotopic values were analyzed.

Results showed that C3 and C4 plants exhibit mass dependent (even Hg isotopes) and mass independent Hg isotope fractionation (odd Hg isotopes). Both C3 and C4 plants are enriched in light isotopes, but the degree of mass fractionation is approximately three times greater in C3 plants, than in C4 plants. Hg in both C3 and C4 plants exhibit negative MIF isotope effect which reported as depletion "and no clear MIF effect. These findings suggest a connection between the Hg isotopic composition and the photosynthetic pathway.

In addition, the leaves are slightly more fractionated than the roots. Differences in the degree of MIF between roots and leaves suggest that they obtain Hg from different sources.

**Keywords:** Mercury isotopes, mass independent fractionation, photosynthetic pathways, isotope fractionation

\*Sorumlu Yazar / Corresponding Author: Ayça DOĞRUL SELVER, aycaselver@ksu.edu.tr

**ToCite:** DOĞRUL SELVER, A., (2020). STABLE MERCURY ISOTOPE FRACTIONATION BEHAVIOURS OF PLANTS. *Kahramanmaraş Sütçü İmam Üniversitesi Mühendislik Bilimleri Dergisi*, 23(4), 197-209.

## INTRODUCTION

Mercury (Hg) is a toxic global pollutant and it can be emitted to the atmosphere by natural and anthropogenic processes (Driscoll, Mason, Chan, Jacob, & Pirrone, 2013; Lamborg et al., 2002; Pirrone, Keeler, & Nriagu, 1996; Schroeder, 1998). The elemental gaseous form of Hg has long residence time (~1yr) in the atmosphere (Schroeder, 1998) therefore it can be transported long distances before being oxidized or deposited (Durnford, Dastoor, Figueras-Nieto, & Ryjkov, 2010; Lindberg et al., 2007). In addition when Hg is methylated, it becomes bioaccumulative which then poses a serious health problems. Therefore, to gain understanding of the source, fate and transformation of Hg in the environment is important. Studies to date showed that different natural samples vary in their Hg isotope compositions which suggest the use of Hg isotopes for source fingerprinting and for understanding transformation reactions.

Hg has seven stable isotopes whose relative abundances are  $^{196}\text{Hg}$  (0.15%),  $^{198}\text{Hg}$  (9.97 %),  $^{199}\text{Hg}$  (16.87 %),  $^{200}\text{Hg}$  (23.1 %),  $^{201}\text{Hg}$  (13.18%),  $^{202}\text{Hg}$  (29.86%), and  $^{204}\text{Hg}$  (6.86%) (Zadnik, Specht, & Begemann, 1989). Hg isotopes have been extensively used to understand fractionation behavior of different Hg isotopes in various natural samples (Biswas, Blum, Bergquist, Keeler, & Xie, 2008; Cai & Chen, 2016; Das, Salters, & Odom, 2009; S Ghosh, Xu, Humayun, & Odom, 2008; Zheng, Obrist, Weis, & Bergquist, 2016) and to trace Hg contaminant sources (Hintelmann & Zheng, 2011; Yin, Feng, Li, Yu, & Du, 2014). On the other hand, studies on Hg isotopes in terrestrial and aquatic vegetation is limited (Carignan, Estrade, Sonke, & Donard, 2009; S Ghosh et al., 2008; Sulata Ghosh, 2010; Yin, Feng, & Meng, 2013).

Mercury isotopes show both mass dependent (MDF) and mass independent isotope fractionation (MIF). Among seven Hg isotopes, even numbered Hg isotopes (especially  $\delta^{202}\text{Hg}$ ) show MDF. On the other hand, odd isotopes of Hg ( $\delta^{199}\text{Hg}$  and  $\delta^{201}\text{Hg}$ ) usually undergo MIF and produce negative isotopic anomalies (expressed as  $\Delta^{199}\text{Hg}$  and  $\Delta^{201}\text{Hg}$ ).  $\Delta^{199}\text{Hg}$  and  $\Delta^{201}\text{Hg}$  are a measure of the deviation from predicted MDF line. In 2007, Bergquist and Blum reported MIF of Hg isotopes in fish samples and reported up to 2.5‰ fractionation in odd Hg isotopes. Following to this study, MIF of odd Hg isotopes has been found in many natural samples such as sediments (Donovan, Blum, Yee, Gehrke, & Singer, 2013; Foucher, Hintelmann, Al, & MacQuarrie, 2013; Gehrke, Blum, & Marvin-DiPasquale, 2011), atmospheric samples (Sulata Ghosh, 2010; Yin et al., 2013; Yuan et al., 2015), lichens and mosses (Blum et al., 2012; S Ghosh et al., 2008; Sulata Ghosh, 2010). Photodegradation, photochemical reduction, abiotic reduction and evaporation are the mechanisms which are suggested to cause MIF (Bergquist & Blum, 2007; Sanghamitra Ghosh, Schauble, Lacrampe Couloume, Blum, & Bergquist, 2013; Zheng & Hintelmann, 2010).

The magnetic isotope effect (MIE) and the nuclear volume effect (NVE) are the most probable mechanisms causing MIF of odd isotope.

NVE is related with the nuclear volume and radius which is not proportional to the mass number. Isotopes have same charge but different neutron numbers and therefore a change in the neutron number result in the change in nuclear charge distribution which ultimately result in NVE. For heavier isotopes (lower nuclear charge density), the nuclear charge is distributed over a bigger volume while for smaller isotopes it is distributed over a small volume (higher nuclear charge density). On the other hand, odd isotopes have different behaviors, because of the nuclear energy splitting in the spectral lines. The MIE occurs when there is a spin-selective chemical reaction and it sorts nuclei according to their spins and magnetic moments (Buchachenko et al, 1976, Buchachenko, 2000). Among seven isotopes, even isotopes are spinless and non-magnetic but odd isotopes ( $^{199}\text{Hg}$  and  $^{201}\text{Hg}$ ) have non zero nuclear spins and magnetic moments therefore MIE only affects the odd isotopes. The result of magnetic isotope effect is fractionation of magnetic and non-magnetic isotopes in a chemical reaction (Buchachenko, 2000) and this depends on nuclear spin quantum number.

In this study, carbon and Hg isotope ratios of terrestrial plants were analyzed and interpreted together to understand (a) if there is any difference in Hg isotope signatures of plant samples which have different photosynthetic pathways (b) if there is a difference in the Hg isotopic fractionation in different parts of plants (mainly roots and leaves) (c) if



MDF and MIF occurs in terrestrial plants.

## METHOD

### *Sampling and Sample Preparation*

Plant samples were collected in St. Marks Wildlife Refuge, Florida and in Black Water River State Park, Pensacola, Florida. Identification of plant samples were done by Dr. Loren Anderson in the Department of Biology at FSU and by experts in Tallahassee Nurseries (Table 1).

Plants were divided into three sub-samples: leaves, stems and roots if available. Some of the plants were trees, and tree roots could not be collected in St. Marks Wildlife Refuge. Upon arrival to laboratory, each part was cleaned with Kimwipes to get rid of dust, soil and other particles. After being freeze dried, plant samples were ground into powder for further sample preparation.

For the carbon isotopic measurements, approximately 100 micrograms of ground plant samples were put in tin capsules.

For the mercury isotopic measurement, 2-3 grams of ground freeze dried sample was dissolved in aqua regia (3:1 14 N HNO<sub>3</sub> to 12 N HCl) and left on the hot plate (~50°C) for 8 hours and at room temperature for 7 days. At the end of 7 days, this solution was filtered through 100 micron filter paper. After filtering the samples, concentrated NaOH is added to solutions to reduce the acidity.

**Table 1.** Numbers, Names and Photosynthetic Pathways of Samples (PB: Pensacola Blackwater River Park Samples, SM: St. Mark's Samples)

SAMPLE NUMBER	SAMPLE NAME	PHOTOSYNTHETIC PATHWAY
PB1	Ambrosia Artemisiifolia	C3
PB2	Panicum Virgatum	C4
PB3	Chasmanthium Laxum	C3
PB4	Grass	C3
PB5	Vaccinium Corymbosum	C3
PB7	Vaxxinium Elliottii	C3
PB9	Clerhra Alnifolia	C3
PB10	Chamaecyparis Thyoides	C3
PB11	Ilex Opaca	C3
SM-1	Quercus virginiana	C3
SM-2	Myrica cerifera	C3
SM-3	Opuntia Stricta	CAM
SM-4	Lipidium Virginicum	C3
SM-6	Juniperus Virginiana (Red cedar)	C3
SM-7	Similax Sp.	C3
SM-8	Salt Bush	C3
SM-9	Grass	C4

### *Instrumental Analyses*

#### *Mercury Isotopic Analyses*

Mercury isotopic analysis methodology is developed by Ghosh, 2008. The sample solution was introduced to Thermo Finnigan *Neptune* multi collector inductively coupled plasma by a *CETAC HGX-200* cold vapor hydride generator (in NHMFL, Florida State University). Sample solution is introduced into the hydride generator along with

1-2 % SnCl<sub>2</sub> in a 1N HCl matrix to reduce the divalent mercury (Hg<sup>+2</sup>) in the solution and releases elemental mercury into gaseous phase. This cold vapor is introduced into the MC-ICP-MS to measure mercury isotopic ratios.

The 1 ppb mercury standard which was diluted from the 10 ppm standard reference material of National Institute of Standards and Technology (NIST SRM 3133) was used during analysis.

Seven adjustable Faraday cups were used for mercury isotope ratio measurements for mass numbers of 198, 199, 200, 201, 202, and 204 and also <sup>204</sup>Pb interference on <sup>204</sup>Hg was monitored at 206. Raw isotope ratios of <sup>198</sup>Hg/<sup>200</sup>Hg, <sup>199</sup>Hg/<sup>200</sup>Hg, <sup>201</sup>Hg/<sup>200</sup>Hg, <sup>202</sup>Hg/<sup>200</sup>Hg and <sup>204</sup>Hg/<sup>200</sup>Hg were calculated from the respective ion currents. For minimizing effects of instrumental fractionation, isotope ratios were determined by sample standard bracketing technique. Hg isotope ratios are reported relative to NIST-3133 Hg standard in δ (‰) notation (Eq.1);

$$\delta^N\text{Hg} = \left[ \frac{\left( \frac{^A\text{Hg}}{^{200}\text{Hg}} \right)_{\text{SAMPLE}}}{\left( \frac{^A\text{Hg}}{^{200}\text{Hg}} \right)_{\text{NIST3133}}} - 1 \right] \times 1000 \quad (1)$$

where A is the mass of each Hg isotope between 199 and 204 amu.

### Carbon Isotopic Analyses

For the carbon isotopic measurements, ground plant samples are put in tin capsules and loaded in the auto-sampler of a Carlo Erba Elemental Analyzer (EA) that is interfaced to a Finnigan MAT delta Plus XP stable isotope ratio mass spectrometer (IRMS). The sample is first introduced into the combustion column of the EA to produce a gas mixture of CO<sub>2</sub>, N<sub>2</sub>, SO<sub>3</sub>, SO<sub>2</sub>, NxOx and etc. The gas mixture is transported in ultra-pure He (as a Carrier gas) through the reduction column in the EA which is packed with copper as a reducer. In the reduction column, gases that are transferred from combustion column are converted into a mixture of CO<sub>2</sub>, N<sub>2</sub>, H<sub>2</sub>O, and SO<sub>2</sub>. The gas mixture is passed through a water trap to remove water. After removal of water, the gas mixture is transported through a GC (Gas Chromatography) column to be separated into its molecular components and the separated CO<sub>2</sub> molecules (eluted after N<sub>2</sub>) are transferred into the IRMS for C isotope measurements. The results are reported in the standard δ in reference to the international VPDB standard (Eq.2).

$$\delta^{13}\text{C} = \left[ \frac{\left( \frac{^{13}\text{C}}{^{12}\text{C}} \right)_{\text{SAMPLE}}}{\left( \frac{^{13}\text{C}}{^{12}\text{C}} \right)_{\text{STANDARD}}} - 1 \right] \times 1000 \quad (2)$$

## RESULTS AND DISCUSSION

14 of the samples are C3 plants having δ<sup>13</sup>C value of -30 to -26 ‰. The δ<sup>13</sup>C values of one CAM and two C4 plants ranges between -14 to -15‰ (Table 2). The difference in the δ<sup>13</sup>C values of above and below ground parts is 1‰ or less which does not make any difference in the photosynthetic type of plants.

C3 and C4 type of plants are enriched in light isotopes and depleted in heavy isotopes and have small difference in magnitude of fractionation. On the other hand, the flower and the main body (SM-3-F and SM-3-L respectively) of one CAM plant are enriched in heavy isotopes and therefore different from the rest of the plant samples. There is big analytical uncertainty associated with sample SM-3 but the data appear to best indicate an absence of any isotope

fractionation effects relative to the standard. (Table 3 and Figure 1).

As mentioned in the sampling part, it was not possible to obtain roots of all the samples and low ion currents (<150-200 milivolts) caused inaccurate isotopic measurements for stems of the samples therefore it was not possible to report all parts of the plant samples. In general, the highest signal intensities were obtained from leaves following by roots. There is just one stem sample that ran well.

When different plant parts are compared (roots and leaves of C3 plants), it was observed that both leaves and roots are enriched in light isotopes and depleted in heavy isotopes but the roots show slightly higher fractionation than the leaves (Table 4 and figure 2).

Previous studies gave similar results. For example; (Yin et al., 2013) reported average  $\delta^{202}\text{Hg}$  value of -3,28 ‰ for rice plant which is much more depleted than the leaves used in this study (-0,61 ‰ for leaves of C3 plants). Similarly,  $\delta^{202}\text{Hg}$  values reported to be around -2,0 to -2,6 ‰ for leaves of deciduous and coniferous trees (Demers, Blum, & Zak, 2013; Jiskra et al., 2015; Yin et al., 2013). this negative  $\delta^{202}\text{Hg}$  values observed is possibly due to photochemical reduction and loss of Hg from the surface of the leaves (Yin et al., 2013). Indeed, other studies also showed MDF of even isotopes during biological processes such as photoreduction, methylation and volatilization.

**Table 2.**  $\delta^{13}\text{C}$  Values of the Plant Samples

<b>SAMPLE NUMBER</b>	<b><math>\delta^{13}\text{C}</math> (‰)</b>
<b>PB1</b>	-30.45
<b>PB2</b>	-15.28
<b>PB3</b>	-30.41
<b>PB4</b>	-28.22
<b>PB5</b>	-30.96
<b>PB7</b>	-30.02
<b>PB9</b>	-28.72
<b>PB10</b>	-30.22
<b>PB11</b>	-28.72
<b>SM-1</b>	-28.74
<b>SM-2</b>	-27.51
<b>SM-3</b>	-13.94
<b>SM-4</b>	-27.78
<b>SM-6</b>	-26.91
<b>SM-7</b>	-28.36
<b>SM-8</b>	-29.02
<b>SM-9</b>	-14.46

Taking all the samples and plant parts together, it can be said that even mass number isotopes indicate mass dependent fractionation while odd isotopes show mass independent fractionation. In all the measured samples, the delta values plotted against the respective isotope masses define a linear line. The odd isotopes deviate from this line and show negative anomaly. This deviation is expressed as  $\Delta^{199}\text{Hg}$  and  $\Delta^{201}\text{Hg}$ . In other words, the degree of mass independent fractionation is indicated by  $\Delta^{201}\text{Hg}$  and  $\Delta^{199}\text{Hg}$  values and these are calculated as follows (Eq.3);

$$\Delta^{\text{A}}\text{Hg} = \delta^{\text{A}}\text{Hg}_{\text{measured}} - \delta^{\text{A}}\text{Hg}_{\text{MDF}} \quad (3)$$

where  $\delta^{\text{A}}\text{Hg}_{\text{MDF}}$  is calculated by using slope and interception of the mass dependent line.

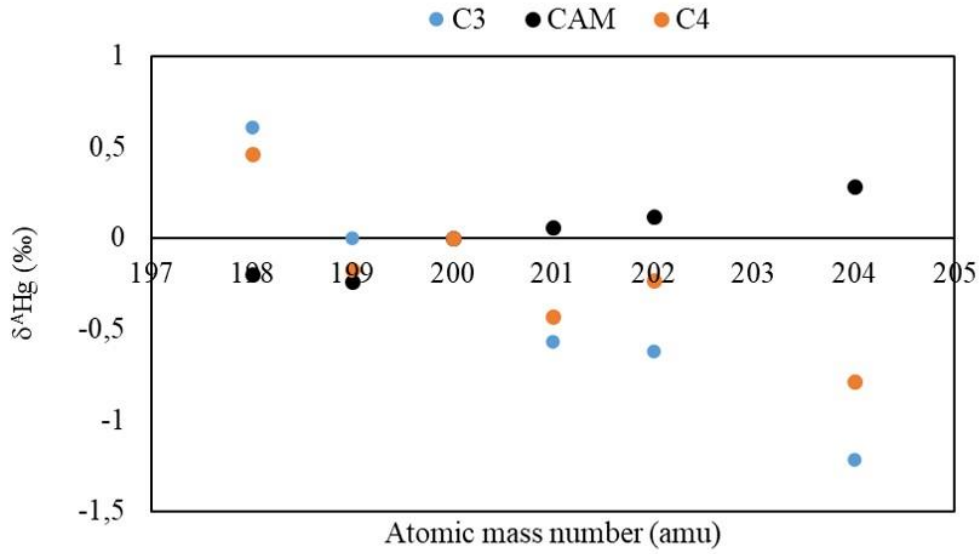
In all the samples,  $\Delta^{199}\text{Hg}$  values range between -0,09 and -0,60 ‰ and  $\Delta^{201}\text{Hg}$  values are between -0,03‰ and -

0,49 ‰ with average values being -0,28 and -0,22 respectively (Table 3). It is clear in the Figure 3 that C4 plants have the highest negative MIF degree (especially  $\Delta^{199}\text{Hg}$ ) compared to C3 and CAM plants. In contrast, CAM plant have slightly positive  $\Delta^{201}\text{Hg}$  deviation however considering the number of CAM plant samples (only 1) and the analytical uncertainty associated with this sample, this interpretation is open to discussion. Taking these into consideration, it can still be suggest that the degree of MIF of odd Hg isotopes can be related to the photosynthetic type of plants. For comparison, Hg isotopic data of rice plants taken from Yin et al. (2013) were used,  $\Delta^{199}\text{Hg}$  and  $\Delta^{201}\text{Hg}$  values (average of leaves and roots) was plotted on the diagram (Figure 4). It is clear that rice plant, which is also a C3 plant, plots close to C3 plant data point however they are not clustered.

**Table 3.**  $\delta^A\text{Hg}/^{200}\text{Hg}$  Values (‰),  $\Delta^{201}\text{Hg}$  and  $\Delta^{199}\text{Hg}$  Values and  $\Delta/\Delta$  Ratios of Different Parts of the Plants (L: leaves, R:roots, S: stems, B: berries).

	$\delta^{198}\text{Hg}$ (‰)	$\delta^{199}\text{Hg}$ (‰)	$\delta^{201}\text{Hg}$ (‰)	$\delta^{202}\text{Hg}$ (‰)	$\delta^{204}\text{Hg}$ (‰)	$\Delta^{199}\text{Hg}$ (‰)	$\Delta^{201}\text{Hg}$ (‰)	$\Delta^{199}\text{Hg}/\Delta^{201}\text{Hg}$	
Pensacola Samples	PB1-R	0,62	-0,23	-0,54	-0,72	-1,02	-0,47	-0,3	0,64
	PB1-L	0,78	0,1	-0,65	-0,89	-1,66	-0,17	-0,22	1,33
	PB2-R*	0,46	-0,06	-0,58	-0,21	-0,87	-0,4	-0,39	0,97
	PB2-L	0,89	-0,13	-0,69	-0,75	-1,43	-0,57	-0,37	0,65
	PB3-R	0,53	0,13	-0,7	-0,79	-1,55	-0,12	-0,25	2,07
	PB3-L	0,79	0,06	-0,53	-0,68	-1,33	-0,32	-0,22	0,68
	PB4-L	1,22	0,38	-0,55	-0,73	-1,59	-0,22	-0,28	1,27
	PB5-L	0,98	0,19	-0,7	-0,78	-1,68	-0,33	-0,35	1,03
	PB5-R	0,52	-0,11	-0,67	-0,74	-1,32	-0,35	-0,24	0,69
	PB6-L	0,22	-0,48	-0,26	0,08	-0,34	-0,6	-0,24	0,4
	PB7-R	0,82	-0,12	-0,58	-0,73	-1,26	-0,51	-0,26	0,51
	PB9-R	0,92	0,26	-0,78	-1,02	-2,1	-0,21	-0,23	1,1
	PB10-R	0,84	0,22	-0,71	-0,87	-1,91	-0,21	-0,22	1,09
PB11-R	0,68	-0,06	-0,69	-0,83	-1,16	-0,37	-0,36	0,99	
Saint Marks Samples	SM-1-L	0,38	-0,05	-0,33	-0,4	-0,86	-0,22	-0,1	0,46
	SM-2-S	-0,19	-0,28	-0,29	0,12	0,42	-0,17	-0,1	0,57
	SM-2-L	0,31	-0,06	-0,3	-0,23	-0,62	-0,13	-0,11	0,8
	SM-3-F*	0	-0,08	0,05	0,03	-0,07	-0,09	0,07	-0,81
	SM-3-L	-0,4	-0,4	0,07	0,2	0,63	-0,17	-0,03	0,2
	SM-4-L	1,55	0,69	-1,0	-1,59	-2,94	-0,11	-0,22	2,01
	SM-6-B	0,23	-0,14	-0,4	-0,09	-0,35	-0,13	-0,26	1,96
	SM-6-L	0,78	0,2	-0,66	-1,01	-2,04	-0,12	-0,06	0,53
	SM-7-L	0,17	-0,18	-0,39	-0,22	-0,42	-0,15	-0,2	1,29
SM-8-L	0,02	-0,49	-0,67	-0,26	-0,56	-0,49	-0,49	1,00	
SM-9*	0,03	-0,32	-0,02	0,27	-0,06	-0,34	-0,14	0,41	

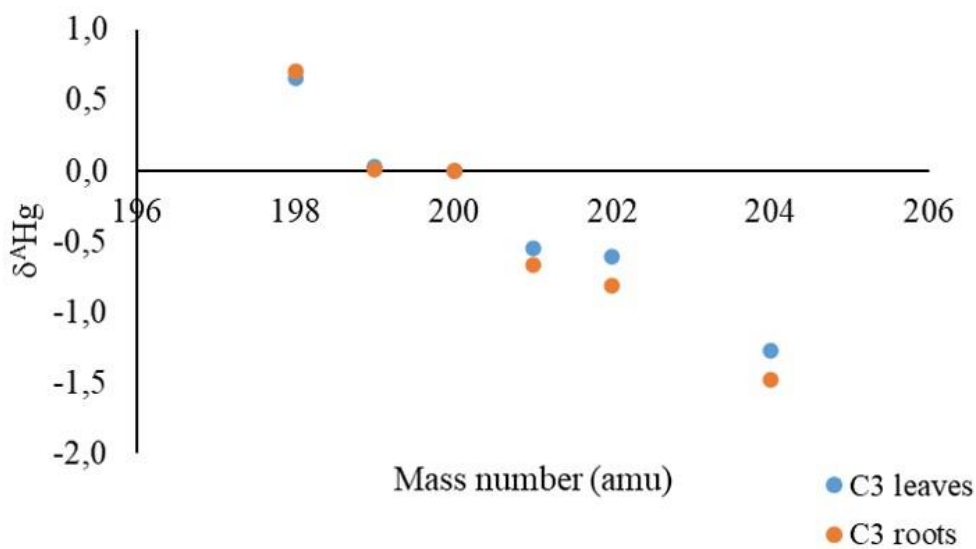
\* indicates C4 and CAM plants



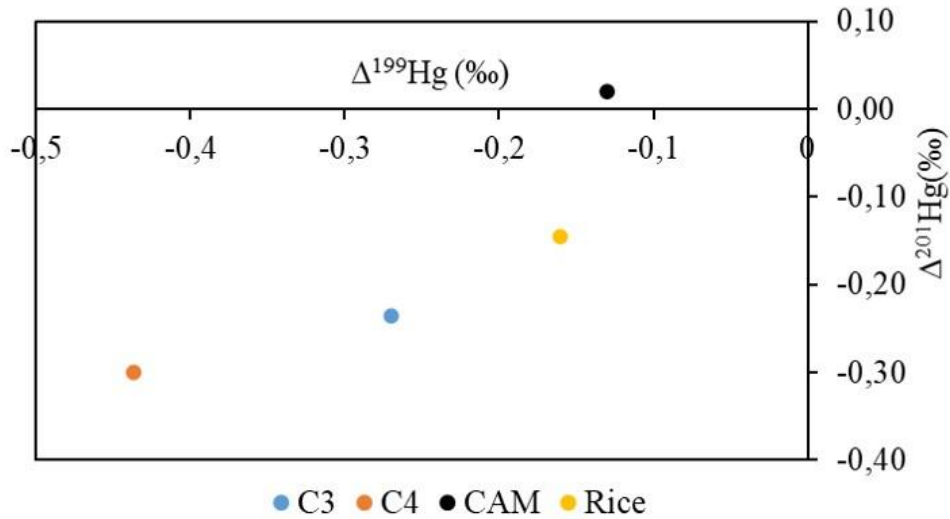
**Figure 1.**  $\delta^A \text{Hg}$  (‰) vs Atomic Mass Number Plots of C3, C4 and CAM Plants

**Table 4.** Average  $\delta^A \text{Hg}/^{200}\text{Hg}$  values (‰),  $\Delta^{201}\text{Hg}$  and  $\Delta^{199}\text{Hg}$  values and  $\Delta/\Delta$  ratios of All Samples, Pensacola Samples, Saint Mark's Samples, Different Parts of the Plants and of C3, C4 and CAM Plants

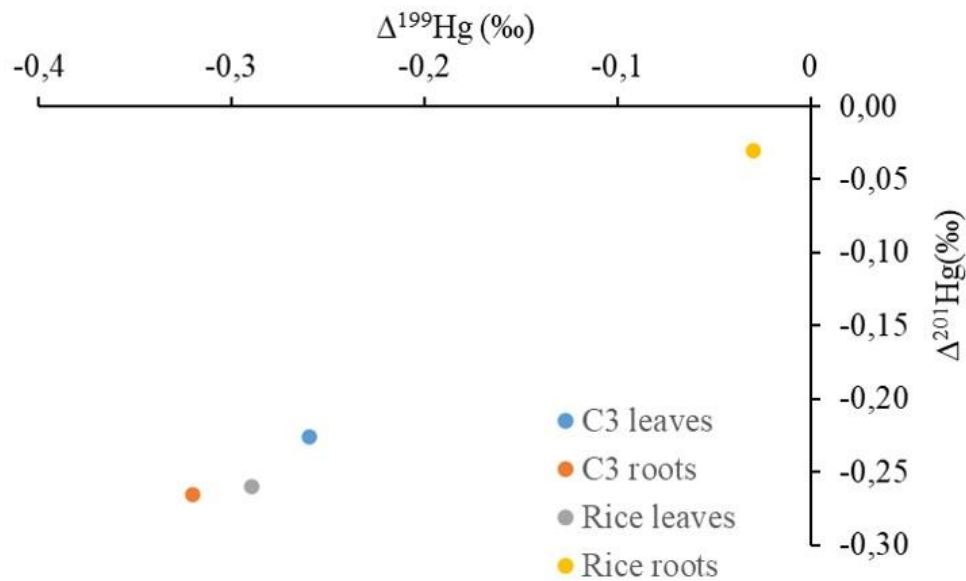
	$\delta^{198}\text{Hg}$ (‰)	$\delta^{199}\text{Hg}$ (‰)	$\delta^{201}\text{Hg}$ (‰)	$\delta^{202}\text{Hg}$ (‰)	$\delta^{204}\text{Hg}$ (‰)	$\Delta^{199}\text{Hg}$ (‰)	$\Delta^{201}\text{Hg}$ (‰)
<b>Average all</b>	0,53	-0,04	-0,50	-0,51	-1,04	-0,28	-0,22
<b>Average C3</b>	0,61	0,002	-0,57	-0,62	-1,21	-0,27	-0,24
<b>Average C4</b>	0,46	-0,17	-0,43	-0,23	-0,78	-0,44	-0,30
<b>Average CAM</b>	-0,2	-0,24	0,06	0,12	0,28	-0,13	0,02



**Figure 2.** The Fractionation Difference Between Roots and Leaves of C3 Plants



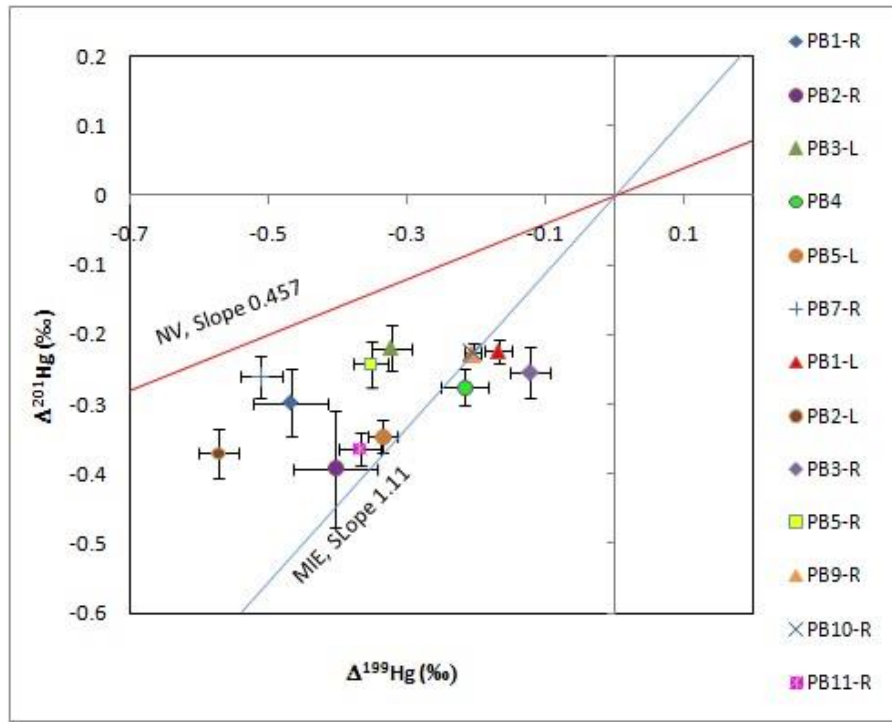
**Figure 3.** Average  $\Delta^{201}\text{Hg}$  vs  $\Delta^{199}\text{Hg}$  Plots of C3, C4 and CAM Plants. Rice Plant (Leaves And Roots Average) Results Are Taken From Yin et al. (2013)



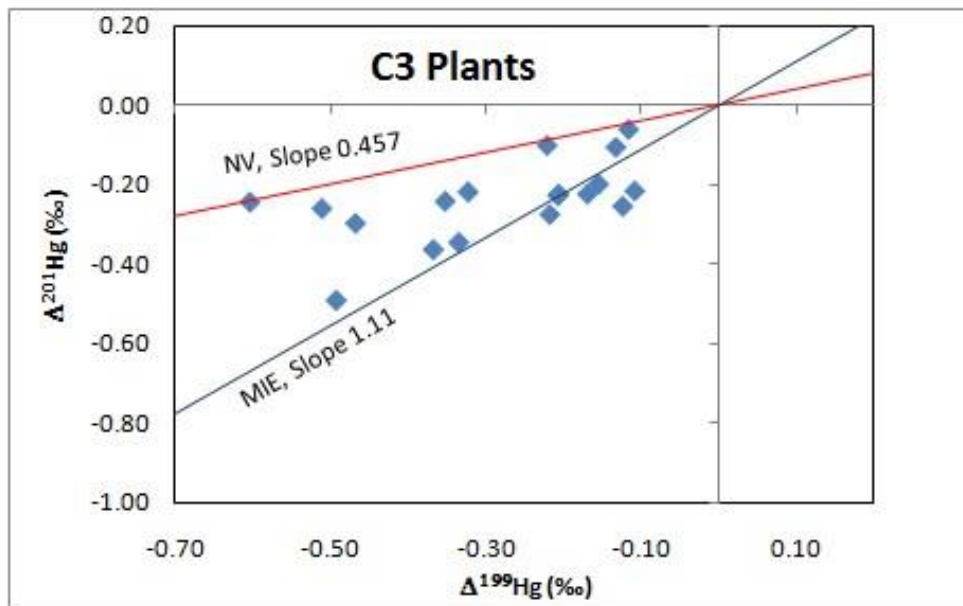
**Figure 4.** Average  $\Delta^{201}\text{Hg}$  vs  $\Delta^{199}\text{Hg}$  Plots of C3 Plant Parts. Rice Plant Data are Taken from Yin et al. (2013)

To understand the possible cause for MIF observed in plants,  $\Delta^{201}\text{Hg}/\Delta^{199}\text{Hg}$  ratios produced by the effects of magnetic isotope effect (MIE, blue lines) and nuclear volume (NV, red lines) were plotted on the  $\Delta^{199}\text{Hg}$  vs  $\Delta^{201}\text{Hg}$  diagram, with  $\Delta^{201}\text{Hg}/\Delta^{199}\text{Hg}$  ratios of 1.11 and 0.457 respectively (S Ghosh et al., 2008). Figure 5 and 6 indicate that MIF in these plant samples cannot be solely explained by either MIE or NV effect. A combination of both effects is likely responsible for the negative  $\Delta^{201}\text{Hg}$  and  $\Delta^{199}\text{Hg}$  values observed.

In addition, using MIF and NV effect lines it can also be suggested that MIF differences between roots and leaves (Figure 5) cannot be accounted for by either the NV or the MIE. The most simple explanation is that leaves and roots have acquired some of their mercury from different sources that already had been isotopically fractionated independent of their masses. In 2010, Ghosh found large differences between the  $\Delta^{199}\text{Hg}$  and  $\Delta^{201}\text{Hg}$  values of epiphytes (negative deviations) and the atmosphere ( $\sim 0$  or slightly positive deviations) and suggested that MIF effects can be produced within plants (Ghosh, 2010). Therefore, the isotopic differences in root-leaf pairs found in this study may also be due to *in vivo* effects as well.



**Figure 5.**  $\Delta^{199}\text{Hg}$  vs  $\Delta^{201}\text{Hg}$  Plot for Pensacola Plant Samples (Blue Line  $\Delta^{201}\text{Hg}/\Delta^{199}\text{Hg} = 1.11$ , Red Line  $\Delta^{201}\text{Hg}/\Delta^{199}\text{Hg} = 0.4569$ ). Error Bars Indicate 1SE Internal Precision on Each Sample.



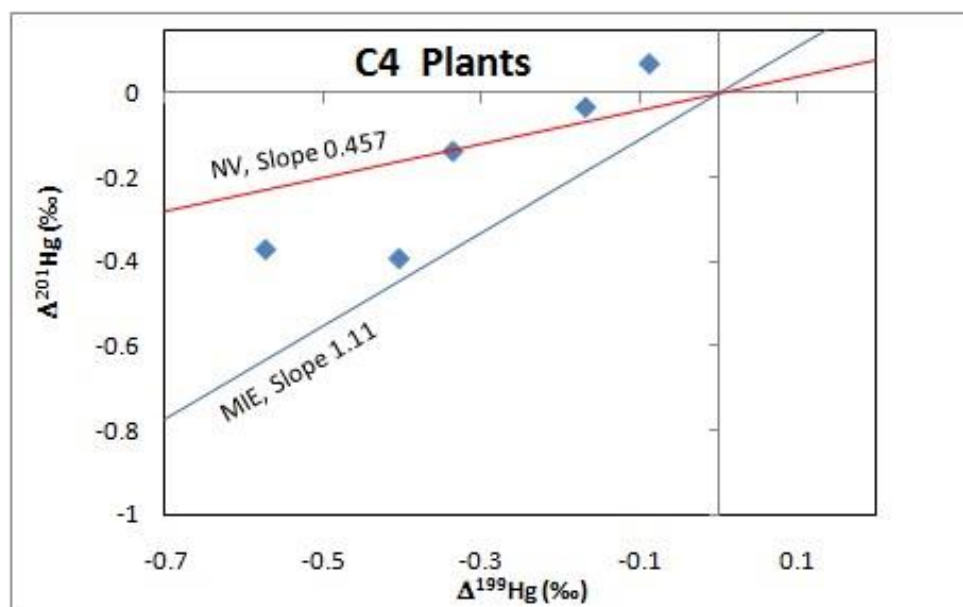


**Figure 6.**  $\Delta^{199}\text{Hg}$  vs.  $\Delta^{201}\text{Hg}$  Plot for C3 and C4 Plants (Blue Line  $\Delta^{201}\text{Hg}/\Delta^{199}\text{Hg}=1.11$ , Red Line  $\Delta^{201}\text{Hg}/\Delta^{199}\text{Hg}=0.457$ ).

## CONCLUSION

In the present study, Hg and C stable isotopic compositions of terrestrial plants were analyzed to understand if the Hg isotopic features of plants differ with different photosynthetic pathways and to understand the possible differences between above and below ground parts. Results showed that both C3 and C4 plants showed light Hg isotope enrichment, with mass dependent fractionation being approximately 3 times greater in the C3 plants than in C4 plants ( $-0.29\text{‰}/\text{amu}$ ) compared to ( $-0.09\text{‰}/\text{amu}$ ). The Hg isotopic signature of the single CAM plant is different than that of the C3 and C4 plants and showed light-isotope depletion. Together, these findings may suggest that there is a relationship between Hg isotopic composition in plants and their photosynthetic pathways.

Hg isotopic signatures of leaves and roots showed that both parts are enriched in light isotopes however roots fractionated slightly more than the leaves. In both parts of the plants odd isotopes of Hg showed negative MIF but the degree of MIF is different which cannot be explained only by known processes, if both roots and leaves obtain their mercury from same source. Considering the previous studies showing no MIF in atmospheric samples but negative MIF in leaves, it can be suggested that *in vivo* reactions in plants contribute to Hg isotopic fractionation in plants.

As a conclusion, this study provides an important step toward understanding biogeochemical cycle of Hg and improves our understanding of Hg isotope fractionation behavior in different plant types and in different organs of plants however there is a need for additional focused sampling and experiments on plants grown in controlled environment.

## ACKNOWLEDGEMENT

This work was financially supported by the Ministry of National Education of Turkey.

## REFERENCES

- Bergquist, B. A., & Blum, J. D. (2007). Mass-Dependent and -Independent Fractionation of Hg Isotopes by Photoreduction in Aquatic Systems. *Science*, 318(5849), 417 LP – 420. <https://doi.org/10.1126/science.1148050>
- Biswas, A., Blum, J. D., Bergquist, B. A., Keeler, G. J., & Xie, Z. (2008). Natural mercury isotope variation in coal deposits and organic soils. *Environmental Science and Technology*, 42(22), 8303–8309. <https://doi.org/10.1021/es801444b>



- Blum, J. D., Johnson, M. W., Gleason, J. D., Demers, J. D., Landis, M. S., & Krupa, S. (2012). Mercury Concentration and Isotopic Composition of Epiphytic Tree Lichens in the Athabasca Oil Sands Region. In K. E. B. T.-D. in E. S. Percy (Ed.), *Alberta Oil Sands* (Vol. 11, pp. 373–390). Elsevier. <https://doi.org/https://doi.org/10.1016/B978-0-08-097760-7.00016-0>
- Cai, H., & Chen, J. (2016). Mass-independent fractionation of even mercury isotopes. *Science Bulletin*, 61(2), 116–124. <https://doi.org/10.1007/s11434-015-0968-8>
- Carignan, J., Estrade, N., Sonke, J. E., & Donard, O. F. X. (2009). Odd Isotope Deficits in Atmospheric Hg Measured in Lichens. *Environmental Science & Technology*, 43(15), 5660–5664. <https://doi.org/10.1021/es900578v>
- Das, R., Salters, V. J. M., & Odom, A. L. (2009). A case for in vivo mass-independent fractionation of mercury isotopes in fish. *Geochemistry, Geophysics, Geosystems*, 10(11), 1–12. <https://doi.org/10.1029/2009GC002617>
- Demers, J. D., Blum, J. D., & Zak, D. R. (2013). Mercury isotopes in a forested ecosystem: Implications for air-surface exchange dynamics and the global mercury cycle. *Global Biogeochemical Cycles*, 27(1), 222–238. <https://doi.org/10.1002/gbc.20021>
- Donovan, P. M., Blum, J. D., Yee, D., Gehrke, G. E., & Singer, M. B. (2013). An isotopic record of mercury in San Francisco Bay sediment. *Chemical Geology*, 349–350, 87–98. <https://doi.org/10.1016/j.chemgeo.2013.04.017>
- Driscoll, C. T., Mason, R. P., Chan, H. M., Jacob, D. J., & Pirrone, N. (2013). Mercury as a Global Pollutant: Sources, Pathways, and Effects. *Environmental Science & Technology*, 47, 4967–4983.
- Durnford, D., Dastoor, A., Figueras-Nieto, D., & Ryjkov, A. (2010). Long range transport of mercury to the Arctic and across Canada. *Atmospheric Chemistry and Physics*, 10(13), 6063–6086. <https://doi.org/10.5194/acp-10-6063-2010>
- Foucher, D., Hintelmann, H., Al, T. A., & MacQuarrie, K. T. (2013). Mercury isotope fractionation in waters and sediments of the Murray Brook mine watershed (New Brunswick, Canada): Tracing mercury contamination and transformation. *Chemical Geology*, 336, 87–95. <https://doi.org/10.1016/j.chemgeo.2012.04.014>
- Gehrke, G. E., Blum, J. D., & Marvin-DiPasquale, M. (2011). Sources of mercury to San Francisco Bay surface sediment as revealed by mercury stable isotopes. *Geochimica et Cosmochimica Acta*, 75(3), 691–705. <https://doi.org/10.1016/j.gca.2010.11.012>
- Ghosh, S., Xu, Y., Humayun, M., & Odom, L. (2008). Mass-independent fractionation of mercury isotopes in the environment. *Geochemistry, Geophysics, Geosystems*, 9(3), 1–10. <https://doi.org/10.1029/2007GC001827>
- Ghosh, Sanghamitra, Schauble, E. A., Lacrampe Couloume, G., Blum, J. D., & Bergquist, B. A. (2013). Estimation of nuclear volume dependent fractionation of mercury isotopes in equilibrium liquid-vapor evaporation experiments. *Chemical Geology*, 336, 5–12. <https://doi.org/10.1016/j.chemgeo.2012.01.008>
- Ghosh, Sulata. (2010). *Isotopic Composition of Mercury in the Atmosphere*.
- Hintelmann, H., & Zheng, W. (2011, November 18). Tracking Geochemical Transformations and Transport of Mercury through Isotope Fractionation. *Environmental Chemistry and Toxicology of Mercury*. <https://doi.org/doi:10.1002/9781118146644.ch9>
- Jiskra, M., Wiederhold, J. G., Skyllberg, U., Kronberg, R. M., Hajdas, I., & Kretzschmar, R. (2015). Mercury Deposition and Re-emission Pathways in Boreal Forest Soils Investigated with Hg Isotope Signatures. *Environmental Science and Technology*, 49(12), 7188–7196. <https://doi.org/10.1021/acs.est.5b00742>
- Lamborg, C. H., Fitzgerald, W. F., Damman, A. W. H., Benoit, J. M., Balcom, P. H., & Engstrom, D. R. (2002). Modern and historic atmospheric mercury fluxes in both hemispheres: Global and regional mercury cycling implications. *Global Biogeochemical Cycles*, 16(4), 51-1-51–11. <https://doi.org/10.1029/2001gb001847>

Lindberg, S., Bullock, R., Ebinghaus, R., Engstrom, D., Feng, X., Fitzgerald, W., ... Seigneur, C. (2007). A Synthesis of Progress and Uncertainties in Attributing the Sources of Mercury in Deposition. Source: *Ambio*, 36(1), 19–32.

Pirrone, N., Keeler, G. J., & Nriagu, J. O. (1996). Regional differences in worldwide emissions of mercury to the atmosphere. *Atmospheric Environment*, 30(17), 2981–2987. [https://doi.org/10.1016/1352-2310\(95\)00498-X](https://doi.org/10.1016/1352-2310(95)00498-X)  
Schroeder, H. (1998). Atmospheric Mercury-An Overview. *Atmospheric Environment*, 32(5).

Yin, R., Feng, X., Li, X., Yu, B., & Du, B. (2014). Trends and advances in mercury stable isotopes as a geochemical tracer. *Trends in Environmental Analytical Chemistry*, 2, 1–10. <https://doi.org/10.1016/j.teac.2014.03.001>

Yin, R., Feng, X., & Meng, B. (2013). Stable Mercury Isotope Variation in Rice Plants (*Oryza sativa* L.) from the Wanshan Mercury Mining District, SW China. *Environmental Science & Technology*, 47(5), 2238–2245. <https://doi.org/10.1021/es304302a>

Yuan, S., Zhang, Y., Chen, J., Kang, S., Zhang, J., Feng, X., ... Huang, Q. (2015). Large Variation of Mercury Isotope Composition During a Single Precipitation Event at Lhasa City, Tibetan Plateau, China. *Procedia Earth and Planetary Science*, 13, 282–286. <https://doi.org/10.1016/j.proeps.2015.07.066>

Zadnik, M. G., Specht, S., & Begemann, F. (1989). Revised isotopic composition of terrestrial mercury. *International Journal of Mass Spectrometry and Ion Processes*, 89(1), 103–110. [https://doi.org/https://doi.org/10.1016/0168-1176\(89\)85035-9](https://doi.org/https://doi.org/10.1016/0168-1176(89)85035-9)

Zheng, W., & Hintelmann, H. (2010). Nuclear Field Shift Effect in Isotope Fractionation of Mercury during Abiotic Reduction in the Absence of Light. *The Journal of Physical Chemistry A*, 114(12), 4238–4245. <https://doi.org/10.1021/jp910353y>

Zheng, W., Obrist, D., Weis, D., & Bergquist, B. A. (2016). Mercury isotope compositions across North American forests. *Global Biogeochemical Cycles*, 30(10), 1475–1492. <https://doi.org/10.1002/2015GB005323>



# Kahramanmaraş Sutcu Imam University Journal of Engineering Sciences



Geliş Tarihi : 06.08.2020  
Kabul Tarihi : 14.10.2020

Received Date : 06.08.2020  
Accepted Date : 14.10.2020

## KURUTULMUŞ NAR (*Punica granatum*) KABUĞU TOZUNUN GLUTENSİZ BİSKÜVİLERİN TEKSTÜREL, DUYUSAL VE BAZI FİZİKOKİMYASAL ÖZELLİKLERİ ÜZERİNE ETKİSİ

### EFFECT OF DRIED POMEGRANATE (*Punica granatum*) PEEL POWDER ON TEXTURAL, SENSORY AND SOME PHYSICO-CHEMICAL CHARACTERISTICS OF GLUTEN-FREE BISCUITS

Sibel BÖLEK<sup>1</sup> (ORCID: 0000-0003-4697-9416)

<sup>1</sup> Sağlık Bilimleri Üniversitesi, Gıda Teknolojisi Ana Bilim Dalı, İstanbul, Türkiye

\*Sorumlu Yazar / Corresponding Author: Sibel Bölek, sibel.bolek@sbu.edu.tr

#### ÖZET

Glutensiz bir diyet çölyak hastalığının tedavisinde etkin bir rol oynamaktadır. Bu çalışmada, zengin fenolik madde içeriği ve yüksek antioksidan özelliklerine rağmen gıda endüstrisinde atık olarak nitelendirilen nar kabuğu tozunun glutensiz fonksiyonel gıda üretiminde kullanım olanakları araştırılmıştır. Bu amaçla glutensiz bisküvi formülasyonuna %0, %4, %8 ve %12 olmak üzere 4 farklı oranda nar kabuğu tozu buğday unu ile ikame edilmiştir. Nar kabuğu tozunun bisküvilerin renk, nem, kül, yağ, protein, diyet lif, toplam fenolik madde, antioksidan aktivite değerleri ile tekstürel ve duyuşsal özellikleri üzerine etkisi incelenmiştir. Bisküvi formülasyonuna nar kabuğu tozu ilavesi, antioksidan aktivite, toplam fenolik madde ve diyet lif içeriklerinde istatistiksel olarak önemli düzeyde artış sağlamıştır ( $p<0.05$ ). Bisküvi hamurunun ve bisküvilerin tekstürel özellikleri de nar kabuğu tozu ilavesinden istatistiksel olarak önemli düzeyde etkilenmiştir. Bisküvi formülasyonundaki nar kabuğu tozu oranı arttıkça duyuşsal panelden alınan puanlarda düşüş görülmüştür. Ancak duyuşsal panelden alınan puanların hepsi duyuşsal panel için orta değer olarak belirlenen 3 puanın üzerinde olduğundan bisküvi formülasyonuna %12 düzeyine kadar nar kabuğu tozu ilavesinin duyuşsal olarak kabul edilebilir bir ürün elde edilmesine olanak sağladığı ortaya çıkarılmıştır.

**Anahtar Kelimeler:** Bisküvi, *Punica granatum*, diyet lif, antioksidan aktivite, duyuşsal analiz

#### ABSTRACT

A gluten-free diet plays an active role in the treatment of celiac disease. In this study, the possibilities of using pomegranate peel powder, which is considered as waste in the food industry despite its rich phenolic content and high antioxidant properties, in gluten-free functional food production were investigated. For this purpose, the gluten-free wheat flour was substituted by pomegranate peel powder at levels of 0, 4, 8 and 12%. The effect of pomegranate peel powder on color, moisture, ash, oil, protein, dietary fiber, total phenolic content, antioxidant activity, textural and sensory properties of biscuits was investigated. The addition of pomegranate peel powder to the biscuit formulation provided a statistically significant increase in antioxidant activity, total phenolic substance and dietary fiber content of biscuits ( $p<0.05$ ). The textural properties of biscuit dough and biscuits were also significantly affected by pomegranate peel powder substitution. As the rate of pomegranate peel powder in the biscuit formulation increased, the scores obtained from the sensory panel decreased. However, since the scores obtained from the sensory panel were all above 3 point determined as the middle value for sensory panel, it was revealed that the addition of pomegranate peel powder to the biscuit formulation up to 12% enables acceptable product in terms of sensory properties.

**Keywords:** Biscuit, *Punica granatum*, dietary fiber, antioxidant activity, sensory analysis

\*Sorumlu Yazar / Corresponding Author: Sibel BÖLEK, sibel.bolek@sbu.edu.tr

**ToCite:** BOLEK, S. (2020). KURUTULMUŞ NAR (*PUNİCA GRANATUM*) KABUĞU TOZUNUN GLUTENSİZ BİSKÜVİLERİN TEKSTÜREL, DUYUSAL VE BAZI FİZİKOKİMYASAL ÖZELLİKLERİ ÜZERİNE ETKİSİ *Kahramanmaraş Sütçü İmam Üniversitesi Mühendislik Bilimleri Dergisi*, 23(4), 209-218.

## GİRİŞ

Fırıncılık ürünleri nispeten uzun raf ömürleri, lezzetleri oluşları, ucuz oluşları, kolay taşınabilir olmaları gibi sebeplerle Dünya'nın her yerinde hemen her yaş grubunda yaygın olarak tüketilmektedir (Oluwamukomi, Oluwalana ve Akinbowale, 2011). Bununla beraber fırıncılık ürünlerinin dengeli beslenmeye yardımcı olmaktan ziyade tüketenlere boş kaloriler sağladığı düşünülmektedir. Bu nedenle önemli düzeyde tüketilme oranlarına sahip olan bu ürünlerin diyet lifi, antioksidan aktivite, vitamin ve mineral içeriği açısından zenginleştirilmesi son derece önemlidir. Diğer taraftan böyle zenginleştirilmiş fırıncılık ürünleri genel kabul edilen tanımıyla "normal diyetin bir parçası olarak tüketilen ve sağlığı iyileştirme ya da hastalık riskini azaltma potansiyeline sahip biyolojik açıdan aktif bileşenleri içeren gıdalar" (Aksoylu, Çağındı ve Köse, 2012) olan fonksiyonel gıda eldesine olanak sağlamaktadır. Son yıllarda fonksiyonel gıdalara olan eğilimin artmasının nedeni, yapılan araştırmaların fonksiyonel gıdaların çeşitli kanser türlerine yakalanma riskini azaltma, kötü huylu kolesterolü düşürmede etkili olarak koroner kalp hastalıklarını önleme, tip-2 diyabetin oluşma sıklığının azaltılmasında etkili olma gibi potansiyellerini ortaya koymasının yanında sindirim, bağırsak ve bağışıklık sistemlerinin iyileştirilmesine katkıda bulunabileceklerinin ispatlaması sonucu bu ürünlerin tüketiciye daha sağlıklı bir görünüm kazandırmasıyla ilgilidir [Lin vd., 2016; Schaafsma ve Pakan, 1999; Wang ve Zhou, 2004]. Bu amaçla fırıncılık ürünlerinin zenginleştirildiği birçok çalışma gerçekleştirilmiştir. Pasqualone vd. (2014) bisküvi formülasyonuna üzüm posası ekstraktı ilave etmişlerdir. Çalışmalarının sonucunda bisküvi örneklerinin toplam fenolik madde ve antioksidan aktivite değerlerinin arttığını saptamışlardır. Gawlik-Dziki vd. (2013) ekmeği kurutulup öğütülmüş soğan ile zenginleştirmişlerdir. Yürütülen çalışmanın sonucunda ekmeğin formülasyonuna %3 düzeyinde soğan ilavesinin ekmeğin duyusal özelliklerinde olumsuz bir değişime neden olmadan antioksidan aktivite değerlerinde artış sağladığı ortaya konulmuştur. Kinoa yapraklarının ekmeğin zenginleştirilmesinde kullanıldığı bir çalışmada ekmeğin formülasyonundaki buğday ununun %1-5 oranında kinoa yaprağı ile ikame edilmesinin ekmeğin toplam fenolik madde içeriğinde artış sağladığı sonucuna ulaşılmıştır (Świeca, Sęczyk, Gawlik-Dziki ve Dziki, 2014). Bisküvilerin zenginleştirilmesinde pirinç kepeklerinin kullanıldığı bir çalışmanın sonucunda bisküvilerin protein içeriklerinde önemli oranda artış sağlanmış dolayısıyla pirinç kepeğinin bisküvilerin besleyici değerini arttırmada kullanılabileceği sonucuna ulaşılmıştır (Yadav, Yadav ve Chaudhary, 2011).

Gıda endüstrisinde işlem sırasında ve sonrasında pek çok gıda atığı oluşmaktadır. Bu atıklar genellikle imha edilmekte ya da ekonomik değeri nispeten daha az olan hayvan yemi, gübre vb. olarak değerlendirilmektedir. Söz konusu atıkların insan beslenmesinde kullanım olanakları üzerinde ise yeterince durulmamaktadır. Meyve ve sebze işleme endüstrisinde oluşan atıklar genellikle beslenme açısından önemli olan diyet lifi, pektin, antioksidanlar, esansiyel yağ asitleri, vitaminler gibi değerli bileşenleri içermektedir.

Nar Lythraceae familyasının *Punica* cinsinden çok yıllık bir bitki olup hem ticari hem de kültürel anlamda önemli değere sahip olan bir meyvedir. Nar meyvesinin ticari türü olan *Punica granatum* L. Dünya'da çekirdekli elma olarak da bilinmektedir (Kurt ve Şahin, 2013). Nar protein, karbonhidrat, yağ, toplam fenolik madde, vitamin ve mineral madde açısından oldukça zengin bir meyvedir (Al-Maiman ve Ahmad, 2002). İçerdiği bileşenlerin sağlık üzerindeki son derece olumlu etkileri nedeniyle pek çok ülkede gıda takviyesi ve ilaç etken maddesi olarak kullanılmaktadır (Özdemir, Soyer, Tağı ve Turan, 2014). Diğer taraftan nar meyvesinin kabukları da proantosiyanidinler, flavonoidler ve kondanse tanenler yönünden zengindir (Guo vd., 2003). Ayrıca kabuk kısmının antioksidan ve antimikrobiyal etkisinin meyvenin diğer kısımlarından daha fazla olduğu da yapılan araştırmalarla ortaya konulmuştur (Liv d., 2006; Negi, Jayaparaksha, 2003). Tüm bunların yanında nar meyvesinin kabuğu zengin bir lif kaynağıdır (Akhtar, Ismail, Fraternal ve Sestili (2015).

Bisküvi fırıncılık ürünleri içerisinde en yaygın olarak üretilen ve tüketilen gıdalardan biridir. Ayrıca bisküvi yoğun çalışma temposu ve hızlı yaşam tarzının getirdiği alıştırmalıklarla beslenme kültüründe sıklıkla ana öğün geçiştirmek amacıyla da tüketilebilmektedir. Bu nedenle bisküvinin fonksiyonel bileşenlerce zenginleştirilmesi gittikçe önem kazanmaktadır.

Bu çalışmanın amacı; antioksidanlar ve diyet lifi başta olmak üzere biyoaktif bileşenlerce zengin bir gıda atığı olan nar kabuğunu glutensiz bisküvi formülasyonuna ilave ederek özellikle çölyak hastaları için glutensiz fonksiyonel bir gıda elde etmektir. Nar kabuğu tozunun yüksek antioksidan aktivitesi ve besleyici özellikleri nedeniyle fırıncılık

ürünlerinde kullanıldığı çalışmalar mevcuttur fakat nar kabuğu tozunun glutensiz bisküvi formülasyonuna ilave edildiği bir çalışmanın literatürde mevcut olmaması çalışmanın özgün değerini oluşturmaktadır. Bu çalışma ile bisküvilere sağlık açısından fonksiyonel özellik kazandırılırken bir gıda atığına da geri dönüşüm olanağı sağlanması amaçlanmaktadır.

## **MATERYAL VE METOT**

Çalışmada kullanılan Hicaz türü narlar, *Punica granatum*, Antalya’da yerel bir satıcıdan temin edilmiştir. Bisküvi hamurunun hazırlanmasında kullanılan glutensiz buğday unu, toz şeker, tereyağı, yağsız süt tozu ve tuz ticari yerel bir marketten satın alınmıştır. Kullanılan kimyasallar analitik veya yüksek saflıkta kimyasallar olup, Sigma-Aldrich (St. Louis.MO, ABD) firmasından satın alınmıştır.

### ***Nar Kabuğu Tozunun Hazırlanması***

Nar meyvelerinin kabukları Al-Zoreky (2009) tarafından belirtilen şekilde manuel olarak soyulmuş ve damıtık su ile iyice yıkanmıştır. Küçük parçalara ayrılan kabuklar etüv kullanılarak (Memmert UNB400, Almanya) 60°C’de yaklaşık 6 saat %7 nem oranına kadar kurutulmuştur. Analizlere kadar -18°C’de LDPE poşetlerde bekletilen kabuklar analizlerden önce bir öğütücü (Delongi KG 79) yardımıyla 150 µm inceliğine öğütülmüştür.

### ***Bisküvilerin Hazırlanması***

Bisküvi hamuru AACC (10-54, 2000) yönteminde küçük modifikasyonlarla bir homojenizatör (KitchenAid, Artisan 5KSM175PSEER) kullanılarak hazırlanmıştır. Bisküvi hamurunda Munaza vd. (2012) tarafından peynir altı suyu proteini konsantresi ile zenginleştirilmiş bisküvi yapımına benzer şekilde buğday unu (100 g), toz şeker (30 g), tereyağı (10 g), yağsız süt tozu (2.0 g), amonyum bikarbonat (1.0 g), lesitin (1.0 g), sodyum bikarbonat (0.5 g), tuz (0.3 g) ve damıtık su (20 mL) kullanılmıştır. Buğday unu ve nar kabuğu tozu ikame edilerek aşağıdaki şekilde 4 ayrı karışım hazırlanmıştır.

T0: %0 nar kabuğu tozu, %100 buğday unu içeren bisküvi  
T1: %4 nar kabuğu tozu, %96 buğday unu içeren bisküvi  
T2: %8 nar kabuğu tozu, %92 buğday unu içeren bisküvi  
T3: %12 nar kabuğu tozu, %88 buğday unu içeren bisküvi

Karışımlarda kullanılan oranlar ön denemelerle özgün olacak şekilde belirlenmiştir. Bisküvi hamurunun şekillendirilmesinde AACC (10-50.05, 2000) yöntemi kullanılmıştır 55.0 mm çaplı kesme kalıbı ile şekil verilen hamurlar bir elektrikli fırın (Arçelik SUF 5000 MGSI) kullanılarak 200°C’de 15 dakika boyunca pişirilmiştir.

Fiziksel, kimyasal, tekstürel ve duyuşal özelliklerin belirlenmesi için ayrı ayrı üretim yapılarak bekleme süresinden bisküvinin ölçülecek özelliklerinin etkilenmesi engellenmiştir.

### ***Hammaddelerin Kimyasal Kompozisyonlarının Belirlenmesi***

Bisküvi üretiminde kullanılacak unda ve kurutulmuş nar kabuklarında nem, kül, protein, yağ ve diyet lif tayini AOAC [20]’da belirtilen standart prosedüre göre yapılmıştır.

### ***Bisküvi Hamurunun Tekstürel Özelliklerinin Belirlenmesi***

Bisküvi hamurunun tekstürel özellikleri bir tekstür analizörü (TA.XT Plus, Stable Micro Systems, England) kullanılarak belirlenmiştir. Analizde 25 kg’lık yük hücresi ve 35 mm’lik silindirik alüminyum prob kullanılmıştır. Test hızı ve test sonrası hızı 1 mm/s olarak ayarlanmıştır. Sertlik, esneklik, yapışkanlık, bağlılık değerleri belirlenmiştir.

### ***Bisküvilerde Yapılan Analizler***

### ***Bisküvilerin Kimyasal Kompozisyonlarının Belirlenmesi***

Bisküvilerin nem, kül, yağ, protein ve diyet lif içerikleri AOAC (2005)'da belirtilen standart prosedür kullanılarak belirlenmiştir.

### **Renk Tayini**

Bisküvilerin yüzey renklerini ölçmek için Minolta DP-301 (Osaka, Japonya) model bir kolorimetre kullanılmıştır. Renk tespitinde Hunter renk parametreleri (L\* (parlaklık), a\*(kırmızılık) ve b\*(sarılık) değerleri) göz önünde bulundurulmuştur. L\*= 93.3, a\*=0.3162 ve b\*= 0.3321 (beyaz plaka) değerleri kalibrasyon için referans olarak kullanılmıştır.

### **Antioksidan Aktivite Tayini**

Analiz için farklı konsantrasyonlarda örnek ekstraktları (10-40µg/mL) hazırlanarak etanol ile 2 mL'ye seyreltilmiştir. Üzerine etanol ile hazırlanan DPPH çözeltisinden (1 mM) 500 µL ilave edilmiştir. Daha sonra vorteks ile karıştırılıp, karanlıkta 30°C'de 30 dk inkübe edilmiştir. Kör olarak etanol kullanılmıştır. Absorbans 517 nm'de köre karşı ölçülmüştür. Absorbanstaki azalma DPPH serbest radikal süpürme aktivitesini göstermiştir. Elde edilen absorbans değerlerinden % inhibisyon değerleri eşitlik 1 kullanılarak hesaplanmıştır (Ye, Wang, Liu ve Ng, 2000).

$$\% \text{ inhibisyon} = [(A_{\text{DPPH}} - A_{\text{ekstrakt}}) / A_{\text{DPPH}}] \times 100 \quad (1)$$

$A_{\text{DPPH}}$ : DPPH şahit örneğin absorbans değeri

$A_{\text{ekstrakt}}$ : Örnek ekstraktın absorbans değeri

### **Toplam Fenolik Madde Tayini**

Bisküvilerin toplam fenolik madde içerikleri Cemeroğlu (2010) tarafından önerilen yöntemde küçük modifikasyonlar yapılarak belirlenmiştir. 5 g örnek alınıp 50 mL %80'lik metil alkol içerisinde homojenize edilmiştir. Homojenat bir behere alınıp 5 dk süreyle kaynatılmıştır. Ekstrakt Whatman 4 filtre kağıdından filtre edilmiştir. Beherdeki kalıntı üzerine tekrar 50 mL %80'lik metil alkol eklenip 10 dk daha kaynatılmıştır. Her iki ekstrakt 100 mL lik balon jode birleştirilip soğumaya bırakılmıştır. Soğuduktan sonra balon joje çizgisine kadar saf suyla tamamlanmıştır. Ekstraktan 50 mL'lik balon joje içerisine 5 mL alınıp üzerine 5 mL saf su ilave edilmiştir. Daha sonra üzerine 0.5 mL Folin-cioalciu ayracı eklenip balon iyice çalkalanmıştır. 3 dk beklendikten sonra üzerine 1 mL %36'luk sodyum karbonat çözeltisi eklenen balon, saf su ile tekrar çizgisine kadar tamamlandıktan sonra tekrar iyice çalkalanıp karanlık bir ortamda 1 saat bekletilmiştir. Bekleme süresi sonunda spektrofotometrede 725 nm dalga boyunda okuma yapılmıştır.

Stok çözeltinin hazırlanması: 0.1 gr gallik asit 100 mL metanolla seyreltilmiştir.

Standart çözeltilerin hazırlanması: 0, 0.4, 0.8, 1.2, 1.6, 2 mg/mL konsantrasyonda çözeltiler gerekli seyreltmeler yapılarak hazırlanmıştır. Her bir örnek için okunan absorbans değerlerine karşı konsantrasyon miktarı kalibrasyon grafiğinden belirlenmiş, sonuçlar seyreltme katsayıları dikkate alınarak mg/100g olarak gallik asit cinsinden hesaplanmıştır

### **Tekstürel Özelliklerin Tayini**

Bisküvilerin tekstürel özellikleri bir tekstür analizörü (TA.XT Plus, Stable Micro Systems, England) kullanılarak belirlenmiştir. Analizde 5 kg'lık yük hücresi ve 2 mm'lik silindirik alüminyum prob kullanılmıştır. Test hızı 0,2 mm/s ve test sonrası hızı 0.5 mm/s olarak ayarlanmıştır. Bisküvilerin sertlik ve kırılma değeri belirlenmiştir.

### **Duyusal Analiz**

Bisküvi örnekleri görünüş, koku, doku, koku, lezzet ve genel izlenim bakımından kıyaslanarak duyu panel tarafından en beğenilen örneği bulmak amacıyla 5 puanlı hedonik skala (1= Hiç beğenmedim, 2= Beğenmedim, 3= Ne beğendim ne beğenmedim, 4= Beğendim, 5= Çok beğendim) kullanılmıştır (Meilgaard, Civille ve Carr, 2016). Analiz ISO 8586 (2012) normlarına uygun olarak gerçekleştirilmiştir. Bisküvilerin panelistlere sunulurken kullanıldığı porselen tabaklar rastgele 3 haneli rakamlarla kodlanarak daha önceden belirlenmiş yaş aralığı 20-30 arasında değişen yarı-eğitilmiş 80 paneliste (46 kadın 34 erkek) sunulmuştur. Analiz 3 tekerrürlü olarak uygulanmıştır.

Analiz ortamı beyaz floresan ampul kullanılarak aydınlatılmıştır. Her uygulamada panelistlere 4 farklı örnek sunulmuştur. Örnek sunumları arasında ağızda oluşan kalıntı tadı gidermek için su kullanılmıştır.

### İstatistiksel Analiz

Tüm üretimler üç tekerrürlü yapılmış ve elde edilen örneklerin analizleri de 3 paralel olarak gerçekleştirilmiştir. Analizlerden elde edilen veriler SPSS (version 15 for windows, SPSS, Inc., Chicago, IL, USA) istatistiksel paket programı ile Duncan çoklu karşılaştırma testi ile 0.05 güven aralığı kullanılarak analiz edilmiştir.

## BULGULAR VE TARTIŞMA

### Hammaddenin Özellikleri

Bisküvi üretiminde kullanılan unun ve nar kabuklarının kimyasal kompozisyonları Tablo 1’de verilmiştir. Nar kabuğunun diyet lif açısından oldukça zengin bir kaynak olduğu sonucuna ulaşılmıştır. Ayrıca nar kabuğunun gıdalarda bulunan mineral madde içeriğinin bir göstergesi olan kül oranı da (Yurtseven ve Baran, 2000) yüksek bulunmuştur. Sonuçlar literatürde nar kabuğunun kimyasal kompozisyonun belirlendiği çalışmalarla uyumludur [Al-Rawahi, Rahman, Guizani, Essa, 2013; Galaz vd., 2017; Ibrahim, 2010).

**Tablo 1.** Hammaddelerin Kimyasal Kompozisyonları

Hammadde	Nem (%)	Kül (%)	Yağ (%)	Protein (%)	Diyet Lif (%)
Un	10.55±0.02	0.52±0.01	0.99±0.04	1.6±0.07	2.95±0.03
Nar Kabuğu Tozu	5.96±0.05	4.08±0.03	3.10±0.07	2.70±0.06	40,65±0,09

### Bisküvi Hamurunun Tekstürel Özellikleri

Bisküvi hamurunun tekstürel özellikleri Tablo 2’de verilmiştir. Bisküvi formülasyonuna nar kabuğu tozu ilavesi bisküvi hamurunun tüm tekstürel özelliklerini istatistiksel olarak önemli düzeyde etkilemiştir ( $p<0.05$ ). Bisküvi formülasyonuna nar kabuğu tozu ilavesi bisküvi hamurunun sertlik ve yapışkanlık değerlerinde artışa neden olmuştur. Bunun nedeni nar kabuklarının yüksek lif içeriği ile açıklanabilir. Benzer sonuçlar Psyllium lifinin bisküvi hamurunun tekstürel özellikleri üzerine etkisinin araştırıldığı çalışmanın (Raymundo, Fradinho ve Nunes, 2014) sonucunda da elde edilmiştir. Diğer taraftan nar kabuğu tozu ilavesinin bisküvi hamurunun esneklik ve bağlılık değerlerinde azalmaya neden olduğu gözlemlenmiştir ( $p<0.05$ ). Bağlılık değeri hamurun gluten içeriğiyle önemli ölçüde ilişkili olduğundan (Saha vd., 2011) formülasyonda buğday unu miktarı azalıp nar kabuğu tozu ilavesi arttıkça hamurun bağlılık değeri istatistiksel olarak önemli düzeyde azalmıştır ( $p<0.05$ ). Elde edilen sonuçlar, yüksek proteinli bisküvi eldesi için buğday unu ile *Spirulina platensis*’in ikame edildiği çalışmanın sonuçlarıyla uyumludur (Singh, Singh, Jha, Rasane, Gautam, 2015).

**Tablo 2.** Bisküvi Hamurunun Tekstürel Özellikleri

Uygulama	Sertlik (N)	Esneklik	Yapışkanlık (N)	Bağlılık (N x s)
T <sub>0</sub>	24.05±0.08 <sup>d</sup>	0.707±0.03 <sup>a</sup>	0.24±0.07 <sup>d</sup>	47.66±0.12 <sup>a</sup>
T <sub>1</sub>	25.52±0.06 <sup>c</sup>	0.686±0.03 <sup>b</sup>	0.25±0.05 <sup>c</sup>	41.36±0.10 <sup>b</sup>
T <sub>2</sub>	26.22±0.06 <sup>b</sup>	0.664±0.02 <sup>c</sup>	0.26±0.04 <sup>b</sup>	36.42±0.09 <sup>c</sup>
T <sub>3</sub>	27.06±0.07 <sup>a</sup>	0.642±0.03 <sup>d</sup>	0.27±0.03 <sup>a</sup>	31.88±0.08 <sup>d</sup>

a-d  $p<0.05$  Aynı sütundaki farklı harfler istatistiki açıdan farklıdır.

### Bisküvilerin Kimyasal Kompozisyonları

Kontrol bisküvilerinin ve nar kabuğu tozu ilave edilmiş bisküvilerin kimyasal kompozisyonları Tablo 3'te verilmiştir. Bisküvi formülasyonuna nar kabuğu tozu ilavesi bisküvilerin nem değerlerinde istatistiksel olarak önemli düzeyde artışa neden olmuştur ( $p<0.05$ ). Bu sonuç bisküvilerin nar kabuğu tozu ilavesi ile artan diyet lif içeriği sayesinde su tutma kapasitelerinin artması ile açıklanabilir. Mango kabuklarının bisküvi formülasyonuna ilave edildiği çalışmada bisküvilerin nem değerleri için benzer sonuçlar elde edilmiştir (Ashoush ve Gadallah, 2011). Bisküvilerin kül oranı nar kabuğu tozu ilavesi ile artış göstermiştir. Fakat bu artış istatistiksel olarak önemli düzeyde olmamıştır ( $p>0.05$ ). Bisküvi formülasyonuna nar kabuğu tozu ilavesi bisküvilerin yağ içeriğinde de istatistiksel olarak önemli olmayan düzeyde bir azalmaya neden olmuştur. ( $p>0.05$ ). Diğer taraftan, bisküvi formülasyonuna ilave edilen nar kabuğu tozu oranı arttıkça bisküvilerin protein oranı ve diyet lif içerikleri önemli düzeyde artış göstermiştir ( $p<0.05$ ). Bu sonuç nar kabuğu tozunun özellikle çölyak hastası bireyler için fırıncılık ürünlerinde potansiyel bir protein kaynağı olabileceğini göstermektedir.

**Tablo 3.** Bisküvilerin Kimyasal Kompozisyonları

Uygulama	Nem (%)	Kül (%)	Yağ (%)	Protein (%)	Diyet lif (%)
T <sub>0</sub>	2.48±0.03 <sup>d</sup>	1.95±0.02 <sup>a</sup>	20.62±0.02 <sup>a</sup>	0.86±0.05 <sup>a</sup>	2.38±0.03 <sup>d</sup>
T <sub>1</sub>	3.10±0.02 <sup>c</sup>	2.07±0.03 <sup>a</sup>	19.05±0.05 <sup>b</sup>	0.98±0.02 <sup>b</sup>	2.60±0.07 <sup>c</sup>
T <sub>2</sub>	3.36±0.01 <sup>b</sup>	2.25±0.02 <sup>a</sup>	18.02±0.04 <sup>c</sup>	1.45±0.01 <sup>c</sup>	4.82±0.08 <sup>b</sup>
T <sub>3</sub>	3.68±0.07 <sup>a</sup>	2.64±0.01 <sup>a</sup>	17.12±0.03 <sup>d</sup>	1.82±0.02 <sup>d</sup>	6.28±0.05 <sup>a</sup>

a-d  $p<0.05$  Aynı sütundaki farklı harfler istatistiki açıdan farklıdır

### Bisküvilerin Renk Değerleri

Kontrol bisküvilerinin ve nar kabuğu tozu ilave edilmiş bisküvilerin L\*, a\*, b\* değerleri Tablo 4'te verilmiştir. Bisküvi formülasyonuna nar kabuğu tozu ilavesi bisküvilerin renk değerlerini istatistiksel olarak önemli düzeyde etkilemiştir ( $p<0.05$ ). Bisküvi formülasyonundaki nar kabuğu tozu oranı arttıkça bisküvilerin L\* ve b\* değerlerinde düşüş gözlenirken, a\* değerlerinde artış olduğu saptanmıştır. L\* ve b\* değerlerindeki azalma bisküvi formülasyonundaki nar kabuğu tozu oranı arttıkça bisküvilerin pişirilmesi esnasında enzimatik ve enzimatik olmayan esmerleşme reaksiyonlarının daha fazla gerçekleşmesiyle açıklanabilir. Diğer taraftan nar kabuğundaki antosiyaninler sıcaklık etkisi ile renk değişimine uğrayabilmektedir (Nizamlioğlu ve Nas, 2010; Uzuner, Onsekizoglu ve Acar, 2011). Bisküvi formülasyonunda nar kabuğu tozu oranı arttıkça a\* değerinin artması nar kabuğunun rengindeki kırmızılıkla ilişkilendirilebilir.

**Tablo 4.** Bisküvilerin L\*,a\*,b\* Değerleri

Uygulama	L*	a*	b*
T <sub>0</sub>	66.22±0.07 <sup>a</sup>	11.48±0.02 <sup>a</sup>	32.22±0.06 <sup>a</sup>
T <sub>1</sub>	50.34±0.04 <sup>b</sup>	11.96±0.03 <sup>a</sup>	26.32±0.05 <sup>b</sup>
T <sub>2</sub>	42.22±0.04 <sup>c</sup>	12.44±0.02 <sup>b</sup>	24.46±0.04 <sup>c</sup>
T <sub>3</sub>	35.06±0.03 <sup>d</sup>	13.15±0.01 <sup>b</sup>	20.20±0.03 <sup>d</sup>

a-d  $p<0.05$  Aynı sütundaki farklı harfler istatistiki açıdan farklıdır

### Bisküvilerin Antioksidan Aktivite ve Toplam Fenolik Madde İçerikleri

Nar kabuğu tozunun, kontrol bisküvilerinin ve nar kabuğu tozu ilave edilmiş bisküvilerin antioksidan aktivite ve toplam fenolik madde içerikleri Tablo 5'te verilmiştir. Bisküvi formülasyonuna nar kabuğu tozu ilavesi ile bisküvilerin antioksidan aktivite ve toplam fenolik madde içeriklerini istatistiksel olarak önemli düzeyde artış



gerçekleşmiştir ( $p<0.05$ ). Bu durum nar kabuğunun toplam fenolik madde ve antioksidanlarca oldukça zengin olmasından ileri gelmiştir.

**Tablo 5.** Bisküvilerin Antioksidan Aktivite ve Toplam Fenolik Madde İçerikleri

Uygulama	Toplam Fenolik Madde (mg GAE/100 g)	DPPH (%)
Nar kabuğu tozu	1379.02±2.12	86.50±1.48
T <sub>0</sub>	88.66±1.07 <sup>a</sup>	26.62±1.03 <sup>a</sup>
T <sub>1</sub>	118.26±1.02 <sup>b</sup>	36.90±1.16 <sup>b</sup>
T <sub>2</sub>	142.21±1.14 <sup>c</sup>	45.44±1.02 <sup>c</sup>
T <sub>3</sub>	155.07±1.03 <sup>d</sup>	50.15±1.05 <sup>d</sup>

a-d  $p<0.05$  Aynı sütundaki farklı harfler istatistiki açıdan farklıdır

### ***Bisküvilerin Tekstürel Özellikleri***

Kontrol bisküvilerinin ve nar kabuğu tozu ilave edilmiş bisküvilerin tekstürel özellikleri Tablo 6'da verilmiştir. Bisküvilerin tekstürel kalitesini belirlemede genel olarak kullanılan sertlik ve kırılgenlik değerleri belirlenmiştir (Banerjee, Singh, Jha ve Mitra, 2014; Castillo, 2018; González, Gallo, Correa ve Gallo-García). Bisküvi formülasyonuna nar kabuğu tozu ilavesi bisküvilerin sertlik ve kırılgenlik değerlerini istatistiksel olarak önemli düzeyde etkilemiştir ( $p<0.05$ ). Bisküvi formülasyonundaki nar kabuğu tozu oranı arttıkça bisküvilerin sertlik ve kırılgenlik değerlerinde artış görülmüştür. Bu durum nar kabuğu tozunun yüksek lif içeriği ile daha kompakt bir bisküvi tekstürü oluşturmasıyla açıklanabilir. Bisküvilerin tekstürel özelliklerinin değişimi ile ilgili benzer sonuçlar bisküvilerin yüksek lif içeriğine sahip gıdalarla zenginleştirildiği çalışmalarda da elde edilmiştir (Kulkarni ve Joshi; 2013; Singh, Rana, Sahi, Lohani ve Chand, 2012).

**Tablo 6.** Bisküvilerin Tekstürel Özellikleri

Uygulama	Sertlik (N)	Kırılgenlik (N)
T <sub>0</sub>	29.54±0.07 <sup>a</sup>	25.41±0.02 <sup>a</sup>
T <sub>1</sub>	31.36±0.04 <sup>b</sup>	27.88±0.03 <sup>b</sup>
T <sub>2</sub>	34.41±0.04 <sup>c</sup>	30.48±0.02 <sup>c</sup>
T <sub>3</sub>	37.84±0.03 <sup>d</sup>	33.63±0.01 <sup>d</sup>

a-d  $p<0.05$  Aynı sütundaki farklı harfler istatistiki açıdan farklıdır

### ***Bisküvilerin Duyusal Özellikleri***

Kontrol bisküvilerinin ve nar kabuğu tozu ilave edilmiş bisküvilerin duyusal özellikleri Tablo 7'de verilmiştir. Nar kabuğu tozu ilavesi bisküvilerin duyusal özelliklerini olumsuz yönde etkilemiştir. Nar kabuğu tozu ilaveli bisküvilerin duyusal özellikleri kontrol bisküvilerine göre duyusal panelden daha düşük puanlar almıştır ancak %4 nar kabuğu tozu ilaveli bisküvilerin duyusal panelden aldığı puanlar ile kontrol bisküvilerin duyusal panelden aldığı puanlar arasında istatistiksel olarak anlamlı bir fark bulunamamıştır ( $p>0.05$ ). Nar kabuğu tozu ilavesi %4'ü geçtikçe duyusal özelliklerde istatistiksel olarak önemli düzeyde düşüş gerçekleşmiştir ( $p<0.05$ ). Ancak, yine de duyusal panelden alınan puanların hepsi duyusal panel için orta değer olarak belirlenen 3 puanın (ne beğendim ne beğenmedim) üzerinde olduğundan bisküvi formülasyonuna %12 düzeyine kadar nar kabuğu tozu ilavesinin duyusal olarak kabul edilebilir bir ürün elde edilmesine olanak sağladığı ortaya çıkarılmıştır.

**Tablo 7.** Bisküvilerin Duyusal Özellikleri

Uygulama	Görünüş	Koku	Doku	Lezzet	Genel İzlenim
T <sub>0</sub>	4.98±0.3 <sup>a</sup>	4.92±0.2 <sup>a</sup>	4.95±0.4 <sup>a</sup>	4.94±0.2 <sup>a</sup>	4.93±0.3 <sup>a</sup>
T <sub>1</sub>	4.72±0.2 <sup>a</sup>	4.87±0.4 <sup>a</sup>	4.85±0.5 <sup>a</sup>	4.66±0.2 <sup>a</sup>	4.50±0.2 <sup>a</sup>
T <sub>2</sub>	4.01±0.2 <sup>b</sup>	3.78±0.2 <sup>b</sup>	3.54±0.4 <sup>b</sup>	3.65±0.1 <sup>b</sup>	3.82±0.3 <sup>b</sup>
T <sub>3</sub>	3.08±0.6 <sup>c</sup>	3.04±0.1 <sup>c</sup>	3.08±0.3 <sup>c</sup>	3.00±0.2 <sup>c</sup>	3.18±0.4 <sup>c</sup>

a-d p <0.05 Aynı sütundaki farklı harfler istatistiki açıdan farklıdır

## SONUÇ

Bu çalışmada yüksek antioksidan aktivite ve toplam fenolik madde içeriğine rağmen gıda endüstrisinde atık olarak nitelendirilen nar kabuğu tozunun yaygın olarak tüketilmekle birlikte besleyici değeri düşük bir gıda olan bisküviye katılma olanakları araştırılmıştır. Bisküvi formülasyonuna nar kabuğu tozu ilavesi bisküvilerin diyet lif, protein, antioksidan aktivite ve toplam fenolik madde içeriğinin istatistiksel olarak anlamlı düzeyde artışını sağlamıştır (p<0.05). Nar kabuğu tozunun glutensiz bisküvilerin protein miktarında artış sağlaması çölyak hastaları için fırıncılık ürünlerinde potansiyel bir protein kaynağı olabileceği sonucunu ortaya koymuştur. Diğer taraftan nar kabuğu tozu bisküvi hamurunun ve bisküvilerin tekstürel özelliklerinde istatistiksel olarak önemli düzeyde değişikliklere neden olmuştur. Diyet lif içeriği oldukça zengin olan nar kabuğu tozu hem bisküvilerin hem de bisküvi hamurlarının sertlik değerlerinde artışa neden olmuştur. Bisküvilerin renk değerleri de bisküvi formülasyonuna nar kabuğu tozu ilavesinden önemli düzeyde etkilenmiş, L\* ve b\* değerlerinde azalma görülürken a\* değerlerinde artış görülmüştür (p<0.05). Nar kabuğu tozu ilavesi bisküvilerin duyusal özelliklerini de önemli düzeyde etkilemiştir. Bisküvi formülasyonundaki nar kabuğu tozu oranı arttıkça duyusal panelden alınan puanlarda düşüş görülmüştür. Ancak duyusal panelden alınan tüm puanlar 3 puanın (ne beğendim ne beğenmedim) üzerinde olduğundan bisküvi formülasyonuna %12 düzeyine kadar nar kabuğu tozu ilavesinin duyusal olarak kabul edilebilir bir ürün elde edilmesine olanak sağladığı ortaya çıkarılmıştır. Bununla birlikte, bisküvi formülasyonuna daha fazla süt tozu ve farklı aroma maddelerinin ilavesiyle bisküvilerin duyusal özelliklerinin geliştirilmesi mümkün olabilir. Gelecek çalışmalar nar kabuğu tozu içeren gıdaların insan sağlığı üzerindeki pozitif etkilerini doğrulamaya yönelik olarak planlanmalıdır.

## KAYNAKLAR

AACC (2000). Method no.10-54. Approved methods of the American Association of Cereal Chemists (10th ed.). St Paul, Minnesota, USA: Association of Cereal Chemists.

Akhtar, S., Ismail, T., Fraternali, D., Sestili, P. (2015). Pomegranate peel and peel extracts: Chemistry and food features. Food Chemistry, 174, 417-425.

Aksoylu, Z., Çağındı, Ö., Köse, E. (2012). Bisküvinin Fonksiyonel Bileşenlerce Zenginleştirilmesi. Academic Food Journal/Akademik GIDA, 10(3).

Al-Maiman, S. A., Ahmad, D. (2002). Changes in physical and chemical properties during pomegranate (Punica granatum L.) fruit maturation. Food Chemistry, 76(4), 437-441.

Al-Rawahi, A. S., Rahman, M. S., Guizani, N., Essa, M. M. (2013). Chemical composition, water sorption isotherm, and phenolic contents in fresh and dried pomegranate peels. Drying Technology, 31(3), 257-263.

Al-Zoreky, N. S. (2009). Antimicrobial activity of pomegranate (Punica granatum L.) fruit peels. International Journal of Food Microbiology, 134(3), 244-248.

AOAC. (2005). Official methods of analysis (18th ed.) Arlington, VA: Association of Official Analytical Chemists.

Ashoush, I. S., Gadallah, M. G. E. (2011). Utilization of mango peels and seed kernels powders as sources of phytochemicals in biscuit. World Journal of Dairy & Food Sciences, 6(1), 35-42.

- Banerjee, C., Singh, R., Jha, A., Mitra, J. (2014). Effect of inulin on textural and sensory characteristics of sorghum based high fibre biscuits using response surface methodology. *Journal Of Food Science and Technology*, 51(10), 2762-2768.
- Galaz, P., Valdenegro, M., Ramírez, C., Nuñez, H., Almonacid, S., Simpson, R. (2017). Effect of drum drying temperature on drying kinetic and polyphenol contents in pomegranate peel. *Journal of Food Engineering*, 208, 19-27.
- Gawlik-Dziki, U., Świeca, M., Dziki, D., Baraniak, B., Tomiło, J., Czyż, J. (2013). Quality and antioxidant properties of breads enriched with dry onion (*Allium cepa* L.) skin. *Food Chemistry*, 138(2-3), 1621-1628.
- González, J. D. T., Gallo, R. T., Correa, D. A., Gallo-García, L. A., Castillo, P. M. (2018). Instrumental Assessment of Textural Parameters of Colombian Lemon Biscuits. *Contemporary Engineering Sciences*, 11(22), 1085 - 1102
- Guo, C., Yang, J., Wei, J., Li, Y., Xu, J., Jiang, Y. (2003). Antioxidant activities of peel, pulp and seed fractions of common fruits as determined by FRAP assay. *Nutrition Research*, 23(12), 1719-1726.
- Ibrahim, M. I. (2010). Efficiency of pomegranate peel extract as antimicrobial, antioxidant and protective agents. *World Journal of Agricultural Sciences*, 6(4), 338-344.
- International Organization for Standardization (ISO) 8586. (2012). *Sensory Analysis- General guidelines for the selection, training and monitoring of selected assessors and expert sensory assessors*.
- Kulkarni, A. S., Joshi, D. C. (2013). Effect of replacement of wheat flour with pumpkin powder on textural and sensory qualities of biscuit. *International Food Research Journal*, 20(2), 587.
- Kurt, H., Şahin, G. (2013). Bir Ziraat Coğrafyası Çalışması: Türkiye’de Nar (*Punica granatum* L.) Tarimi. *Marmara Coğrafya Dergisi*, (27), 551-574.
- Li, Y., Guo, C., Yang, J., Wei, J., Xu, J., Cheng, S. (2006). Evaluation of antioxidant properties of pomegranate peel extract in comparison with pomegranate pulp extract. *Food Chemistry*, 96(2), 254-260.
- Lin, D., Xiao, M., Zhao, J., Li, Z., Xing, B., Li, X., Kong, M., Li, L., Zhang, Q., Yaowen, L., Chen H., Qin, W., Wu H., Chen, S. (2016). An overview of plant phenolic compounds and their importance in human nutrition and management of type 2 diabetes. *Molecules*, 21(10), 1374.
- Meilgaard, M. C., Civille, G. V., Carr, B. T. (2016). *Sensory evaluation techniques* (5th ed., pp. 123-152). Boca Raton: CRC Press.
- Munaza, B., Prasad, S. G. M., Gayas, B. (2012). Whey protein concentrate enriched biscuits. *International Journal of Scientific and Research Publications*, 2(8), 1-4.
- Negi, P. S., Jayaprakasha, G. K. (2003). Antioxidant and antibacterial activities of *Punica granatum* peel extracts. *Journal of Food Science*, 68(4), 1473-1477.
- Nizamloğlu, N. M., Nas, S. (2010). Meyve ve sebzelerde bulunan fenolik bileşikler; yapıları ve önemleri. *Gıda Teknolojileri Elektronik Dergisi*, 5(1), 20-35.
- Oluwamukomi, M. O., Oluwalana, I. B., Akinbowale, O. F. (2011). Physicochemical and sensory properties of wheat-cassava composite biscuit enriched with soy flour. *African Journal of Food Science*, 5(2), 50-56.
- Özdemir, H., Soyer, A., Tağı, Ş., & Turan, M. (2014). Nar kabuğu ekstraktının antimikrobiyel ve antioksidan aktivitesinin köfte kalitesine etkisi. *GIDA*, 39(6), 355-362.
- Pasqualone, A., Bianco, A. M., Paradiso, V. M., Summo, C., Gambacorta, G., Caponio, F. (2014). Physico-chemical, sensory and volatile profiles of biscuits enriched with grape marc extract. *Food Research International*, 65, 385-393.
- Raymundo, A., Fradinho, P., Nunes, M. C. (2014). Effect of Psyllium fibre content on the textural and rheological characteristics of biscuit and biscuit dough. *Bioactive Carbohydrates And Dietary Fibre*, 3(2), 96-105.

- Saha, S., Gupta, A., Singh, S. R. K., Bharti, N., Singh, K. P., Mahajan, V., Gupta, H. S. (2011). Compositional and varietal influence of finger millet flour on rheological properties of dough and quality of biscuit. *LWT-Food Science and Technology*, 44(3), 616-621.
- Schaafsma, A., Pakan, I. (1999). Short term effects of a chicken egg shell powder enriched dairy-based products on bone mineral density in persons with osteoporosis or osteopenia. *Bratislavske Lekarske Listy*, 100(12), 651-656.
- Singh, A., Rana, I., Sahi, N. C., Lohani, U. C., Chand, K. (2012). Optimization of process variables for preparation of apple pomace-black soyflour based biscuits. *International Journal of Food, Agriculture & Veterinary Sciences*, 2(1), 101-106.
- Singh, P., Singh, R., Jha, A., Rasane, P., Gautam, A. K. (2015). Optimization of a process for high fibre and high protein biscuit. *Journal of Food Science And Technology*, 52(3), 1394-1403.
- Świeca, M., Sęczyk, Ł., Gawlik-Dziki, U., Dziki, D. (2014). Bread enriched with quinoa leaves–The influence of protein–phenolics interactions on the nutritional and antioxidant quality. *Food Chemistry*, 162, 54-62.
- Uzuner, S., Onsekizoglu, P., Acar, J. (2011). Effects of processing techniques and cold storage on ellagic acid concentration and some quality parameters of pomegranate juice. *GIDA/The Journal of FOOD*, 36(5).
- Wang, R., Zhou, W. (2004). Stability of tea catechins in the bread making process. *Journal of Agricultural and Food Chemistry*, 52, 8224–8229.
- Yadav, R. B., Yadav, B. S., Chaudhary, D. (2011). Extraction, characterization and utilization of rice bran protein concentrate for biscuit making. *British Food Journal*, 113(9), 1173-1182.
- Ye, X. Y., Wang, H. X., Liu, F., Ng, T. B. (2000). Ribonuclease, cell-free translation-inhibitory and superoxide radical scavenging activities of the iron-binding protein lactoferrin from bovine milk. *The International Journal Of Biochemistry & Cell Biology*, 32(2), 235-241. Cemeroglu B, 2010. *Gıda Analizleri, Gıda Teknolojisi Yayınları Derneği Yayınları*, No:39, 2. Baskı Ankara.
- Yurtseven, E., Baran, H. Y. (2000). Sulama suyu tuzluluğu ve su miktarlarının brokkolide (*Brassica oleracea botrytis*) verim ve mineral madde içeriğine etkisi. *Turkish Journal of Agriculture and Forestry*, 24(2), 185-190.



# Kahramanmaraş Sutcu Imam University

## Journal of Engineering Sciences



Geliş Tarihi : 14.08.2020  
Kabul Tarihi : 23.10.2020

Received Date : 14.08.2020  
Accepted Date : 23.10.2020

### TİTANYUM DİOKSİT SENTEZİ (TiO<sub>2</sub>)

### SYNTHESIS OF TITANIUM DIOXIDE (TiO<sub>2</sub>)

Serdar GÖÇER<sup>1</sup> (ORCID: 0000-0003-0443-8045)

Binnaz Zeynep ZAIMOĞLU<sup>1</sup> (ORCID: 0000-0002-9573-4781)

Kevser CIRIK<sup>2\*</sup> (ORCID: 0000-0002-1756-553X)

<sup>1</sup> Department of Environmental Engineering, Çukurova University, Adana, Turkey

<sup>2</sup> Department of Environmental Engineering, Kahramanmaraş Sutcu Imam University, Kahramanmaraş, Turkey

\*Sorumlu Yazar / Corresponding Author: Kevser CIRIK, kcirik@ksu.edu.tr

#### ÖZET

Titanyum dioksit (TiO<sub>2</sub>), çevre dostu, sentezi kolay, stabil ve ucuz bir katalizör olarak, çoğunlukla su arıtımı gibi çevresel iyileştirme amaçlı hafif aktiviteye sahip bir katalizör olarak kabul edilmektedir. Bu çalışmada, TiO<sub>2</sub>, kristal yapıları belirlemek için X-Ray difraksiyon cihazı (XRD), enerji dağıtıcı X-ışını spektroskopisi (EDX) ile donatılmış taramalı elektron mikroskobu (SEM), parçacık boyutunu belirlemek için BET analizi, ve bağları belirlemek için FT-IR analizi kullanılarak sentezlenmiş ve karakterize edilmiştir. Sonuçlar, 2θ piklerde 25°, 38°, 48°'de TiO<sub>2</sub> nanopartiküllerinin varlığı tespit edilirken, 65° ve 70° piklerde TiO tespit edildiğini göstermektedir. EDX analizi sonuçlarına göre; Ti, O, Au ve C elementleri belirlenmiştir. FT-IR analizine göre, 450 cm<sup>-1</sup>'de oluşan pik TiO<sub>2</sub> varlığını gösterir. BET analizine göre; TiO<sub>2</sub>'nin yüzey alanı 65 m<sup>2</sup>/g olarak belirlendi ve bu ticari TiO<sub>2</sub>'den (40 m<sup>2</sup>/g) önemli ölçüde yüksektir. Sonuçlar, literatürde kullanılanlara göre azalan sıcaklıklarda TiO<sub>2</sub> elde etmenin mümkün olduğunu göstermektedir. Ek olarak, oda sıcaklığında sentezlenen TiO<sub>2</sub> karakterizasyonu, yüksek sıcaklıklarda (>400C°) gerçekleştirilen önceki çalışma sonuçlarından elde edilen sonuçlarla karşılaştırıldığında benzerdir.

**Anahtar Kelimeler:** Titanyum Dioksit, Nanopartiküller, Titanyum Dioksit Sentezi

#### ABSTRACT

Titanium dioxide (TiO<sub>2</sub>) is regarded as an environmentally friendly, easy-to-synthesis, stable and inexpensive catalyst, often as a mildly active catalyst for environmental improvement purposes such as water treatment. In this study, TiO<sub>2</sub> was synthesized and characterized using an X-Ray diffraction instrument (XRD) to determine the crystal structures, scanning electron microscopy (SEM), equipped with energy-dispersive X-ray spectroscopy (EDX), BET analysis to determine particles size, and FT-IR analysis to determine bonds TiO<sub>2</sub>. Results show that while the presence of TiO<sub>2</sub> nanoparticles at 25°, 38°, 48° at 2θ peaks was detected, TiO was detected at 65° and 70° peaks. According to the results of EDX analysis; Ti, O, Au, and C elements are detected. According to FT-IR analysis, the peak formed at 450 cm<sup>-1</sup> shows the presence of TiO<sub>2</sub>. According to BET analysis; the surface region of TiO<sub>2</sub> was identified as 65 m<sup>2</sup>/g which was significantly higher than that of commercial TiO<sub>2</sub> (40 m<sup>2</sup>/g). The results show that it is acceptable to achieve TiO<sub>2</sub> at decrease temperatures according to those used in the literature. Additionally, the characterization of synthesized TiO<sub>2</sub> at room temperature is similar compared to the results obtained from previous study results that have been conducted under high temperatures (>400°C).

**Keywords:** Titanium Dioxide, Nanoparticles, Titanium Dioxide Synthesis

\*Sorumlu Yazar / Corresponding Author: Kevser CIRIK, kcirik@ksu.edu.tr

**To Cite:** GOCER S., ZAIMOGLU, Z., & CIRIK, K., (2020). TİTANYUM DİOKSİT SENTEZİ (TiO<sub>2</sub>). *Kahramanmaraş Sütçü İmam Üniversitesi Mühendislik Bilimleri Dergisi*, 23(4), 219-226.

## 1. INTRODUCTION

Titanium dioxide nanoparticles are among the most used nanomaterials due to their high stability, anti-corrosion properties, surface activities, and photocatalytic properties. These properties appear as stable for the extensive use of TiO<sub>2</sub> substances in diverse areas including light activity, hydrogen production, and such as wastewater treatment. (Burke, A., et al., 2008; Nakata, K., et al., 2013; G.L. Chiarello, et al., 2017; W. Zhou, et al., 2014; Z. Xing, et al., 2018). In recent years, optical and electronic characteristics of nanomaterials, which become severely size dependant have attracted attention to the preparation of nanoparticle semi-conductors (M. Tomkiewicz, 2000). Titanium nanoparticles with very thin dimensions are encouraging in many practices such as wastewater treatment, adsorbents, and catalytic fields (G. Ramakrishna, 2003; M.M. Rahman, et al., 1999; E. Pelizzetti, et al., 1993). In almost all of these conditions, when the particle size is reduced greatly, due to the large surface area, some recent optical properties can be expected (S. Sahni, et al., 2007). The synthesis of titanium dioxide nanoparticles consists of four different methods; these, sol-gel process (Q. Zhang, L. Gao, 2003), hydrothermal methods (P.D. Cozzoli, et al., 2003), solvothermal methods (C.S. Kim, et al., 2003), and emulsion precipitation (G. Ramakrishna, H.N. Ghosh, et al., 2003). Many of them were succeeded by synthesizing high purity of (>99%) TiO<sub>2</sub>. However, it is important to be easily reproducible at the industrial level by avoiding dangerous reagents (Zadeh, E.K, et al., 2017; Mezni, A., et al., 2017; Ojeda, M., et al., 2017; Lusvardi, G., et al., 2017). By using this approach, the purpose of this study was the synthesis and characterization of TiO<sub>2</sub> nanoparticles by avoiding harmful chemicals.

In this study, TiO<sub>2</sub> was synthesized in a procedure containing 50 mL titanium isopropoxide (C<sub>12</sub>H<sub>28</sub>O<sub>4</sub>Ti), ≥99.8, 200 mL H<sub>2</sub>O, and 1gr CO(NH<sub>2</sub>)<sub>2</sub>. The materials characterization was performed using an X-Ray diffraction instrument (XRD) to determine the crystal structures of TiO<sub>2</sub> particle, SEM, EDX, and BET analysis to determine particle size and crystal properties, FT-IR analysis to determine chemical bonds TiO<sub>2</sub>.

## 2. MATERIAL AND METHODS

### 2.1. Preparations of Titanium Dioxide (TiO<sub>2</sub>)

The procedure reported in the literature have been tested and (Lusvardi, G., et al., 2017). TiO<sub>2</sub> synthesis was carried out with the best, simplest, and cheapest procedure. The used reagents are titanium isopropoxide (C<sub>12</sub>H<sub>28</sub>O<sub>4</sub>Ti), ≥99.8, and urea (CO(NH<sub>2</sub>)<sub>2</sub>) (Lusvardi, G., et al., 2017). The reagents used for TiO<sub>2</sub> synthesizes are given in Table 1.

**Table 1. Reagents for TiO<sub>2</sub> Synthesis**

Compounds	Amounts
C <sub>12</sub> H <sub>28</sub> Ti	50mL
H <sub>2</sub> O	200mL
CO(NH <sub>2</sub> ) <sub>2</sub>	1gr

Distilled water (H<sub>2</sub>O) and CO(NH<sub>2</sub>)<sub>2</sub> were placed in a beaker and mixed for five minutes with the aid of a magnetic stirrer. Then, C<sub>12</sub>H<sub>28</sub>Ti was added drop by drop to this solution, and stirring continued for thirty minutes. This solution was kept in a water bath at 90 C° for one hour. Finally, the product was separated by drying at 80 C° for 12 hours. (Lusvardi, G., et al., 2017).

### 2.2. Analyses of Nanoparticles

#### 2.2.1. X-Ray diffraction (XRD)

The diffraction patterns of synthesized TiO<sub>2</sub> nanoparticle substances were achieved with a high-resolution electron microscope (HRTEM, Tecnai G2, F30). X-ray diffraction (XRD) diffraction was made using a Miniflex II model (Malik S., et al. 2018).

### 2.2.2. Scanning electron microscopy-energy distribution spectrophotometer (SEM-EDX)

The samples were coated with the gold plated mixture and given to the SEM (Carl Zeiss, EVO 50 model, Germany) and EDX (Bruker AXS Microanalysis GmbH, Germany) devices. Inorganic chemical composition was also determined using an EDX (EDX, analyzer to determine the inorganic composition).

### 2.2.3. Fourier transform infrared spectrophotometer-attenuated total reflection (FTIR-ATR) analysis

Characterization of important functional groups of metabolites was measured using the FTIR-ATR device (Perkin Elmer Spectrum 400, Germany) located in the KSU ÜSKİM laboratory. The collected nanoparticle substances were dried at 50°C for 24 hours before FT-IR measurements. Characterization of functional groups were determined according to the procedures given by Şahinkaya et al. (2018) and Hu et al. (2013).

### 2.2.4. BET analysis

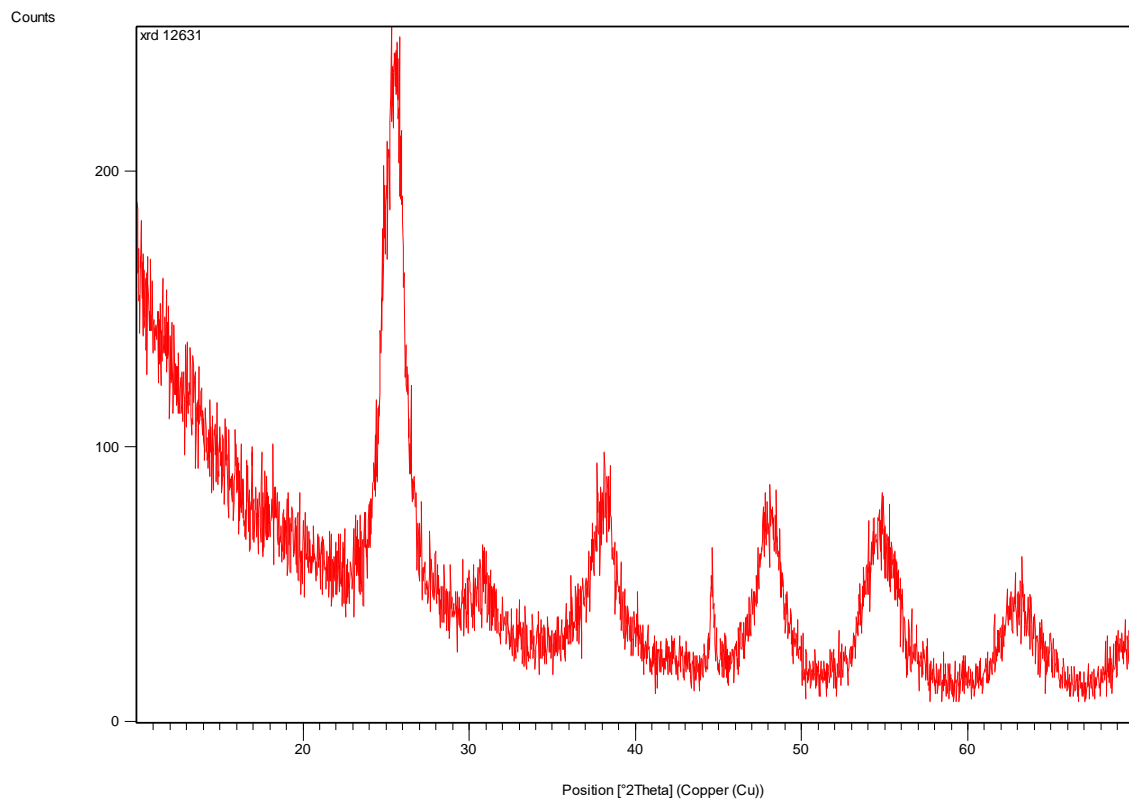
The surface area and nanoparticle size of the synthesized titanium nanoparticles were analyzed by the BET surface area. The BET surface area was determined by N<sub>2</sub> gas using a Tristar 3000. Samples were dried under N<sub>2</sub> gas at 110 C° 15 hours before BET analysis (Martinson, C. A., et al. 2009).

## 3. RESULTS AND DISCUSSION

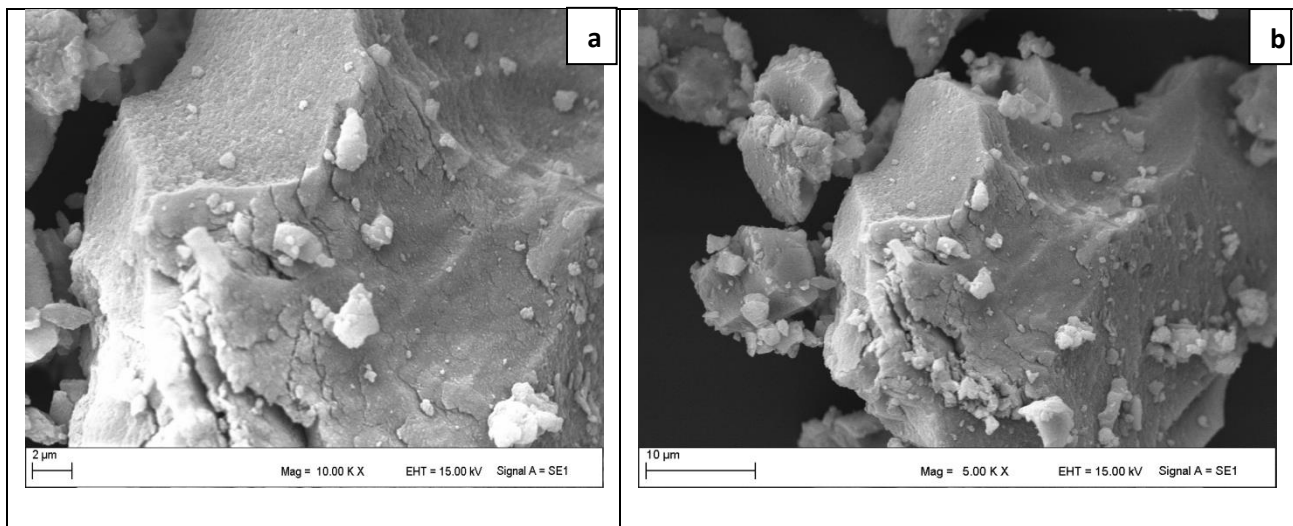
### 3.1. Characterization of Synthesized TiO<sub>2</sub> Particles

TiO<sub>2</sub> is a strong, relatively cheap, easy to prepare, and non-toxic material (Mulmi et al., 2004). It consists of three different crystal structures, anatase, rutile, and brookite (Sekiya et al., 2004). The XRD plot of the prepared TiO<sub>2</sub> nanoparticle shows the presence of very large peaks. Large peaks either show particles with very small crystal size or show that the particles are semi-crystal in nature (C.L. Yeha, et al., 2004). XRD analysis of the synthesized TiO<sub>2</sub> nanoparticles was done in the range of 2θ 20-80. The XRD analysis of TiO<sub>2</sub> nanoparticles is shown in Figure 1. According to the XRD results of the synthesized titanium dioxide nanoparticles, the presence of peak points indicates that there is a crystal structure. Although the presence of the peaks symbolizing TiO<sub>2</sub> was detected, significant peaks could not be obtained. In addition, the dominant peaks observed at 45° and 65° indicate the presence of titanium oxide. While the presence of TiO<sub>2</sub> nanoparticle peaks was detected at 25°, 38°, 48° at 2θ, TiO nanoparticle substance was detected at 65° and 70° peaks (Figure 1). The obtained results are similar to the literature (Vijayalakshmi, R., et al. 2012, Abdulmajeed, B.A., et al. 2019). It is observed titanium dioxide nanoparticle substance has been successfully synthesized.

Figure 2 shows the SEM images of the synthesized TiO<sub>2</sub>. The EDX analysis of TiO<sub>2</sub> is shown in Figure 3A. SEM and EDX were used to qualitatively determine the morphology, size, and composition of the synthesized titanium dioxide. At the selected area EDX spectrum shows a strong signal in the titanium area and confirms the formation of TiO<sub>2</sub>. In this case, the nanoparticle substances are obtained to adhere to each other. Similar to our results, Srikanth et al. (2018) found that pure crystalline particles were in the form of spherical and rod-shaped clusters and pellets. At the same time, to obtain chemical compounds and surface atom distributions of the synthesized TiO<sub>2</sub>, EDX spectra were performed in the selected areas on the surface of the nanoparticle substance. EDX elemental analysis was performed to identify the chemical components of nanoparticle substances. The presence and formation of titanium dioxide nanoparticle material were determined in the EDX spectrum region in the selected area. According to the results of EDX analysis; Ti, O, Au, and C elements are detected as shown in Figure 3B.



**Figure 1.** X-ray diffraction (XRD) of Titanium Dioxide ( $\text{TiO}_2$ ) particles





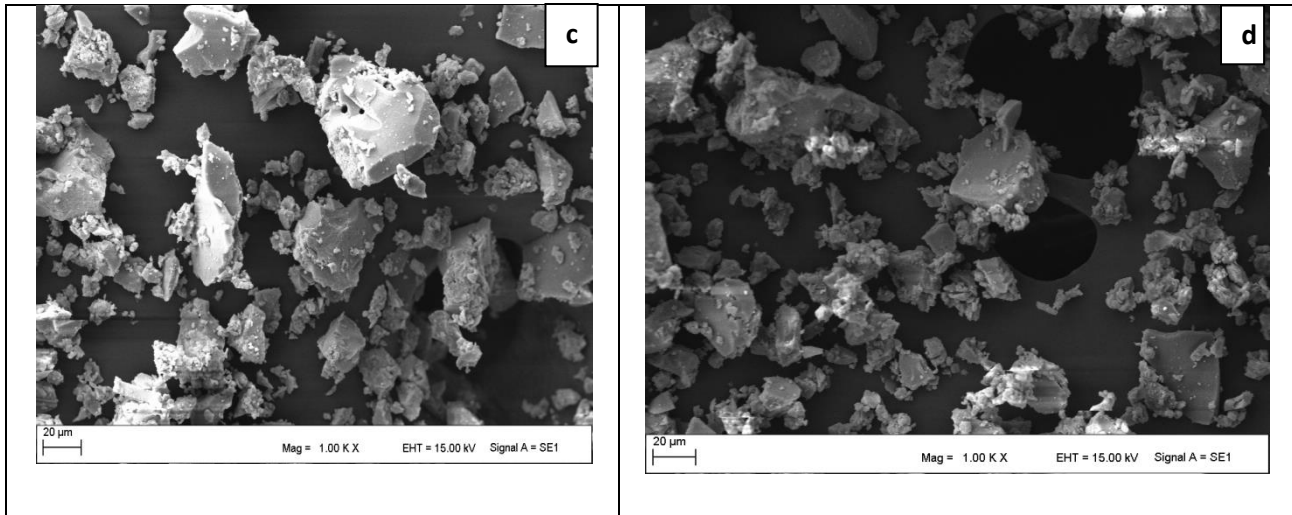


**Figure 2.** SEM images of different sizes of Titanium Dioxide (TiO<sub>2</sub>) particles a) 10kx, b) 5kx, c) 1kx, d) 1kx

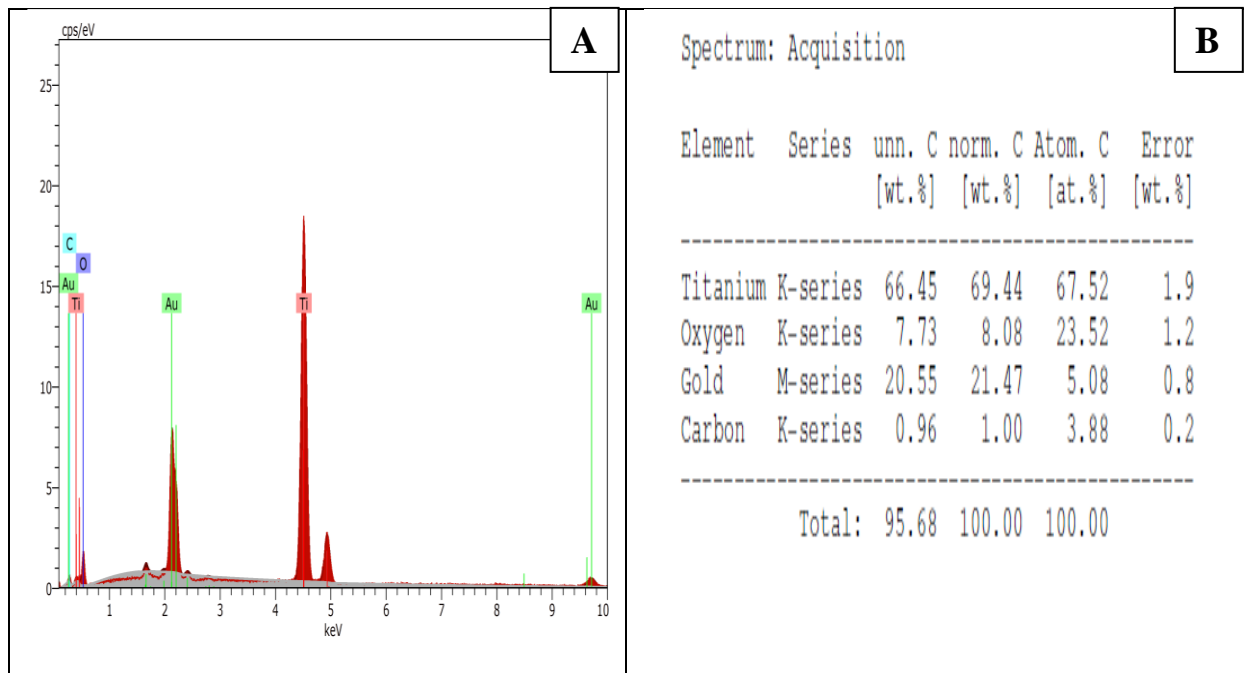


**Figure 3. A:** EDX results of Titanium Dioxide (TiO<sub>2</sub>) particles; **B:** EDX-Element content results of Titanium Dioxide (TiO<sub>2</sub>) particles

Due to its nanoparticle structure, Ti and O are relatively higher than other elements. According to EDX results, the titanium content of the synthesized nanoparticle substance was relatively high (Figure 3B).

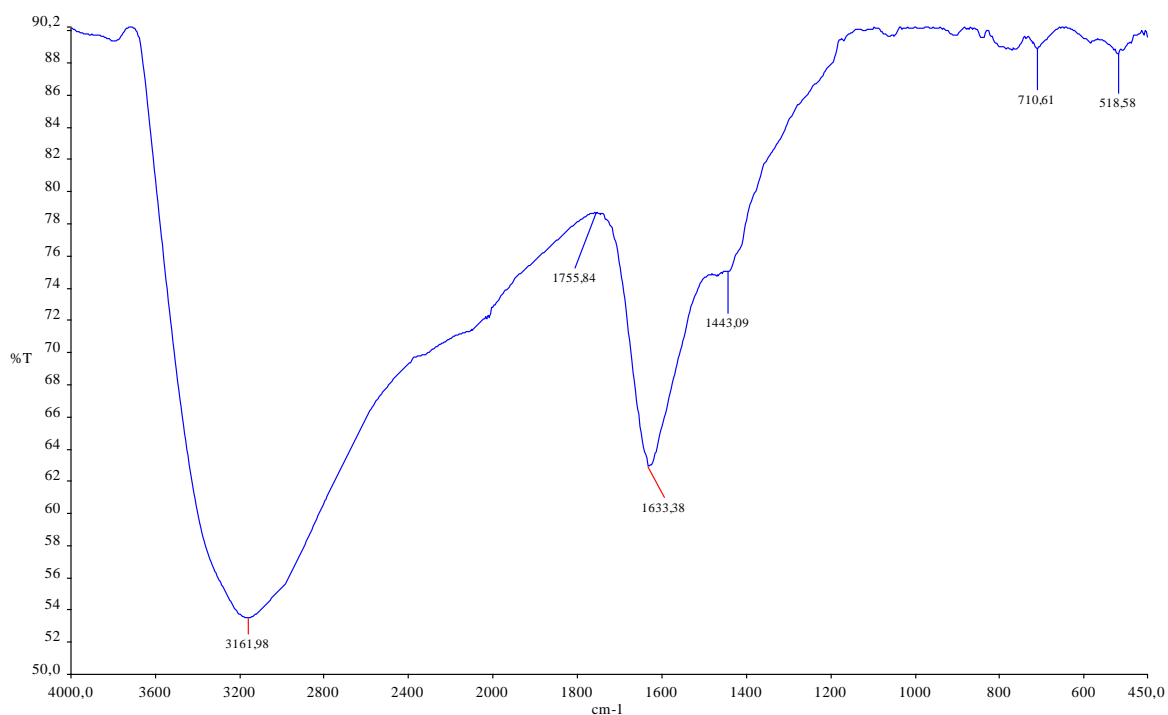


**Figure 4.** Titanium dioxide ( $\text{TiO}_2$ ) FT-IR spectrum

FT-IR spectrum analysis was achieved to determine the characterization and chemical structure of the synthesized nanoparticle substances. The FT-IR spectrum of titanium dioxide is shown in Figure 4. The peak points obtained in the synthesized nanoparticle materials have been shown to be at 3200, 1800, 1600, 1400, 650, and 450  $\text{cm}^{-1}$ . The band at 3421  $\text{cm}^{-1}$  corresponds to the weak stretching vibration of the surface hydroxyl groups. The peaks at 1415 and 1359  $\text{cm}^{-1}$  indicate the  $-\text{COO}-$  groups (Gao et al., 2016; Madhavi et al., 2013). Similar results were obtained in this study. Jose A.A et al. (1999) reported that the strong peak in the range of 880 and 450  $\text{cm}^{-1}$  confirmed the presence of  $\text{TiO}_2$  nanoparticle material. They reported that the peak observed at 3391  $\text{cm}^{-1}$  revealed the presence of hydroxyl, possibly due to the lack of recording of the spectra in place and some reabsorption of water from the ambient atmosphere. In the same study, they reported that the peak water of 1638  $\text{cm}^{-1}$  was associated with hydroxyl groups of water. The peak formed at 450  $\text{cm}^{-1}$  indicates the presence of titanium dioxide.

The surface area of nanoparticle substances was identified by the classical BET method. BET analysis was performed to determine the pore sizes and surface area of nanoparticle materials obtained as a result of synthesis. According to the results obtained; The surface area of titanium dioxide nanoparticle material was determined as 65  $\text{m}^2/\text{g}$ . Similar to study results performed by Hussain et al. (2010) surface area of  $\text{TiO}_2$  nanoparticle material was 60-66  $\text{m}^2/\text{g}$ . The results of this study support the findings obtained from other literature studies.

#### 4. CONCLUSION

Synthesized  $\text{TiO}_2$  characterization was carried out using XRD, SEM, and EDX, FT-IR, BET techniques. Results show that the presence of  $\text{TiO}_2$  nanoparticles was detected at 25°, 38°, 48° at  $2\theta$  peaks, while  $\text{TiO}$  nanoparticle substance was detected at 65° and 70° peaks. According to the results of EDX analysis; Ti, O, Au, and C elements are mainly detected. According to FT-IR analysis, the peak formed at 450  $\text{cm}^{-1}$  shows the presence of titanium dioxide. According to BET analysis; the surface area of titanium dioxide nanoparticle substance was determined as 65  $\text{m}^2/\text{g}$  which was significantly higher than that of commercial  $\text{TiO}_2$  (40  $\text{m}^2/\text{g}$ , a non-porous material). The use, research, and development of titanium dioxide nanoparticle material in environmental applications will contribute to the literature.

#### 5. ACKNOWLEDGE

This article was supported by the Scientific Research Unit of Çukurova University. Project No: FDK-2019-11782.

## 6. REFERENCES

- Abdulmajeed, B.A., Hamadullah, S., & Allawi, F.A. (2019). Synthesis and Characterization of Titanium Dioxide Nanoparticles under Different pH Conditions. *Journal of Engineering*, 25(1), 40-50.
- Burke, A., Ito, S., Snaith, H., Bach, U., Kwiatkowski, J., & Gratzel, M. (2008) The function of a TiO<sub>2</sub> compact layer in dye-sensitized solar cells incorporating “planar” organic dyes, *Nano Lett.* 8 977–981.
- Chiarello, G.L., Dozzi, M.V., & Selli, E. (2017) TiO<sub>2</sub>-based materials for photocatalytic hydrogen production, *J. Energy Chem.* 26 250–258.
- Cozzoli, P.D., Kornowski, A., & Weller, H.A (2003). Low-temperature synthesis of soluble and processable organic-capped anatase TiO<sub>2</sub> nanorods. *Journal of the American chemical society*, 125(47), 14539-14548.
- Gao, P., Liu, Z., Sun, D.D., & Ng, W.J. (2014). The efficient separation of surfactant-stabilized oil-water emulsions with a flexible and superhydrophobic graphene–TiO<sub>2</sub> composite membrane. *Journal of Materials Chemistry A*, 2(34), 14082-14088.
- Hu, Y., Liu, Z., Xu, J., Huang, Y., & Song, Y. (2013). Evidence of pressure enhanced CO<sub>2</sub> storage in ZIF-8 probed by FTIR spectroscopy. *Journal of the American Chemical Society*, 135(25), 9287-9290.
- Hussain, M., Ceccarelli, R., Marchisio, D. L., Fino, D., Russo, N., & Geobaldo, F. (2010). Synthesis, characterization, and photocatalytic application of novel TiO<sub>2</sub> nanoparticles. *Chemical Engineering Journal*, 157(1), 45-51.
- Josea A.N., Juan, J.T., Pablo, D., Javier, R.P., Diana, R., & Marta, I.L. (1999). *Appl. Catal., A Gen.* 178, p.191.
- Kim, C. S., Moon, B. K., Park, J. H., Choi, B. C., & Seo, H. J. (2003). Solvothermal synthesis of nanocrystalline TiO<sub>2</sub> in toluene with surfactant. *Journal of Crystal Growth*, 257(3-4), 309-315.
- Lusvardi, G., Barani, C., Giubertoni, F., & Paganelli, G. (2017). Synthesis and Characterization of TiO<sub>2</sub> Nanoparticles for the Reduction of Water Pollutants. *Materials*, 10(10), 1208.
- Madhavi, V., Prasad, T. N. V. K. V., Reddy, A. V. B., Reddy, B. R., & Madhavi, G. (2013). Application of phyto-genic zero-valent iron nanoparticles in the adsorption of hexavalent chromium. *Spectrochimica Acta Part A: Molecular and Biomolecular Spectroscopy*, 116, 17-25.
- Malik, S.N., Ghosh, P.C., Vaidya, A.N., & Mudliar, S.N. (2018). Catalytic Ozone pretreatment of complex textile effluent using Fe<sup>2+</sup> and zero-valent iron nanoparticles. *Journal of hazardous materials*.
- Martinson, C.A., & Reddy, K.J. (2009). Adsorption of arsenic (III) and arsenic (V) by cupric oxide nanoparticles. *Journal of Colloid and Interface Science*, 336(2), 406-411.
- Mezni, A., Saber, N.B., Ibrahim, M.M., Kemary, M.E., Aldalbahi, A., Smiri, L.S., & Altalhi, T. (2017). Facile synthesis of highly thermally stable TiO<sub>2</sub> photocatalysts. *New J. Chem.* , 41, 5021–5030
- Mulmi DD., Sekiya T., Kamiya N., Kurita S., Murakami Y., & Kodaira T. (2004). Optical and electric properties of Nb-doped anatase TiO<sub>2</sub> single crystal, *J. Phys. Chem. Solids* 65: 1181-1185.
- Nakata, K., & Fujishima, A. (2013). TiO<sub>2</sub> photocatalysis: design and applications, *J. Photochem. Photobiol. C* 13, 169–189.
- Ojeda, M., Kumar, D.K., Chen, B., Xuan, J., Maorto-Valer, M.M., Leung, D.Y.C., & Wang, H. (2017). Polymeric templating synthesis of Anatase TiO<sub>2</sub> nanoparticles from low-cost inorganic titanium sources. *Chem. Select*, 2, 702–706.
- Pelizzetti, E., & Minero, C. (1993). Mechanism of the photo-oxidative degradation of organic pollutants over TiO<sub>2</sub> particles. *Electrochimica acta*, 38(1), 47-55.

- Rahman, M. M., Krishna, K. M., Soga, T., Jimbo, T., & Umeno, M. (1999). Optical properties and X-ray photoelectron spectroscopic study of pure and Pb-doped TiO<sub>2</sub> thin films. *Journal of Physics and Chemistry of Solids*, 60(2), 201-210.
- Ramakrishna, G., & Ghosh, H.N. (2003). Optical and photochemical properties of sodium dodecylbenzenesulfonate (DBS)-capped TiO<sub>2</sub> nanoparticles dispersed in nonaqueous solvents. *Langmuir*, 19(3), 505-508.
- Sahinkaya, E., Sahin, A., Yurtsever, A., & Kitis, M. (2018). Concentrate minimization and water recovery enhancement using pellet precipitator in a reverse osmosis process treating textile wastewater. *Journal of environmental management*, 222, 420-427.
- Sahni, S., Reddy, S. B., & Murty, B. S. (2007). Influence of process parameters on the synthesis of nano-titania by sol-gel route. *Materials Science and Engineering: A*, 452, 758-762.
- Sekiya T., Yagisawa T., Kamiya N., Mulmi DD., Kurita S., Murakami Y., & Kodaira T. (2004). Defects in anatase TiO<sub>2</sub> single crystal controlled by heat treatments. *J. Phys. Soc. Jpn.* 73: 703-710.
- Srikanth, R., & Rao, H. J. (2018). Synthesis and Characterization of Titanium dioxide (TiO<sub>2</sub>) Nanoparticles. *Research Journal Of Pharmaceutical Biological And Chemical Sciences*, 9(4), 313-319.
- Tomkiewicz, & M. Catal. (2000). *Today* 58, 115.
- Vijayalakshmi, R., & Rajendran, V. (2012). Synthesis and characterization of nano-TiO<sub>2</sub> via different methods. *Archives of Applied Science Research*, 4(2), 1183-1190.
- Wu, M., Lin, G., Chen, D., Wang, G., He, D., Feng, S., & Xu, R. (2002). Sol-hydrothermal synthesis and hydrothermally structural evolution of nanocrystal titanium dioxide. *Chemistry of materials*, 14(5), 1974-1980.
- Xing, Z., Zhang, J., Cui, J., Yin, J., Zhao, T., Kuang, J., Xiu, Z., Wan, N., & Zhou, W. (2018). Recent advances in floating TiO<sub>2</sub>-based photocatalysts for environmental application, *Appl. Catal. B* 225,452-467.
- Yeha C.L., Yeh, S.H., & Ma, H.K. (2004) *Powder Technol.* 145-1.
- Zadeh, E.K., Zebarjad, S.M., & Janghorban, K. (2017). Optimization of synthesis conditions of N-doped TiO<sub>2</sub> nanoparticles using Taguchi robust design. *Mater. Chem. Phys.* 201, 69-77.
- Zhang, Q., & Gao, L. (2003). Preparation of oxide nanocrystals with tunable morphologies by the moderate hydrothermal method: insights from rutile TiO<sub>2</sub>. *Langmuir*, 19(3), 967-971.
- Zhou, W., Li, W., Wang, J.Q., Qu, Y., Yang, Y., Xie, Y., Zhang, K., Wang, L., Fu, H., & Zhao, D. (2014). Ordered mesoporous Black TiO<sub>2</sub> as highly efficient hydrogen evolution photocatalyst, *J. Am. Chem. Soc.* 136, 9280-9283.



# Kahramanmaraş Sütçü İmam University

## Journal of Engineering Sciences



Geliş Tarihi : 25.08.2020  
Kabul Tarihi : 10.09.2020

Received Date : 25.08.2020  
Accepted Date : 10.09.2020

### TEL ÇEKME İŞLEMİNDE KALIP KALİBRASYON BÖLGESİ UZUNLUĞUNUN 1045 ÇELİK TEL MUKAVEMETİ ÜZERİNE OLAN ETKİSİNİN İNCELENMESİ

#### INVESTIGATING EFFECT OF BEARING LENGTH ON TENSILE STRENGTH OF 1045 STEEL IN WIRE DRAWING OPERATION

*Ekrem ÇELİK<sup>1</sup>* (ORCID: 0000-0002-2641-1049)  
*Fatih ÖZEN<sup>2\*</sup>* (ORCID: 0000-0002-2915-8456)  
*Erdoğan İLHAN<sup>3</sup>* (ORCID: 0000-0002-3873-1680)  
*Salim ASLANLAR<sup>4</sup>* (ORCID: 0000-0001-6676-110X)

<sup>1</sup> Sakarya Uygulamalı Bilimler Üniversitesi, Lisansüstü Eğitim Enstitüsü, Metalürji ve Malzeme Mühendisliği Bölümü, Sakarya.

<sup>2</sup> Batman Üniversitesi, Teknoloji Fakültesi, Makine ve İmalat Mühendisliği Bölümü, Batman.

<sup>3</sup> Sakarya Uygulamalı Bilimler Üniversitesi, Adapazarı Meslek Yüksekokulu, Makine ve Metal Teknolojileri Bölümü, Sakarya.

<sup>4</sup> Sakarya Uygulamalı Bilimler Üniversitesi, Teknoloji Fakültesi, Metalürji ve Malzeme Mühendisliği Bölümü, Sakarya.

\*Sorumlu Yazar / Corresponding Author: Fatih ÖZEN, fatih.ozen@batman.edu.tr

#### ÖZET

Bu çalışmada, tel çekme işleminde kalibrasyon uzunluğunun çekme mukavemeti üzerine olan etkisi incelenmiştir. Kalibrasyon bölgesinin etkisini iki farklı redüksiyon oranı ve filmaşın çapı kullanılarak gösterilmiştir. Elde edilen sonuçlara göre, kalibrasyon bölge uzunluğu arttıkça mukavemet artışı gözlemlenmiştir. Ancak, kalibrasyon boyunun uzun olması üretim esnasında çeşitli imalat problemlerine sebebiyet vermiştir. Çapsal mikrosertlik dağılımları ise kalibrasyon boyu arttıkça aralarındaki farklarda da artış gözlemlenmiştir. Mikrosertliğin artmasının esas sebebinin kalibrasyon boyunun artmasıyla elde edilen yüksek sürtünme kuvvetinin oluşturduğu deformasyon sertleşmesidir.

**Anahtar Kelimeler:** Tel çekme, kalibrasyon uzunluğu, deformasyon sertleşmesi, tel çekme kalıbı.

#### ABSTRACT

In this work, effect of bearing length on tensile strength was investigated. The influence of the bearing length is illustrated using two different reduction ratios and wire diameters. According to the results, the increase in strength was observed as the length of the bearing zone increased. However, the long bearing length caused various manufacturing problems during production. Microhardness distributions in wire cross section, on the other hand, increased as the length of bearing increased. The main reason for the increase of microhardness is the deformation hardening caused by the high friction force obtained by increasing the bearing length.

**Keywords:** Wire drawing, bearing length, deformation hardening, wire drawing die.

\*Sorumlu Yazar / Corresponding Author: Fatih ÖZEN, fatih.ozen@batman.edu.tr

**ToCite:** ÇELİK, E., ÖZEN, F., İLHAN E., & ASLANLAR, S., (2020). TEL ÇEKME İŞLEMİNDE KALIP KALİBRASYON BÖLGESİ UZUNLUĞUNUN 1045 ÇELİK TEL MUKAVEMETİ ÜZERİNE OLAN ETKİSİNİN İNCELENMESİ. *Kahramanmaraş Sütçü İmam Üniversitesi Mühendislik Bilimleri Dergisi*, 23(4), 227-235.

#### INTRODUCTION

Wire drawing is the most common method used to manufacture wire. It is a cold forming process. It is an indispensable technique for the industry because the wire diameters are obtained with high tolerance and low surface roughness, low forming cost and being a serial process (Nilsson & Olsson, 2011). Wire drawing is done by processing semi-finished product called as alloy wire rod sets.

It has usage areas in numerous applications such as welding wires, brake wire, bridge ropes. Defects occurring during production significantly affect the strength of the wire. At the same time, the design of the die has a great influence on wire strength. The strength obtained in pearlitic steels can be increased up to 7 GPa (Wei et al., 2020).

Wire rod is a product obtained after hot processing. After the hot process, a oxide layer forms on the wire rod surface. The presence of oxide layer causes mold wear during wire drawing. For this reason, various deoxidation processes are carried out. Also, Wire circumference is covered with various lubricants to minimize mold wear during wire drawing operation (Gillström & Jarl, 2007). High wear during wire drawing causes friction force that rises unevenly and induces wire breaks.

Plastic deformation and friction forces must be controlled during wire drawing operation. The bearing length in the wire drawing die is of high importance in controlling of the friction forces. If bearing length is long, friction forces increases that causes undesired cases such as breakage and stripping of the outer covering layer. On the other hand, If the bearing length is short, wire rod wire that spring backs cannot provides desired tolerance size (Korchunov et al., 2014) Also, the bearing length plays an important role in the strength of the drawn wire, significantly controlling the amount of deformation hardening. In this study, the effect of the bearing length on the strength and hardness of the drawn wire was investigated. The optimum bearing length were determined.

### MATERIAL AND METHOD

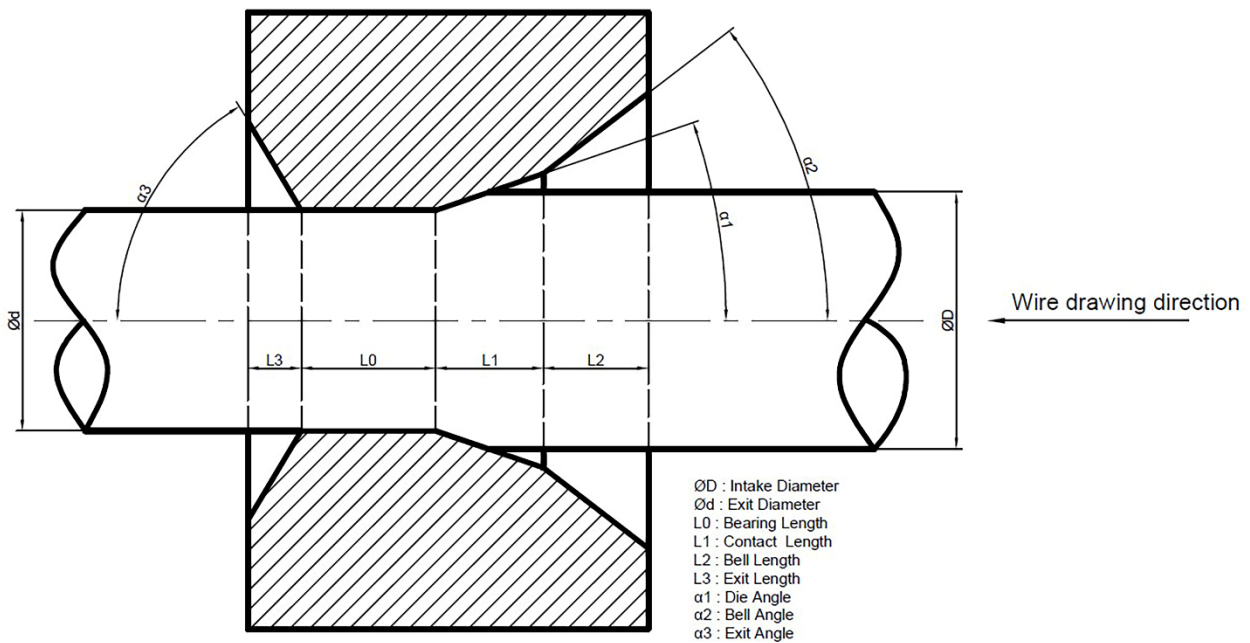


**Figure 1.** The Geometry of Wire Drawing Die

The technical details of wire drawing die manufactured and used experiments is shown in Figure 1. In experiments, the effects of the reduction ratios were also investigated. In the first set of experiments, a wire drawing process was applied from 1.8 mm diameter to 1.6 mm diameter by providing 11.11% rolling ratio. In the second set of experiments, wire drawing was applied from 1.2 mm diameter to 1.1 mm diameter by applying 8.3% rolling ratio. The geometric dimensions of the used dies are presented in Table 1 and 2.

**Table 1.** The Dimensions of Dies for The First Experiments

Die No	ØD	Ød	L0 (%d)	L0 (mm)	L1 (mm)	L2 (mm)	L3 (mm)	α1 (°)	α2 (°)	α3 (°)
1.1			%30.Ød	0.48						
1.2	1.8	1.6	%40.Ød	0.64	12	3	3	6	15	30
1.3			%50.Ød	0.8						
1.4			%60.Ød	0.96						

**Table 2.** The Dimensions of Dies for The Second Experiments

Die No	ØD	Ød	L0 (%d)	L0 (mm)	L1 (mm)	L2 (mm)	L3 (mm)	α1 (°)	α2 (°)	α3 (°)
2.1			%30.Ød	0.33						
2.2	1.2	1.1	%40.Ød	0.44	12	3	3	6	15	30
2.3			%50.Ød	0.55						
2.4			%60.Ød	0.66						

It is essential to minimize the friction force in the wire drawing process. Therefore, various modifications are made on the die and wire. While manufacturing of molds, wire drawing contact surfaces were polished to minimize friction force. Figure 2 shows a wire drawing die with polished surfaces. In order to reduce the friction force between the mold and the wire, zinc phosphate was coated on the wire surface by dipping method. Furthermore, calcium-based solid soap lubricant was used during wire drawing. Figure 3a and 3b show the wire drawing machine and wire drawing test setup. Experiments were carried out on Mekosan wire drawing machine. In both experimental sets, the wire drawing speed was kept constant at 7 m/s.

**Figure 2.** Wire Drawing Die

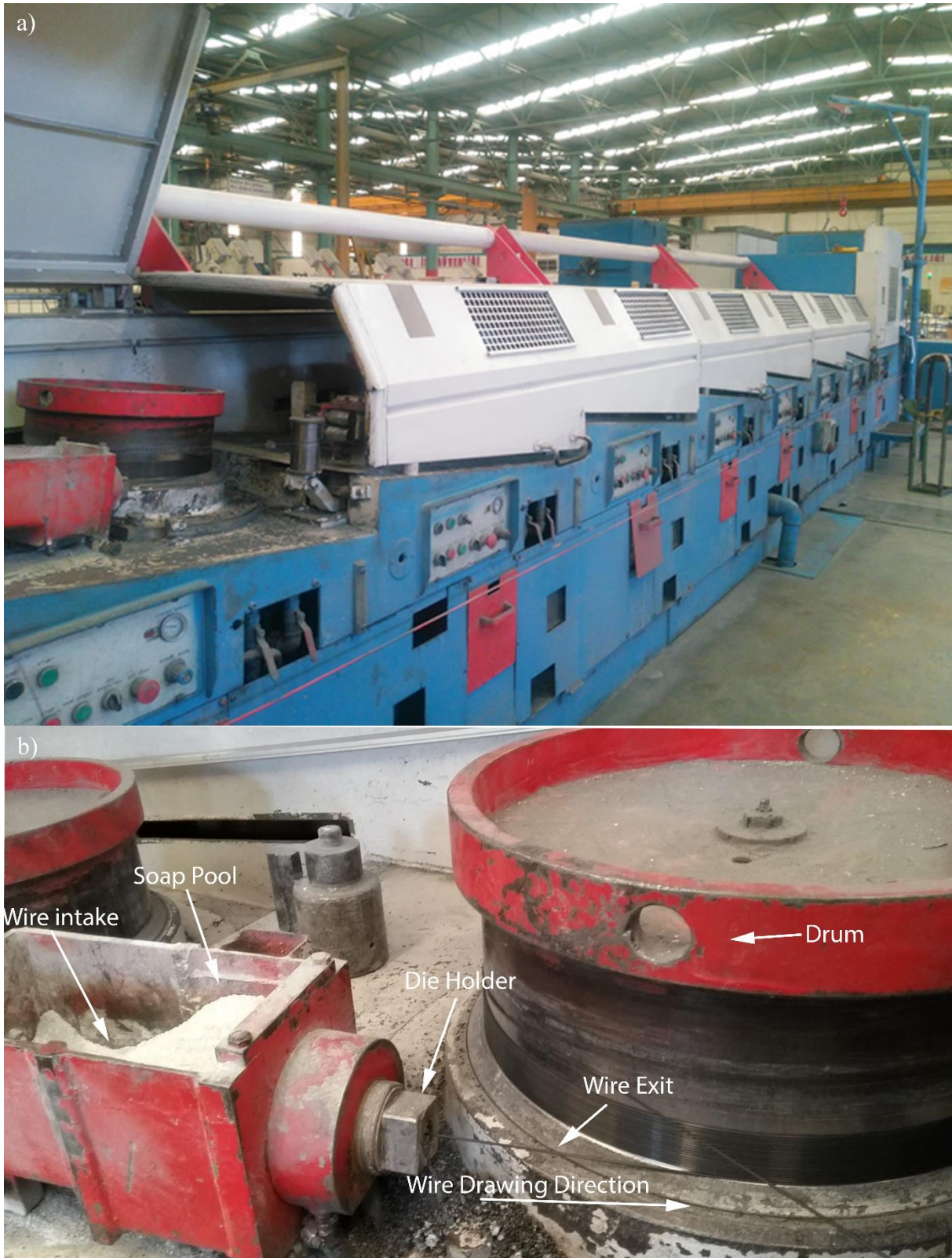


**Figure 3.** a) Wire Drawing Machine and b) Wire Drawing Setup

The length of the wire drawing process for each experiment is 250 000 m. Wire rod material is 1045. Chemical composition of 1045 steel wire is presented in Table 3. Wire rods are reduced to 1.8 and 1.2 mm diameters before the experiment and their strength values are shown in Table 4.



**Table 3.** Chemical Composition of 1045 Steel Wire.

C	Mn	Si	Mo	Cr	Ni	P	S
0.47	0.72	0.39	0.11	0.41	0.48	0.037	0.03

**Table 4.** Wire Strengths Measured Before Experiment.

Wire Material	Wire Diameter (mm)	Tensile Strength (MPa)	Elongation (%)
1045	1.8	1102	18.1
1045	1.2	2141	10.2

Tensile strength measurements were executed Alşa brand tensile device that has 2 ton tensile capacity. Tensile tests were carried out at a speed of 5 m/min. For each experiment, 5 different samples were taken and subjected to tensile testing and then, average values were taken. Microhardness tests were performed with the vickers indentation tip on Wilson Hardness device. Vickers hardness measurement was carried out on the Hv0.2 scale and the force application time was 10 seconds. Metallographic examinations were performed with Nikon Eclipse L150 optical microscope. Samples were etched with 3% Nital solution before metallographic examination.

## RESULTS AND DISCUSSION

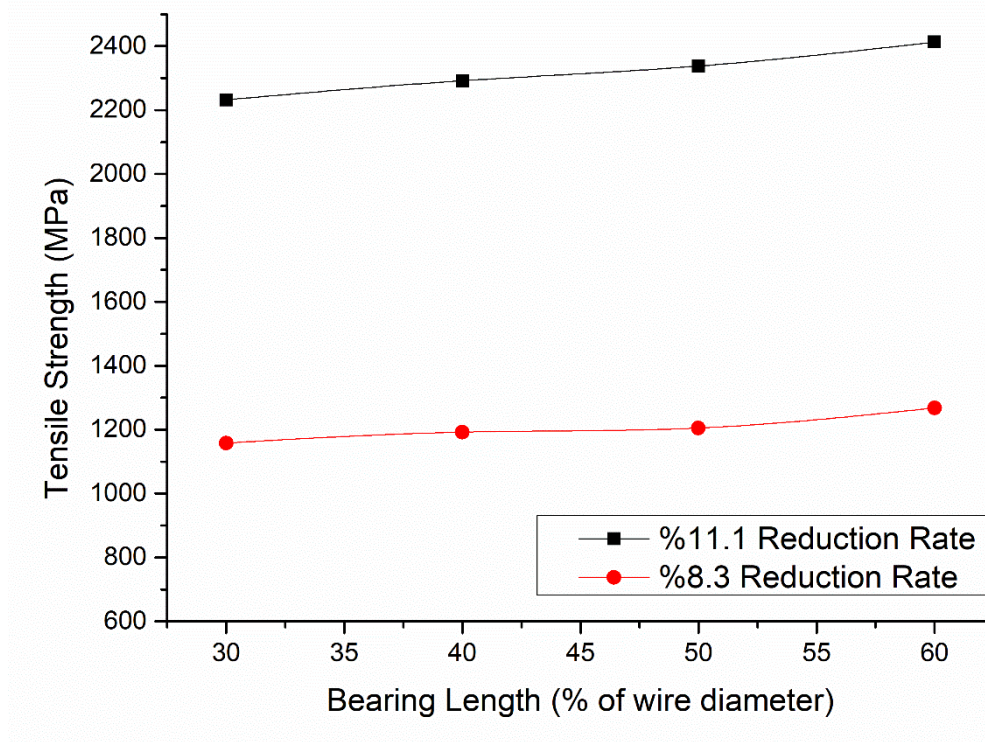


**Figure 4.** Effect of Bearing Length on Tensile Strength under Different Reduction Ranges

The effect of the bearing length on tensile strength under different reduction rates is shown in Figure 4. As the reduction rate increases and the wire thickness decreases, tensile strength of the wire increases due to the deformation hardening phenomenon. As the bearing length increases, an increase in wire strength were taken place.

The 1.2 mm diameter wire, whose cross section has been narrowed by 11.1%, has a tensile strength of 2141 MPa before it is subjected to wire drawing. By increasing the bearing length from 30% of the wire diameter to 60%, the tensile strength increased approximately 200 MPa. This increase amount is approximately 110 MPa for 1.8 mm

diameter wire, whose cross section has been narrowed by 8.3% that had a tensile strength of 1102 Mpa before wire drawing.

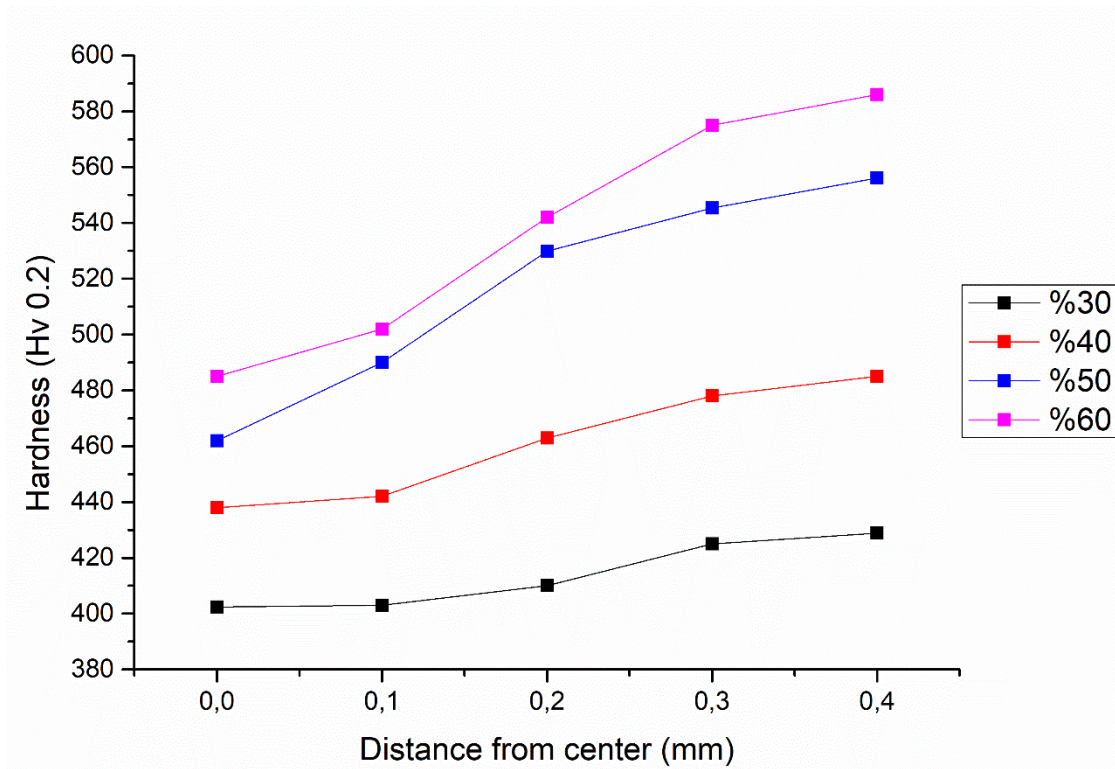


**Figure 5.** Effect of Bearing Length on Hardness Distribution from Wire Cross Section

Figure 5 shows the effect of different bearing length on hardness distribution of cross section in 1.1 mm diameter wire. The hardness increased significantly as progress from the center of the wire to outer diameters. Increases in the bearing length causes elevation in hardness values. As the bearing length increases, the hardness difference between the outer and the center of the wire cross section increases. Hardness elevation is a result of deformation hardening. The amount of hardness is also an indicator of which areas under how much deformed during wire drawing (Sas-Boca et al., 2017). The highest strength on the outer diameter of wire is the main indicative of highest local stress. The amount of hardness is also an indicator of which areas under how much deformation during wire drawing.

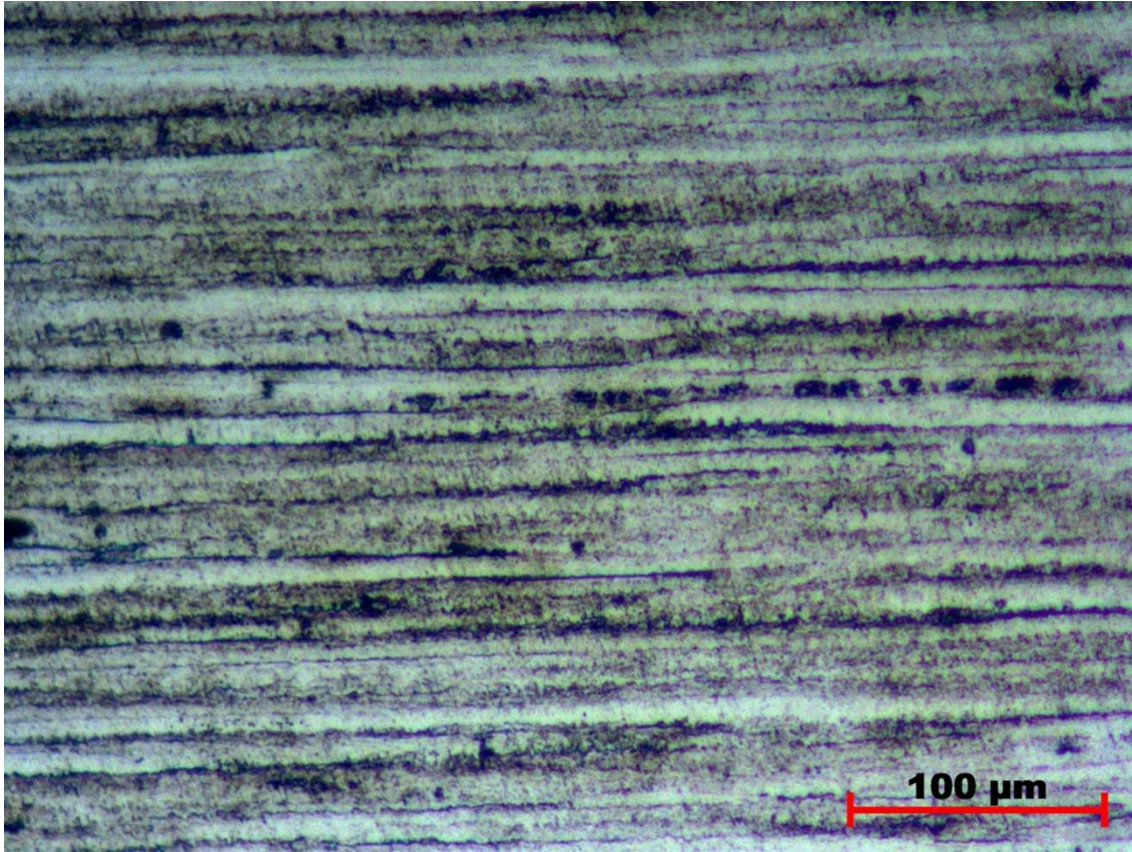


**Figure 6.** Microstructure of the 1.6 mm Diameter Wire

Figure 6 shows the microstructure of the wire with a diameter of 1.6 mm applied an area reduction of 8.3%. Accordingly, the grains are oriented towards the wire drawing direction. Due to the nature of the wire drawing process, rolling lines can easily be seen through cross section. 0.45% C in 1045 wire material did not form a pearlitic structure in the microstructure. Since the ratio of 0.45% C is far from the eutectoid transformation point, the perlite rate is very low. Low perlite ratio limits the amount of deformation hardening to reach high levels (Xu et al., 2019).

Although the brittleness that achieved with deformation hardening is high, deformation accumulation in small sections causes various tension irregularities during wire surface. Was observed that as the bearing length increases, breaks due to irregular stress deposits and coating stripping were occurred. Figure 7.a shows the zinc stripping that takes place at a bearing length of 50%. Zinc coating is stripped due to the high bearing length surface that caused high friction force. In addition to zinc coating zinc-phosphate layer was also stripped (Fig. 7.b).

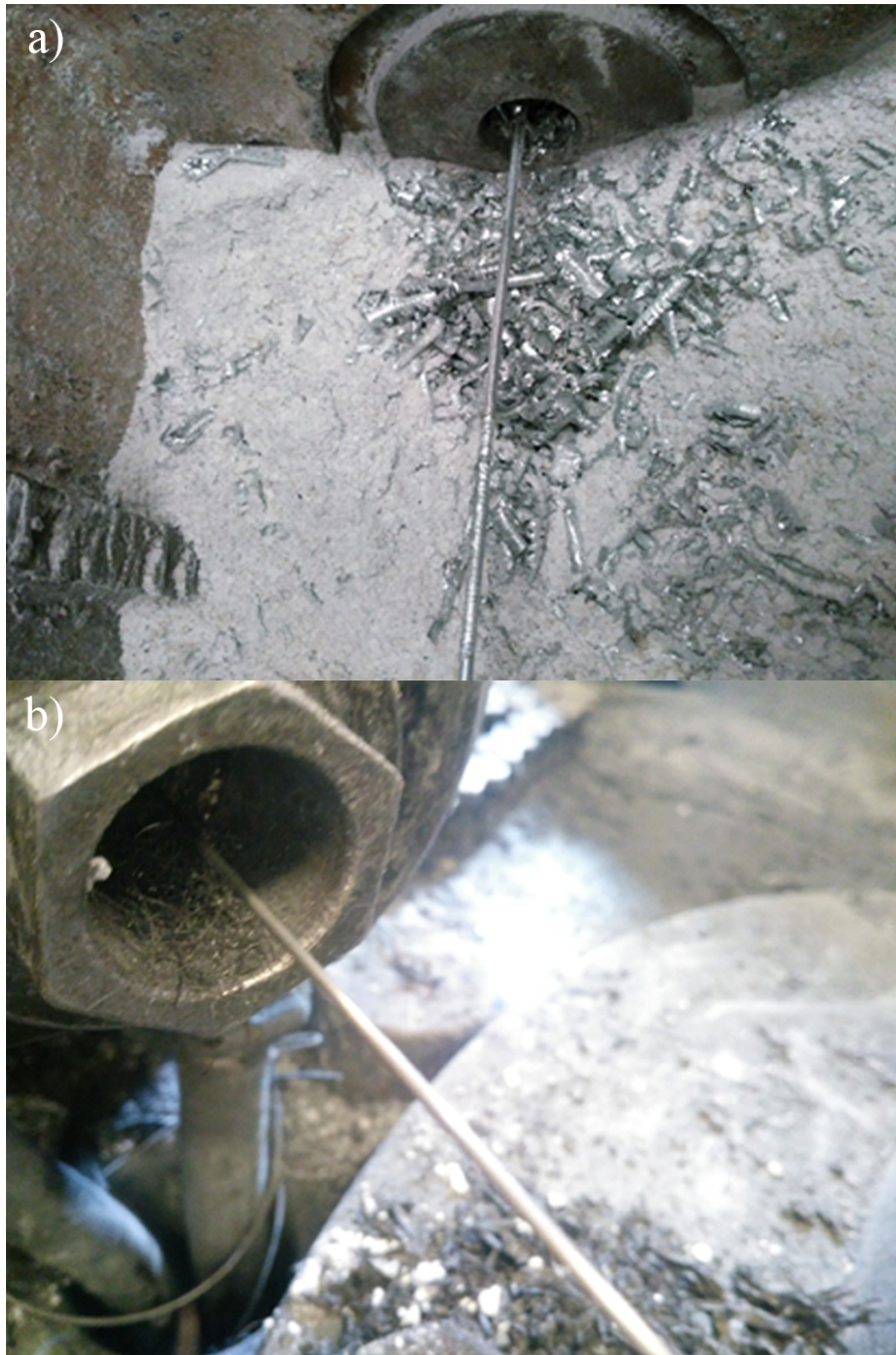


**Figure 6.** a) Zinc and b) Zinc-Phosphate Coating Peel-off with a 50% d Bearing Length (1.8 mm Wire Diameter)

Other problems encountered in high bearing lengths are breakage and scratching during wire drawing. Figure 8 a) and b) shows the surface scratches and rupture surface image formed in 50% and 60% bearing length, respectively. The formation of surface scratches is caused by the ineffectiveness of lubrication as a result of the increased friction force caused by the increased bearing length.

The fracture surface (Figure 8.b) is examined, it can be seen that the tip of the breaking surface is parallel to the drawing direction. In this case, the effect of arranging the grains in the direction of drawing is great. The failure formed due to crack initiations as a result of tension irregularity between the grains. These crack initiations continue in the grain boundary direction, causing the cross section to weaken and then, sudden rupture is developed (Schade, 2006).

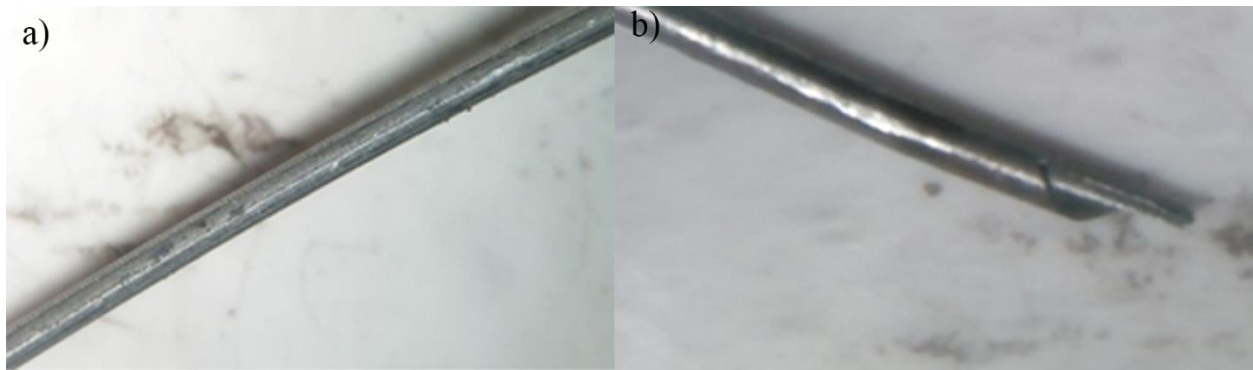


**Figure 8.** a) Scratch and b) Breaking Surface Formation on 1.8 mm Diameter Wire with 50% and 60% Bearing Lengths

## CONCLUSIONS

In the experiments, the effect of different bearing lengths of 1045 steel wires with a diameter of 1.8 and 1.2 mm on strength was investigated in wire drawing operation. The effect of the area reduction rate was also investigated using different reduction rates in both diameters. In the light of the data obtained, the following results can be drawn;

1-As the bearing length increases in all experiments, wire tensile strengths increases. However, this increase causes coating scrapes and irregular wire breaks at 50% bearing length and above. Therefore, it is not recommended to use 50% of wire diameter and higher bearing length in designs.

2-If the bearing length is maintained about 30% and 40% of wire diameter values, wire drawing is done in a healthy way.

3-During the wire drawing process, the increase in the bearing length caused the deformation hardening. Deformation hardening was observed highest at the outermost points of the wire.

4-As bearing length increases, the differences between hardness distribution in the wire cross section were increased. This phenomenon give rise to formation of crack initiations.

5-It is essential to control the friction force during wire drawing. Otherwise, scratches on the outer surface and sudden breaks were formed.

6-Since the amount of carbon in the wire material will affect the perlite ratio, a different bearing length study must be performed for each type of wire materials. Otherwise, it is inevitable to encounter wire breakage and much higher deformation hardening more than expected.

## KAYNAKLAR

Gillström, P., & Jarl, M. (2007). Wear of die after drawing of pickled or reverse bent wire rod. *Wear*, 262(7–8), 858–867. <https://doi.org/10.1016/j.wear.2006.08.016>

Korchunov, A., Gun, G., & Polyakova, M. (2014). Recovery effect in drawing of steel bar for sizing. *Procedia Engineering*, 81, 676–681. <https://doi.org/10.1016/j.proeng.2014.10.059>

Nilsson, M., & Olsson, M. (2011). Tribological testing of some potential PVD and CVD coatings for steel wire drawing dies. *Wear*, 273(1), 55–59. <https://doi.org/10.1016/j.wear.2011.06.020>

Sas-Boca, I. M., Tintelecan, M., Pop, M., Iluțiu-Varvara, D. A., & Mihu, A. M. (2017). The Wire Drawing Process Simulation and the Optimization of Geometry Dies. *Procedia Engineering*, 181, 187–192. <https://doi.org/10.1016/j.proeng.2017.02.368>

Schade, P. (2006). Wire drawing failures and tungsten fracture phenomena. *International Journal of Refractory Metals and Hard Materials*, 24(4), 332–337. <https://doi.org/10.1016/j.ijrmhm.2005.09.003>

Wei, D., Min, X., Hu, X., Xie, Z., & Fang, F. (2020). Microstructure and mechanical properties of cold drawn pearlitic steel wires: Effects of drawing-induced heating. *Materials Science and Engineering A*, 784, 139341. <https://doi.org/10.1016/j.msea.2020.139341>

Xu, P., Liang, Y., Li, J., & Meng, C. (2019). Further improvement in ductility induced by the refined hierarchical structures of pearlite. *Materials Science and Engineering A*, 745, 176–184. <https://doi.org/10.1016/j.msea.2018.12.069>



# Kahramanmaraş Sütçü İmam University

## Journal of Engineering Sciences



Geliş Tarihi : 19.07.2020  
Kabul Tarihi : 30.11.2020

Received Date : 19.07.2020  
Accepted Date : 30.11.2020

### KARAÇAM ODUNUNUN FİZİKSEL ÖZELLİKLERİ ÜZERİNE FARKLI ATMOSFERLERDE UYGULANAN ISIL İŞLEMİN ETKİSİ

### THE EFFECT OF HEAT TREATMENT APPLIED UNDER DIFFERENT ATMOSPHERES ON PHYSICAL PROPERTIES OF BLACKPINE WOOD

Bekir Cihad BAL\* (ORCID: 0000-0001-7097-4132)

<sup>1</sup> Kahramanmaraş Sütçü İmam Üniversitesi, Teknik Bilimler MYO, Malzeme Bölümü, Kahramanmaraş, Türkiye

\*Sorumlu Yazar / Corresponding Author: Bekir Cihad BAL, [bcbal@hotmail.com](mailto:bcbal@hotmail.com)

#### ÖZET

Masif odunun, diğer mühendislik malzemeleri ile kıyaslandığında, yenilenebilir bir malzeme olması, kolay işlenebilmesi, ucuz olması, yoğunluğuna göre mekanik özelliklerinin yüksek olması gibi üstün özellikleri bulunmaktadır. Ancak, biyolojik dayanıklılığı düşüktür ve rutubet alıp verdiğinde daralıp genişlemesi istenmeyen özelliklerindedir. Bu istenmeyen özelliklerini iyileştirmek için değişik metotlar geliştirilmiştir. Isıl işlem metodu bu metotlardan birisidir. Isıl işlem uygulaması, sıcak buhar, sıcak yağ, vakum veya azot gazı atmosferinde uygulanmaktadır. Bu çalışmada, azot gazı, vakum ve hava atmosferlerinde yapılan ısıl işlemin karaçam odununun bazı fiziksel özellikleri üzerine etkisi araştırılmıştır. Test örneklerinin ağırlık kaybı, tam kuru yoğunluk, denge rutubeti yüzdesi, genişleme yüzdeleri ve su alma yüzdeleri belirlenmiştir. Elde edilen verilere göre; sıcaklık arttıkça, ağırlık kaybının arttığı, genişleme ve su almanın azaldığı belirlenmiştir. Ayrıca, hava atmosferinde yapılan ısıl işlem sonuçları ile kıyaslandığında, azot gazı atmosferinde yapılan ısıl işlem sonucunda ağırlık kaybının daha az olduğu tespit edilmiştir.

**Anahtar Kelimeler:** Azot gazı, fiziksel özellikler, ısıl işlem, odun modifikasyonu

#### ABSTRACT

Compared to other engineering materials, solid wood has superior properties such as being a renewable material, easy processing, being cheap and having high mechanical properties according to its density. However, its biological resistance is low and it is undesirable to expand and shrink when moisture is absorbed. Various methods have been developed to improve these undesirable properties. Heat treatment method is one of these methods. Heat treatment is applied in hot steam, hot oil, and vacuum or nitrogen gas atmosphere. In this study, the effect of heat treatment under nitrogen, vacuum and air atmospheres on some physical properties of black pine wood was investigated. Mass loss, oven-dried density, equilibrium moisture content and swelling percentages of the test samples were determined. According to the data obtained; it was determined that as temperature increased, mass loss increased, swelling percentages and water uptake decreased. In addition, when compared to the results of heat treatment under air atmosphere, it was determined that the mass loss was lower as a result of heat treatment under nitrogen atmosphere.

**Keywords:** Wood modification, nitrogen atmosphere, physical properties, heat treatment

\*Sorumlu Yazar / Corresponding Author: Bekir Cihad BAL, [bcbal@hotmail.com](mailto:bcbal@hotmail.com)

**ToCite:** BAL, B.C, (2020). KARAÇAM ODUNUNUN FİZİKSEL ÖZELLİKLERİ ÜZERİNE FARKLI ATMOSFERLERDE UYGULANAN ISIL İŞLEMİN ETKİSİ. *Kahramanmaraş Sütçü İmam Üniversitesi Mühendislik Bilimleri Dergisi*, 23(4), 236-244.

#### GİRİŞ

Odunun fiziksel, kimyasal, mekanik ve biyolojik özellikleri nerede kullanılacağına karar verirken göz önünde bulundurulması gereken önemli özelliklerdendir. Yük altında taşıyıcı elemanlar olarak kullanılacak olan masif

odun veya odun esaslı malzemelerin mekanik özelliklerinin yüksek olması istenir. Yer döşemesi olarak kullanılacak olan odunun aşınma direncinin yüksek olması beklenir. Açık alanlarda kullanılacak olan odun türlerinin biyolojik dayanıklılığının yüksek olması istenir. Ahşap yapı elemanları, mobilya ve yer döşemeleri gibi bazı kullanım yerlerinde ise odunun fiziksel özelliklerinden olan denge rutubetinin ve odunun daralma ve genişleme yüzdelerinin düşük olması gerekir.

Odunun bu fiziksel özelliklerini iyileştirmek için çeşitli modifikasyon yöntemleri geliştirilmiştir. Bunlar; odunun liflere nüfuz eden bir fenolik reçine ile emprenyesi, odundaki hidroksil gruplarının asetil gruplarına dönüştürülmesi, ısı işleme tabi tutulması, polimerik hücre çeperi bileşenleri arasında formaldehit kullanılarak çapraz bağlar oluşturulması, polietilen glikol ile muamele edilerek genişletilmesi ve genişlemiş halin korunmasıyla boyutsal sabitliğin sağlanması şeklindedir (Yıldız, 1994). Bu yöntemlerden özellikle ısı işlem modifikasyonu son yıllarda endüstriyel olarak çok uygulanan yöntemlerdendir. Farklı ülkelerde farklı ısı işlem modifikasyon yöntemleri uygulanmaktadır. Günümüzde en fazla kullanılan ısı işlem metotları Platowood (Hollanda), Thermowood (Finlandiya), Retification ve Le-Bois Perdure (Fransa) ve Oil-heat treatment wood (Almanya) şeklinde olduğu bildirilmiştir (Korkut ve Kocaefe 2009). Türkiye’de ise endüstriyel olarak ısı işlem uygulayan 3 farklı işletme bulunmaktadır. Bu işletmeler Thermowood yöntemi ile üretim yapmaktadır.

Isı işlem modifikasyonunun denge rutubeti miktarı, daralma ve genişleme yüzdeleri gibi fiziksel özelliklerini azalttığı (Almeida ve ark., 2009; Calonego ve ark., 2012; Dubey ve ark., 2012; Gaff and Gasparic 2013; Bal 2013), kimyasal içeriğini değiştirdiği (Brito ve ark., 2008; Korkut ve Kocaefe 2009; Esteves and Pereira 2009; Severo ve ark. 2012), mekanik özelliklerini azalttığı (Jamsa ve Viitaniemi 2001; Esteves ve Pereira 2009), biyolojik dayanıklılığını artırdığı (Kamdem ve ark., 2002; Edlund ve Jermer 2004; Welzbacher ve ark., 2007; Candelier 2013a), yüzey rengini ve parlaklığını değiştirdiği (Kamdem ve ark., 2002; Ayata ve ark., 2017; Karamanoğlu ve Kaymakçı 2018; Ayata ve ark., 2018a; Ayata 2020), yüzey pürüzlülüğünün değiştiği (Ayata ve ark., 2018b) yapılan birçok çalışma ile belirlenmiştir. Ayrıca, ısı işlem esnasında kullanılan ısıtma aracı olan sıcak yağ ile sıcak havanın fiziksel özellikler üzerine etkisi (Sailer ve ark., 2000; Bal 2015; Bal 2016), azot atmosferi ve vakum atmosferinin mekanik özellikler üzerine etkisi (Candelier 2013b; Bal 2018 ) bazı araştırmacılar tarafından belirlenmiştir.

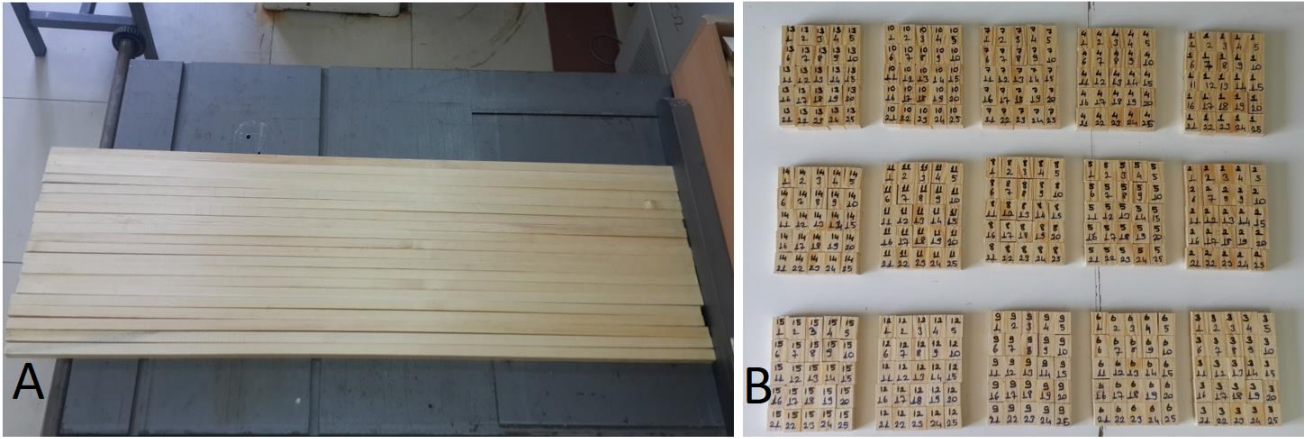
Odunun ısı muamelesi esnasında, ısı taşıma aracı olarak kullanılan hava, yağ, buhar gibi farklı araçların yapılan işlem sonucunda elde edilen çıktılar farklılık gösterebilmektedir. Bu nedenle, farklı ülkelerde kullanılan farklı ısı işlem metotları geliştirilmekte ve yeni metot arayışları da bir taraftan devam ettirilmektedir. Elde edilmeye çalışılan ve tam olarak başarısız olan hedef ise şudur; yapılan ısı işlem sonucunda odunun mekanik özelliklerinin etkilenmemesi sağlamak, buna karşı su alma, daralma-genişleme gibi fiziksel özelliklerin iyileştirilmesi ve biyolojik dayanıklılığın artırılmasıdır. Ancak, bugün için kullanılan ısı işlem metotlarının hepsinde, özellikle biyolojik dayanıklılığı artırmak için yüksek sıcaklıklarda yapılan uygulamalar mekanik özelliklerde azalmaya neden olmaktadır.

Bugüne kadar, farklı ısı işlem metotları kullanılarak farklı odun türleri üzerinde sayısız araştırma yapılmıştır. Ancak, ısı işlem esnasında, kullanılan sıcak hava, sıcak buhar, sıcak bitkisel yağ, azot gazı ve vakum ortamı-metal plaka gibi ısıtma araçlarının ısı işlem sonucunu nasıl etkilediği üzerine yeterli karşılaştırmalı çalışma bulunmamaktadır. Bu nedenle, bu çalışmada, farklı sıcaklıklarda hava atmosferinde, vakum atmosferinde ve azot gazı atmosferinde yapılan ısı işleminin karaçam odununun fiziksel özellikleri üzerine etkisi araştırılmıştır.

## **MATERYAL VE METOT**

### ***Materyal***

Araştırmada deneme materyali olarak kullanılan karaçam tomrukları Kahramanmaraş keresteciler sitesinden rastgele usulle elde edilmiştir. Tomruklar satın alınan yapıldığı kereste atölyesinde keresteye biçilmiştir. Tomruklar kaba biçme sonrası, kalınlıkları yaklaşık 25 mm ve genişlikleri 100 mm olacak şekilde tahtalara biçilmiş ve bu haliyle doğal kurutmaya bırakılmıştır. İki aylık süre sonunda tahtalardan 25 x 25 mm enine kesitinde çıtalar elde edilmiştir (Şekil 1-A). Bu çیتالardan test örnekleri hazırlanmıştır. Aynı çita ya da tahtalardan yan yana kesilen test örnekleri ile test grupları oluşturulmuştur. Fiziksel özelliklerin tespiti için, 3’ü kontrol olmak üzere 15 grup oluşturulmuş ve toplam 375 adet test örneği kesilmiştir (Şekil 1-B). Fiziksel özellikler için, test örnekleri hazırlanırken 150 cm boyunda çیتالardan yan yana kesilen her bir test örneği, 1 nolu gruptan başlayarak, farklı bir gruba dahil edilmiş ve böylece test grupları arasında homojenlik sağlanmaya çalışılmıştır.



Şekil 1. Test örneklerinin hazırlandığı çıtalar (A) ve test örnekleri (B)

### Metot

Test örnekleri kurutma dolabında  $103 \pm 2$  °C’de sıcaklıkta değişmez boyutlara ulaşmaya kadar kurutulmuş, bu durumdaki ölçüleri ve ağırlığı alınmış, bu verilerle tam kuru yoğunlukları belirlenmiştir. Sonra test örnekleri %12 rutubet seviyesine kadar şartlandırılmıştır. Her bir test için bir kontrol grubu oluşturulmuştur. Diğerleri ise deney grubu olarak 180, 200, 220 ve 240°C’de 4 farklı sıcaklıkta 30 dakika ısıtımdan sonra ve 2 saat süre ile ısıtım uygulanmıştır. Isıl işlem uygulaması 3 farklı atmosferde gerçekleştirilmiştir. Bunun için hava atmosferi şartlarında, vakum atmosferi şartlarında ve azot atmosferi şartlarında olmak üzere 3 farklı atmosferde denemeler yapılmıştır. Isıl işlem uygulaması esnasında, hava atmosferi şartlarında yapılan denemelerde etüv içerisine vakum ya da azot gazı uygulanmamıştır. Vakum atmosferi şartlarında yapılan denemelerde vakum 500 mBar uygulanmıştır. İşlem süresince vakum sabit tutulmaya çalışılmıştır. Azot gazı atmosferinde yapılan denemelerde ise, kapak kapatılıp işlem başlatıldıktan sonra, öncelikle etüv içerisine 3 dakika boyunca azot gazı verilmiş, sonra gaz kesilip 50 mBar ile 100 mBar aralığında vakum uygulanıp kapağın kapalı kalması sağlanmış ve sonrasında 50 mBar vakum uygulanırken azot gazı verilmiştir. Böylece ortamdan hava alınmış ve azot gazı atmosferi oluşturulmuştur. Isıl işlem bu ortamda yapılmıştır. Vakum atmosferi ve azot atmosferinde yapılan gruplar ısıl işlem süreci tamamlanınca etüvden alınmış ve hava ile temas etmeyecek şekilde plastik poşetlere konarak soğuyuncaya kadar bekletilmiştir. Bu durumdaki ağırlıkları alınarak ağırlık kaybı hesaplanmıştır. Ayrıca, bu veriler kullanılarak tekrar yoğunluk değerleri (TKY2) belirlenmiştir. Sonra test örnekleri klima dolabında 4 hafta bekletilmiş ve denge rutubeti belirlenmiştir. Daha sonra, deney parçaları değişmez hale gelinceye kadar bir kap içerisinde  $20 \pm 5$  °C sıcaklıkta damıtık su içerisine 2 hafta süre ile batırılmıştır. Sonra tam yaş haldeki son ölçüleri alınmış, bu verilerle genişleme yüzdeleri ve su alma yüzdeleri hesaplanmıştır. Test örneklerinin yoğunluk değerleri TS 2472 numaralı standartta belirtilen esaslara göre, denge rutubeti ve su alma yüzdesinin belirlenmesi için TS 2471, genişleme yüzdesinin belirlenmesi için TS 4084 ve TS 4086 numaralı standartlar kullanılmıştır. Bu standarda göre deney parçaları; kesiti 20 x 20 mm ve lif doğrultusundaki uzunluğu 30 mm olan prizma biçiminde hazırlanmıştır.



Şekil 2. Isıl işlem uygulamasında kullanılan vakumlu etüv, vakum pompası ve azot gazı tüpü



**BULGULAR VE TARTIŞMA**

Kontrol gruplarında ve uygulanan ısı işlem sonucunda deney gruplarında elde edilen ağırlık kaybı, tam kuru yoğunluk değeri, denge rutubet yüzdesi, genişleme yüzdeleri ve su alma yüzdelerine ait bulgular Çizelge 1’de verilmiştir. Ağırlık kaybı, yoğunluk azalması, genişleme yüzdesindeki azalma ve su almadaki azalma en fazla hava atmosferinde yapılan denemelerde ve 240°C elde edilmiştir.

**Tablo 1.** Testler sonunda elde edilen fiziksel özelliklere ait bulgular

			AK	TKY1	TKY2	DRM	TG	RG	HG	SA
Gruplar			%	kg/m <sup>3</sup>	kg/m <sup>3</sup>	%	%	%	%	%
HAŞ	1-Kont.	x	-	498	498	12.6	9.5	5.4	15.0	85
		ss	-	29	29	1.0	0.7	0.5	1.0	6
	2-180°C	x	1.1	501	493	11.2	9.3	5.9	15.2	80
		ss	0.3	30	31	0.4	0.7	0.5	1.2	4
	3-200°C	x	2.1	501	494	11.6	8.8	5.8	14.7	78
		ss	0.5	29	30	0.5	0.6	0.5	1.0	3
	4-220°C	x	3.7	501	492	9.6	7.7	5.0	12.8	75
		ss	0.4	30	31	0.2	0.5	0.5	0.9	5
	5-240°C	x	10.4	496	465	8.1	6.1	3.9	10.0	67
		ss	1.1	33	34	0.3	0.4	0.5	0.8	5
VAŞ	6-Kont.	x	-	494	494	12.6	9.3	5.4	14.8	86
		ss	-	28	28	0.3	0.7	0.5	1.1	5
	7-180°C	x	0.7	497	491	12.2	9.0	5.9	14.9	84
		ss	0.1	32	33	0.2	1.1	0.5	1.5	5
	8-200°C	x	1.5	498	493	11.6	8.8	5.8	14.6	82
		ss	0.2	32	33	0.2	0.7	0.5	1.1	6
	9-220°C	x	3.1	495	488	10.2	7.9	5.1	13.1	78
		ss	0.4	31	33	0.2	0.7	0.6	1.2	5
	10-240°C	x	6.6	496	477	7.8	6.5	4.0	10.5	71
		ss	0.6	31	33	1.0	0.6	0.5	1.0	6
AAŞ	11-Kont.	x	-	496	496	12.8	9.5	5.5	15.0	86
		ss	-	26	26	0.6	0.8	0.6	1.3	5
	12-180°C	x	0.8	496	489	11.5	9.1	5.7	14.8	82
		ss	0.1	29	31	0.2	0.6	0.5	1.0	4
	13-200°C	x	1.4	499	489	11.7	8.6	5.7	14.4	80
		ss	0.2	36	30	0.3	0.7	0.6	1.2	4
	14-220°C	x	2.7	495	487	10.3	7.9	5.0	13.0	76
		ss	0.5	29	32	0.4	0.7	0.6	1.3	4
	15-240°C	x	5.1	494	481	7.2	6.9	4.4	11.4	74
		ss	0.6	28	29	1.0	0.6	0.5	1.1	4

AK: ağırlık kaybı, TKY1: ısı işlem öncesi tam kuru yoğunluk değerleri, TKY2: ısı işlem sonrası tam kuru yoğunluk değerleri, DRM: denge rutubeti miktarı, TG: teğet genişleme, RG: radyal genişleme, HG: hacmen genişleme, SA: su alma yüzdesi, x: aritmetik ortalama, SS: standart sapma, HAŞ: hava atmosferi şartları, VAŞ: vakum atmosferi şartları, AAŞ: azot atmosferi şartları.

Çizelge 1’de gösterilen verilere göre, ağırlık kaybını etkileyen iki farklı bağımsız değişken vardır. Bunlar; atmosfer ve sıcaklıktır. Aşağıda Çizelge 2’de bu iki faktörün ağırlık kaybı üzerine etkisini gösteren iki yönlü ANOVA testi sonuçları gösterilmiştir. Bu sonuçlara göre, her iki faktörde ağırlık kaybı üzerine istatistiksel olarak çok ileri düzeyde önemli seviyede etkilidir ( $p < 0.001$ ).

**Tablo 2.** Sıcaklık ve işlem şartlarının ağırlık kaybı üzerine etkisini gösteren ANOVA testi sonuçları

Varyans Kaynağı	Kareler toplamı	SD	Ortalama kareler	F	Sig.
Atmosfer	180,093	2	90,047	375,068	0,000
Sıcaklık	1886,804	3	628,935	2619,681	0,000
Atmosfer * Sıcaklık	220,774	6	36,796	153,264	0,000

Atmosferin ve sıcaklığın ağırlık kaybı üzerine etkisi gösteren ANOVA testi sonuçları Çizelge 2’de verilmiştir. Her iki faktöründe önemli seviyede etkili olduğu belirlenmiştir. Buna ilaveten, hangi şartların ne seviyede etkili olduğu ya da hangi sıcaklık seviyesinin diğerlerinden farklı bir etkiye sahip olduğunu gösteren Duncan testi sonuçları ise Çizelge 3’te verilmiştir. Çizelge 3 incelendiğinde her üç atmosferin ağırlık kaybı bakımından birbirinden farklı olduğu görülmektedir. En fazla ağırlık kaybı %4.3’le hava atmosferi şartlarında gerçekleşmiştir. En az ağırlık kaybı ise %2.49 ile azot atmosferi şartlarında gerçekleşmiştir. Bunun önemli bir sebebinin hava atmosferi şartlarında odunun oksijenle teması sonucu, odun bileşenlerinde hızlı bir bozulmanın gerçekleşmesidir. Vakum atmosferi ve azot atmosferi inert atmosfer olarak bilinmektedir. Ortamda oksijen çok azdır. Odun bileşenleri geç bozulur. Yapılan önceki çalışmalarda benzer sonuçlar rapor edilmiştir (Candelier ve ark., 2013a). Yapılan bu çalışma ile Candelier ve ark., (2013a) tarafından yapılan çalışma arasında ki metod farkı ısıtma sistemi ile ilgilidir. Yapılan bu çalışmada etüv içerisinde ısı transferi, ısı taşınımı (konveksiyon) yöntemi ile sağlanmıştır. Ancak, Candelier ve ark., (2013a) tarafından yapılan çalışma da ise ısı transferi ısı iletimi (kondüksiyon) yöntemi ile metal plakalar aracılığıyla yapılmıştır. Elbette ki bu iki yöntem arasında sonuçlar bakımından farklar oluşması muhtemeldir.

**Tablo 3.** Atmosfer ve sıcaklığın ağırlık kaybına etkisini gösteren Duncan testi sonuçları

Atmosfer	N	Alt Gruplar			Sıcaklık	N	Alt Gruplar			
		1	2	3			1	2	3	4
AAŞ	100	2,49			180°C	75	0,86			
VAŞ	100		2,98		200°C	75		1,65		
HAŞ	100			4,32	220°C	75			3,18	
					240°C	75				7,36

Çizelge 1’de TKY1 değerleri ısıtma işlem uygulaması öncesi her grupta ölçülen tam kuru yoğunluk değerlerini ve TKY2 değerleri ise ısıtma işlem sonrası ölçülen aynı gruptaki tam kuru yoğunluk değerlerini göstermektedir. TKY1 değerleri incelendiğinde gruplar arasındaki yoğunluk farklılığının en fazla 5 kg olduğu görülmektedir. Odun üzerinde yapılan farklı gruplar arasında bu derece düşük yoğunluk farklılığının olması, yapılan işlemin etkisi görebilmek ve yoğunluğun etkisini elimine edebilmek için son derece önemlidir. TKY2 değerleri incelendiğinde artan sıcaklıkla beraber TKY2 değerlerinde bir azalma meydana geldiği ve en fazla azalmanın 240°C’de meydana geldiği görülmektedir. Isıtma işlem muamelesinin odunun yoğunluğu üzerine yapılan önceki çalışmalarda da benzer sonuçlar elde edilmiştir (Korkut ve Güller 2008; Bal 2013).

Yapılan bu çalışmada ısıtma işlem muamelesinin çam odununun denge rutubeti üzerine etkisi de araştırılmıştır. Elde edilen veriler Çizelge 1’de verilmiştir. Denge rutubeti üzerine sıcaklık ve atmosfer şartlarının etkisini gösteren iki yönlü ANOVA testi sonuçları ise Çizelge 4’de gösterilmiştir. Çizelgedeki veriler incelendiğinde sıcaklık ve atmosfer şartlarının denge rutubeti üzerine etkisinin istatistiksel olarak önemli seviyede ( $P < 0.001$ ) etkili olduğu görülmektedir.

**Tablo 4.** Sıcaklık ve atmosfer şartlarının denge rutubeti üzerine etkisini ait ANOVA testi sonuçları

Varyans Kaynağı	Kareler toplamı	SD	Ortalama kareler	F	Sig.
Atmosfer	6,55	2	3,27	11,50	0,000
Sıcaklık	762,99	3	254,33	893,89	0,000
Atmosfer * Sıcaklık	22,81	6	3,80	13,36	0,000

Atmosfer şartlarının ve sıcaklığın denge rutubeti üzerine etkisini gösteren Duncan testi sonuçları Çizelge 5’de verilmiştir. Bu sonuçlara göre hava atmosferi şartları ile azot atmosfer şartlarında yapılan işlemin denge rutubeti üzerine etkileri arasında fark oluşmazken, vakum atmosferi şartlarında yapılan ısıtma işlemi denge rutubeti üzerine diğerlerinden önemli seviyede farklı bulunmuştur. Ayrıca, en yüksek denge rutubeti %12,6 ile kontrol grubunda elde edilmiştir. Çizelgede verilen sıcaklık grupları incelendiğinde, en yüksek denge rutubeti yüzdesinin kontrol gruplarında ve en düşük denge rutubeti yüzdesinin ise 240°C’de işlem gören gruplarda elde edildiği görülmektedir. Isıtma işlem uygulanmış odunun, yapılan önceki çalışmalarda da denge rutubeti ile ilgili olarak benzer sonuçlar elde edilmiştir (Gündüz ve ark., 2008; Bal 2013).

**Tablo 5.** Şartlar ve İşlem sıcaklığının denge rutubetine ait Duncan testi sonuçları

Atmosfer	N	Alt gruplar			Sıcaklık	N	Alt gruplar			
		1	2	3			1	2	3	4
HAŞ	100	10,1			240°C	75	7,7			
AAŞ	100	10,2			220°C	75		10,1		
VAŞ	100		10,5		200°C	75			11,6	
Kontrol	75			12,6	180°C	75			11,6	
					Kontrol	75				12,6

Yapılan denemeler sonunda elde edilen hacmen genişleme yüzdelere sıcaklığın etkisi ve atmosfer şartlarının etkisini gösteren ANOVA testi sonuçları Çizelge 6'da verilmiştir. Elde edilen bu istatistik testi sonuçlarına göre; atmosfer şartlarının hacmen genişleme yüzdesi üzerine etkisi önemsizdir. Ancak, sıcaklığın etkisi istatistiksel olarak önemlidir ( $P < 0.001$ ). Her iki faktörün etkileşimi ise yine önemli olarak belirlenmiştir.

**Tablo 6.** Sıcaklık ve işlem şartlarının hacmen genişleme üzerine etkisini ait ANOVA testi sonuçları

Varyans Kaynağı	Kareler toplamı	SD	Ortalama kareler	F	Sig.
Atmosfer	2,44	2	1,22	0,95	0,388
Sıcaklık	863,55	3	287,85	223,53	0,000
Atmosfer * Sıcaklık	26,89	6	4,48	3,48	0,002

Sıcaklık ve atmosferin hacmen genişleme üzerine etkisini gösteren Duncan testi sonuçları Çizelge 7'de verilmiştir. En küçük hacmen genişleme hava atmosferi şartlarında yapılan denemelerde ölçülmüştür. En büyük hacmen genişleme ise azot gazı atmosferinde yapılan denemelerde ölçülmüştür. Kontrol grubunda ise %14,9 ölçülmüştür. Bu sonuçlara göre ortam şartlarının hacmen genişlemeye etkisi küçük farklılıklarla vardır, ama aradaki farklar önemsiz farklılıklardır (NS) denebilir. Ancak, sıcaklık grupları incelendiğinde, en düşük hacmen genişleme yüzdesi %10,6 olarak 240°C'de işlem gören gruplarda ölçülmüştür. Kontrol grubunda ve 180°C'de işlem gören grupta ise %14,9 olarak ölçülmüştür. Isıl işlem görmüş odun örneklerinin hacmen daralma ve genişleme yüzdelere azalma olduğunu yapılan önceki çalışmalarda da rapor edilmiştir (Almeida ve ark., 2009; Calonego ve ark., 2012; Dubey ve ark., 2012; Gaff and Gasparic 2013; Bal ve Bektaş 2012; Bal 2013).

**Tablo 7.** Atmosfer ve İşlem sıcaklığının hacmen genişlemeye etkisini gösteren Duncan testi

Atmosfer	N	Alt gruplar		Sıcaklık	N	Alt gruplar			
		1	2			1	2	3	4
HAŞ	100	13,2		240°C	75	10,6			
VAŞ	100	13,3		220°C	75		12,9		
AAŞ	100	13,4		200°C	75			14,5	
Kontrol	75		14,9	180°C	75				14,9
				Kontrol	75				14,9

Su alma yüzdesi üzerine sıcaklık ve atmosfer şartlarının etkisini gösteren iki yönlü ANOVA testi sonuçları Çizelge 8'de verilmiştir. Bu çizelgede ki verilere göre her iki faktöründe su alma yüzdesi üzerine etkisi istatistiksel olarak çok ileri düzeyde önemli olduğu bulunmuştur ( $p < 0.001$ ). Ayrıca, her iki faktörün etkileşimi de önemli bulunmuştur ( $p < 0.05$ ).

**Tablo 8.** Sıcaklık ve işlem şartlarının su alma miktarı üzerine ait ANOVA testi sonuçları

Varyans Kaynağı	Kareler toplamı	SD	Ortalama kareler	F	Sig.
Atmosfer	873,047	2	436,523	18,891	0,000
Sıcaklık	5600,650	3	1866,883	80,790	0,000
Atmosfer * Sıcaklık	333,860	6	55,643	2,408	0,027

Su alma testi sonunda elde edilen verilere ait Duncan çoklu karşılaştırma testi sonuçları Çizelge 9'da verilmiştir. Bu sonuçlara göre hava atmosferi şartlarında en düşük su alma yüzdesi ölçülmüştür. Vakum ve azot atmosfer şartları arasında ise bir farklılık bulunmamıştır. Sıcaklık gruplarına göre, tüm sıcaklık gruplarında ölçülen su alma yüzdeleri birbirinden farklıdır. En düşük su alma yüzdesi %70,5 olarak 240°C'de işlem gören gruplarda ölçülmüştür. En yüksek su alma yüzdesi ise %85,5 olarak kontrol grubunda ölçülmüştür. Burada ölçülen, ısıl işlem görmüş odunun, su alma yüzdesi üzerine etkili olan iki önemli faktör bulunmaktadır. Bunlardan birincisi, ısıl işlem görmüş odunun hücre çeperine bağlanan su miktarının ısıl işlem sonrasında hemiselüloz ve selüloz yapısında meydana gelen bozulma nedeniyle azalmasıdır. Bu durum yukarıda Çizelge 5'de gösterilmiştir. Kontrol grubunun denge rutubeti %12'ler seviyesinde iken, 240°C ısıl işlem görmüş grubun denge rutubeti %7'lere kadar azalmıştır. Ayrıca, Çizelge 7'de görülebileceği gibi, ısıl işlem görmüş test örneklerinin hacmen genişleme yüzdeleri de azalmaktadır. Böylece test örneklerinin hacminin azalması içerisindeki boşluklara alabileceği serbest su yüzdesininde azalmasına neden olmaktadır. Benzer sonuçlar Bal ve Bektaş (2012) tarafından rapor edilmiştir.

**Tablo 9.** Su alma testi verilerine ait Duncan çoklu karşılaştırma testi sonuçları

Atmosfer	N	Alt gruplar			Sıcaklık	N	Alt gruplar					
		1	2	3			1	2	3	4	5	
HAŞ	100	74,9			240°C	75	70,5					
AAŞ	100		77,9		220°C	75		76,4				
VAŞ	100		78,8		200°C	75			80,1			
Kontrol	75			85,5	180°C	75				81,8		
					Kontrol	75						85,5

## SONUÇLAR VE ÖNERİLER

Bu çalışmada, farklı atmosferlerde yüksek sıcaklıklarda muamele edilen karaçam odunun fiziksel özelliklerinde meydana gelen değişimler karşılaştırmalı olarak çalışılmıştır. Elde edilen verilere göre şu sonuçlara ulaşılmıştır; Yapılan denemeler sonunda, ısıl işlem sıcaklığı arttıkça, denemeleri yapılan hava, azot gazı ve vakum atmosferlerinin her üçünde de test örneklerinin fiziksel özelliklerinin değiştiği görülmüştür. Odunun denge rutubeti yüzdesinde ısıl işlem uygulaması ile azalma olduğu belirlenmiştir. En fazla azalma 240°C sıcaklıkta işlem gören grupta ve hava atmosferinde yapılan denemelerde elde edilmiştir. Isıl işlem sonucunda test örneklerinin ağırlık kaybı sıcaklık arttıkça artmıştır. En fazla ağırlık kaybı hava atmosferinde yapılan denemelerde elde edilmiştir. En az ağırlık kaybı azot gazı atmosferinde ölçülmüştür. Genişleme yüzdesinde sıcaklık arttıkça istatistiksel olarak önemli seviyede azalma meydana gelmiştir. En fazla azalma hava atmosferinde yapılan denemelerde elde edilmiştir. Ancak, hava, azot ve vakum atmosfer şartları arasında genişleme yüzdesininin azalması bakımından istatistiksel bir farklılık belirlenmemiştir. Test örneklerinin su alma yüzdeleri artan ısıl işlem sıcaklığına bağlı olarak, istatistiksel olarak önemli derecede azalmıştır. En fazla azalma hava atmosferinde meydana gelmiştir. Vakum ile azot gazı atmosferi arasında fark yoktur.

## TEŞEKKÜR

Bu çalışma Kahramanmaraş Sütçü İmam Üniversitesi Bilimsel Araştırma Projeleri Koordinasyon Birimince desteklenmiştir. Proje Numarası: 2016/3-70M. Laboratuvar çalışmaları esnasında yardımcı olan Zeynep Gündeş ve Elif Akçakaya'ya teşekkür ederim.

## KAYNAKLAR

- Almeida, G, Brito, JO, Perre, P. (2009). "Changes in wood-water relationship due to heat treatment assessed on micro-samples of three Eucalyptus species", *Holzforschung*, 63: 80-88.
- Ayata, U., Gürleyen, L., Esteves, B., Gürleyen, T., and Çakıcıer, N. (2017), "Effect of heat treatment (ThermoWood) on some surface properties of parquet beech with different layers of UV system applied", *BioResources*, 12(2), 3876-3889.
- Ayata, Ü , Gürleyen, T , Gürleyen, L . (2018a). Effect of heat treatment on color and glossiness properties of zebrano, sapeli and merbau woods . *Mobilya ve Ahşap Malzeme Araştırmaları Dergisi* , 1 (1) , 11-20 . DOI: 10.33725/mamad.428913
- Ayata, Ü , Gürleyen, T , Gürleyen, L , Çakıcıer, N . (2018b). Determination of surface roughness parameters of heat-treated and untreated scotch pine, oak and beech woods . *Mobilya ve Ahşap Malzeme Araştırmaları Dergisi* , 1 (1) , 46-50 . DOI: 10.33725/mamad.433945
- Ayata, Ü . (2020). Ayous odununun bazı teknolojik özelliklerinin belirlenmesi ve ısıtıl işleminden sonra renk ve parlaklık özellikleri, *Mobilya ve Ahşap Malzeme Araştırmaları Dergisi* , 3 (1) , 22-33 . DOI: 10.33725/mamad.724596
- Bal BC, Bektaş İ (2012) The effects of heat treatment on the physical properties of juvenile wood and mature wood of *E. grandis*, *Bioresources* 7(4): 5117-5127.
- Bal, BC. (2013). "A comparative study of the physical properties of thermally treated poplar wood and plane wood", *BioResources*, 8 (4): 6493-6500.
- Bal. B.C. 2015. Physical properties of beech wood thermally modified in hot oil and in hot air at various temperatures. *Maderas-Ciencia y- Tecno*l 17(4):789-798.
- Bal BC, 2016, Sıcak bitkisel yağ ile muamele edilen toros göknarı odununun bazı fiziksel özellikleri, *KSÜ Mühendislik Bilimleri Dergisi*, 19 (2): 20-26.
- Bal, BC, 2018, A Comparative Study of Some of the Mechanical Properties of Pine Wood Treated in Vacuum, Nitrogen, and Air Atmospheres, *Bioresources*, 13(3), 5504-5511.
- Brito, J.O., Silva, F.G., LEao, M.M. ve Almeida, G., 2008, Chemical Composition changes in Eucalyptus and Pinus Woods submitted to Heat Treatment, *Bioresource Technology* 99 (2008) 8545-8548)
- Calonego, FW, Severo, ETD, Ballarin, AW. (2012). "Physical and mechanical properties of thermally modified wood from *E. Grandis*", *European Journal of Wood and Wood Products*, 70(4): 453-460.
- Candelier, K., Dumarçay, S., Pétrissans, A., Desharnais, L., Gérardin, P., & Pétrissans, M. (2013a). "Comparison of chemical composition and decay durability of heat treated wood cured under different inert atmospheres: Nitrogen or vacuum". *Polymer degradation and Stability*, 98(2), 677-681.
- Candelier, K., Dumarçay, S., Pétrissans, A., Gérardin, P., & Pétrissans, M. (2013b). "Comparison of mechanical properties of heat treated beech wood cured under nitrogen or vacuum". *Polymer degradation and stability*, 98(9), 1762-1765.
- Dubey, MK, Pang, S, Walker, J. (2012). "Changes in chemistry, color, dimensional stability and fungal resistance of *Pinus radiata* D. Don wood with oil heat-treatment", *Holzforschung* 66: 49-57.
- Edlund, ML, Jermer, J. (2004) Durability of heat-treated wood, In Final Workshop COST action E22 "Environmental optimisation of wood protection", Lisboa-Portugal, March 2004.
- Esteves, BM., Pereira, HM. (2009). "Wood modification by heat treatment: A review," *BioResources* 4(1), 370-404
- Gaff, M, Gašparík, M. (2013) "Shrinkage and Stability of Thermo-Mechanically Modified Aspen Wood". *BioResources*, 8(1), 1136-1146.

Gündüz, G., Niemz, P., & Aydemir, D. (2008). Changes in specific gravity and equilibrium moisture content in heat-treated fir (*Abies nordmanniana* subsp. *bornmülleriana* Mattf.) wood. *Drying Technology*, 26(9), 1135-1139.

Karamanoğlu, M , Kaymakçı, A . (2018). Higrotermal yaşlandırma işleminin ısı işlem görmüş kestane odununun renk ve sertlik özellikleri üzerine etkisi . *Mobilya ve Ahşap Malzeme Araştırmaları Dergisi* , 1 (1) , 31-37 . DOI: 10.33725/mamad.429726

Korkut DS., Güller B., 2008, The effects of heat treatment on physical properties and surface roughness of red-bud maple (*Acer trautvetteri* Medw.) wood, *Bioresource technology*, 99 (2008) 2846-2851.

Korkut, S., Kocaefe, D. (2009). "Isıl işlemin odun özellikleri üzerine etkisi". *Düzce Üniversitesi Ormanlık Dergisi*, 5(2), 11-34.

Kamdem, DP, Pizzi A, Jermannaud, A. (2002) "Durability of heat-treated wood". *Holz als Roh-und Werkstoff*, 60 (1): 1-6.

Jamsa S, Viitaniemi P (2001) Heat treatment of wood - Better durability without chemicals, Review on heat treatments of wood, In proceedings of Special Seminar held in Antibes, France.

Sailer, M., Rapp, A. O., Leithoff, H., & Peek, R. D. (2000). Upgrading of wood by application of an oil-heat treatment. *Holz als Roh-und Werkstoff*, 58(1/2), 15-22.

Severo, E.T.D., Calonego, F.W., Sansigolo, C.A. (2012). "Physical and chemical changes in juvenile and mature woods of *Pinus elliottii* var. *elliottii* by thermal modification", *Eur J Wood Prod* 70: 741-747.

TS 2471, (1976). Odunda Fiziksel ve Mekaniksel Deneyler İçin Rutubet Miktarı Tayini, Türk Standartları Enstitüsü, Ankara.

TS 2472, (1976.) Odunda Fiziksel ve Mekaniksel Deneyler İçin Birim Hacim Ağırlığı Tayini, Türk Standartları Enstitüsü, Ankara.

TS 4084, (1983). Odunda Radyal ve Teğet Doğrultuda Şişmenin Tayini, Türk Standartları Enstitüsü, Ankara.

TS 4086, (1983). Odunda Hacimsel Şişmenin Tayini, Türk Standartları Enstitüsü, Ankara.

Welzbacher, CR, Brischke, C, Rapp, AO. (2007) "Influence of treatment temperature and duration on selected biological, mechanical, physical and optical properties of thermally modified timber". *Wood Material Science and Engineering* 2 (2): 66-76.

Yıldız, Ü.C., 1994, Bazı Hızlı Büyüyen Ağaç Türlerinden Hazırlanan Odun-Polimer Kompozitlerinin Fiziksel ve Mekanik Özellikleri, KTÜ, Fen bilimleri Enstitüsü, Doktora Tezi, Trabzon.



# Kahramanmaraş Sütçü İmam University

## Journal of Engineering Sciences



Geliş Tarihi : 12.10.2020  
Kabul Tarihi : 28.11.2020

Received Date : 12.10.2020  
Accepted Date : 28.11.2020

### ADVANCED TECHNOLOGIES FOR FIBER REINFORCED POLYMER COMPOSITE MANUFACTURING: A REVIEW

#### ELYAF TAKVİYELİ POLİMER KOMPOZİT ÜRETİMİ İÇİN İLERİ TEKNOLOJİLER: DERLEME

Çağrı UZAY<sup>1\*</sup> (ORCID: 0000-0002-7713-8951)  
Necdet GEREN<sup>2</sup> (ORCID: 0000-0002-9645-0852)

<sup>1</sup> Kahramanmaraş Sütçü İmam Üniversitesi, Makine Mühendisliği Bölümü, Kahramanmaraş, Türkiye  
<sup>2</sup> Çukurova Üniversitesi, Makine Mühendisliği Bölümü, Adana, Türkiye

\*Sorumlu Yazar / Corresponding Author: Çağrı UZAY, cagriuzay@ksu.edu.tr

#### ABSTRACT

Developments for improving the effectiveness of the composite structures strongly depend on the manufacturing methods. Additionally, the composite manufacturers have put effort into cost-effective and automated fabrication with mechanization. Controlling the imperfections is also an important consideration for the production. This study presents several manufacturing methods for fiber-reinforced polymer composites. It also draws attention to novel techniques that use advanced technology required for the developed composite designs. Besides the conventional methods such as hand lay-up, vacuum bag, resin transfer molding, resin infusion, and autoclave, the advances in hot press molding, pultrusion process, and automated lay-up method were indicated. Moreover, the methods making difference for the hybrid composite designs such as the same qualified resin transfer molding and automated stitching processes were introduced. The advantages and limitations were indicated for the manufacturing methods and the usage purposes were addressed.

**Keywords:** Manufacturing techniques, composite manufacturing, advanced technology, out of autoclave, same qualified resin transfer molding

#### ÖZET

Kompozit yapıların etkinliğini artırmaya yönelik gelişmeler büyük ölçüde imalat yöntemlerine bağlıdır. İlaveten, kompozit üreticileri düşük maliyetli ve otomasyona dayalı imalat için de çaba göstermektedirler. İmalat hatalarının kontrol edilebilir olması da üretim için önemli bir husustur. Bu çalışmada elyaf takviyeli polimer kompozitler için çeşitli imalat yöntemleri sunulmuştur. Ayrıca gelişmiş kompozit tasarımlar için ileri teknoloji kullanmayı gerektiren yenilikçi yöntemlere de dikkat çekmektedir. El yatırması, vakum torbalama, reçine transfer kalıplama, reçine infüzyonu ve otoklav gibi geleneksel yöntemlerin yanı sıra, sıcak baskı kalıplama, pultrüzyon işlemi ve otomatik yerleştirme (istifleme) yöntemlerindeki gelişmeler de belirtilmiştir. Aynı kalitede reçine transfer kalıplama ve otomatik dikişleme işlemleri gibi hibrit kompozit tasarımlarında fark yaratan yöntemler de tanıtılmıştır. İmalat yöntemlerinin birbirlerine göre üstünlükleri ve sınırlamaları belirtilmiş ve kullanım amaçlarına değinilmiştir.

**Anahtar Kelimeler:** İmalat teknikleri, kompozit üretimi, ileri teknoloji, otoklav harici işlemler, aynı kalitede reçine transfer kalıplama

\*Sorumlu Yazar / Corresponding Author: Çağrı UZAY, cagriuzay@ksu.edu.tr

**ToCite:** UZAY, Ç., & GEREN, N., (2020). ADVANCED TECHNOLOGIES FOR FIBER REINFORCED POLYMER COMPOSITE MANUFACTURING. *Kahramanmaraş Sütçü İmam Üniversitesi Mühendislik Bilimleri Dergisi*, 23(4), 245-257.

## INTRODUCTION

The demand for using fiber-reinforced polymer composites have gradually increased day by day in many engineering fields due to their attractive features. In addition, the developments of new polymers and reinforcement types have made the obtaining of the enhanced physical and mechanical properties possible. Besides the high strength and stiffness to weight ratio, the composites and other hybrid forms such as sandwich structures can provide better impact strength, higher fatigue resistance, thermal and acoustic insulation, good electrical and thermal conductivity, better electromagnetic shielding performance, and resistance to other environmental effects (Gibson, 2000). In order to achieve these features, the applied manufacturing method plays an important role in composites' design and construction (Uzey, 2020). Basically, fiber reinforcement is a dimensional (1D) strengthening process and it can be oriented in different directions in a certain matrix surrounding with a suitable forming process to obtain two or three-dimensional structural members (Baker et al., 2004). Therefore, the desired mechanical properties can be combined in a unique composite part based on the reinforcement type, stacking sequence, matrix materials, and manufacturing technique.

Genç (2006) produced glass fiber/vinyl ester composites with three different manufacturing techniques: hand lay-up, vacuum bag, and resin infusion. When the methods were compared, infusion provided the best results and the hand lay-up yielded the lowest results under the flexural, tensile, and impact loading conditions. The vacuum bag method was found a transition between the infusion and hand lay-up. The void content was observed for the specimens fabricated with hand lay-up. Better surface finishes were obtained with vacuum bag methods. It was also concluded that by using the hand lay-up method, a complete fiber wet-out cannot be reached with insufficient matrix materials and a satisfactory product quality strongly depended on the labor. Durgun et al. (2014) also compared the hand lay-up, vacuum bag, and resin infusion methods. They produced carbon/epoxy and glass/epoxy composite specimens and subjected them to tensile and three-point bending tests. For both loading conditions, the strength values increased in the order of hand lay-up, vacuum bag, and resin infusion methods, respectively. Sevkati et al. (2012) revealed the advantages of the VARTM method over the hand lay-up by investigating the bearing load capacity of pin-loaded woven glass/epoxy composites under the tensile test. Kim et al. (2014) produced both circular and square cross-sectional tubes made from carbon fiber prepreg with the autoclave process. The round structure provided two times higher bending strength under three-point flexural loading. Bere et al. (2019) applied the autoclave method to obtain the best tensile properties of carbon/epoxy prepreg composites. They also introduced the steps of the process.

The pultrusion method has also become an attractive technique with the growth of the improved performance of composite constituents. Application fields of the method are widespread particularly in infrastructure and include bridges and decks, cooling tower parts, marine construction, transportation, and energy such as wind power (2020). Several out-of-autoclave techniques such as RTM, VARTM, vacuum-assisted resin infusion method (VARIM) were developed, but in that application dry fabrics are used. In this case, resin impregnation and curing processes become a concern. Without sacrificing the process quality and robustness, an alternative method instead of the autoclave process was introduced called the Same Qualified Resin Transfer Molding (SQRTM). It was developed by Radius Engineering Inc. and SONACA (2020). The prepreg was cured in an enclosed mold with the resin transfer which is the same as prepreg resin. The process also has advantages over the autoclave. Because dimensional accuracy of the part geometry, structural integration, and internal quality may deteriorate since the technique is not carried out in a well-designed mold. Lumley et al. (2020) compared the SQRTM, autoclave, and RTM methods and applied the SQRTM for the manufacturing of moveable wing parts (slats and flaps). They stated that the complex geometrical shapes can be fabricated with better surface quality by applying the SQRTM method.

Briefly, composite technology continues to grow with developed fabrication techniques in which the parts are produced with higher performance and reduced cost. The present study firstly demonstrates commonly used composite manufacturing methods and then introduces the advanced techniques currently emerged for the manufacturing of composite structures. The methods were also discussed comparatively in order to reveal the negative and positive sides of each other.

## CONVENTIONALLY USED METHODS

Several methods are available to manufacture fiber-reinforced polymer (FRP) composites and their hybrid types like sandwich structures. Typically, hand lay-up, vacuum bag, resin transfer molding (RTM), autoclave, resin infusion, pultrusion, filament winding, matching die set compression molding, etc. are the well-known manufacturing methods (Kar, 2017). But mostly, the followings are currently used methods for the fabrication of



composite materials: *hand lay-up, vacuum bagging, RTM, vacuum-assisted resin transfer molding, filament winding, and autoclave methods.*

### **Hand Lay-up Method**

The hand lay-up method, the oldest process, is used for composite manufacturing carried out on an open mold. This process is simple, but a labor-intensive process, and suitable for low-volume production. For instance, in marine applications, large components like boat hulls can be fabricated with this method (Kar, 2017). Reinforcing materials such as chopped strand mats or fiber fabrics are placed manually onto the open mold, and resin is sprayed or poured over the reinforcement materials and the impregnation of them is provided manually. The required curing time is 24–48 hours at room temperature. A catalyst and accelerator that are called a hardener are mixed to the resin in a proper fraction in order to satisfy curing. The mixture is carefully stirred both to prevent void formations within the matrix and to obtain homogeneous matrix material. Figure 1 shows the schematic view of the hand lay-up process.

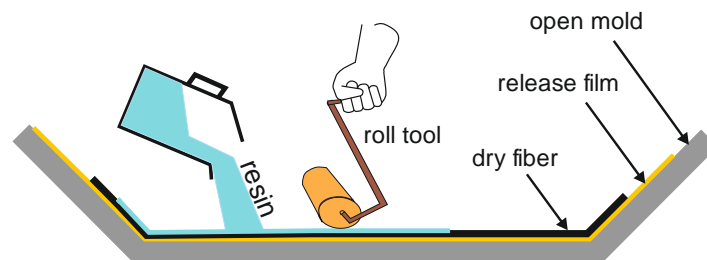


**Figure 1.** Schematic of Hand Lay-up Method

### **Vacuum Bagging Method**

In the vacuum bagging method, the entrapped air during lay-up and excessive resin is removed with a vacuum. After stacking, a peel ply or perforated release film is laid onto the composite laminate. A breather cloth is placed onto the peel ply, in order to absorb excess resin from the laminate. Lastly, the entire system is enclosed with a vacuum bag and the mold surrounding is covered with sealant tape as presented in Figure 2. Then vacuum is applied to the composite material under the bag. This process is more suitable for laboratory applications (Uzay et al., 2019) and provides a high reinforcement with increased fiber volume fraction and improves adhesion bond strength between the composite layers compared to the hand lay-up process. Because the applied vacuum removes most of the air and volatile substance quickly from the laminate (Baker et al., 2004). When compared to the hand lay-up, the method has important advantages such as higher fiber content, better fiber wet out, lower void formation, and decreased volatile emissions. The aerospace industry mainly applies this method since the high production volume is not primarily considered. Moreover, racing car parts and large cruising boats can be fabricated by using a vacuum bagging method. However, the process has some drawbacks such as labor-intensive, a requirement of better labor skills, loss of seal, process cost due to the consumables and equipment (Kar, 2017; Mallick, 2007). In addition to this, Mehdikhani et al. (2019) investigated the reasons for voids in polymer composite materials. The void content within the composites is increasing with the relative humidity. Although the void content obtained with both vacuum bag and autoclave methods is similar up to a relative humidity of 60%, after 60 to 100, the void fraction is increasing exponentially for the vacuum bag method.

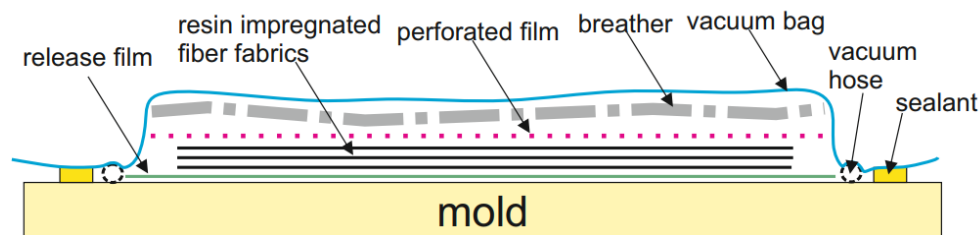


**Figure 2.** Schematic View of the Vacuum Bag Method

### Resin transfer molding (RTM)

Resin transfer molding (RTM) is carried out in a closed mold, and suitable for moderate and high-volume productions. The process mainly contains stacking of the dry reinforcement materials in the base part of the mold, and the other half of the mold is placed over the bottom mold and clamped. The schematic view of the process is presented in Figure 3. After closing the molds, a resin including its hardener is injected. High-quality part requirements such as vehicle body parts, containers, bathtubs, etc. can be achieved by this method. RTM method can be modified with a vacuum assistant for effective resin transfer and impregnation of fiber elements (Kar, 2017). The method is also relatively more suitable for complex shapes compared to hand lay-up and vacuum bag methods (Mallick, 2007).

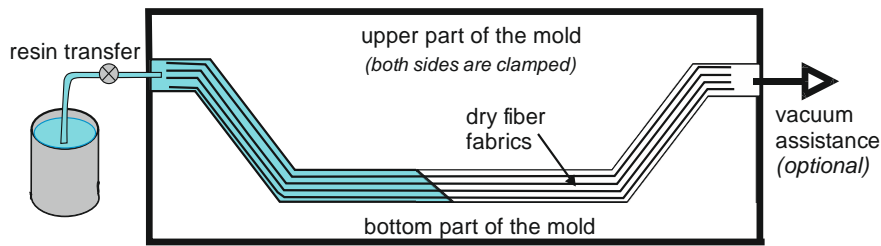


Figure 3. Schematic View of RTM Process

Torres (2019) reviewed the previous studies about monitoring and instrumentation of the process parameters for RTM. Due to its relatively higher ratio of mechanical performance to cost compared to autoclave, the method is still requested. The significant RTM fabrication parameters on surface roughness of the final part were indicated as low profile additives, injection pressure, filler content, a temperature gradient.

### Vacuum-assisted Resin Transfer Molding (VARTM)

In vacuum-assisted RTM (VARTM), the manufacturing is carried out on a single mold in which the composite laminates are stacked on it as the case performed with vacuum bag technique. The process is carried out over the bottom part of the mold only. A peel ply and/or perforated release film is placed over the lamination, and the system is covered with a vacuum bag by using sealant tape. The resin impregnation of the dry composite layers is performed with the aid of a vacuum supply as seen in Figure 4. The vacuum process provides the resin movement. The entrapped air is also removed. The vacuum application increases the fiber concentration and improves adhesion bonding between the composite plies. VARTM technique provides several advantages when compared to the RTM method with lower tooling cost, shorter duration of mold filling by resin. The process efficiency and quality of the final product depend upon sufficient wet-out of the fibers which can be done successfully with a proper resin movement (Kar, 2017).

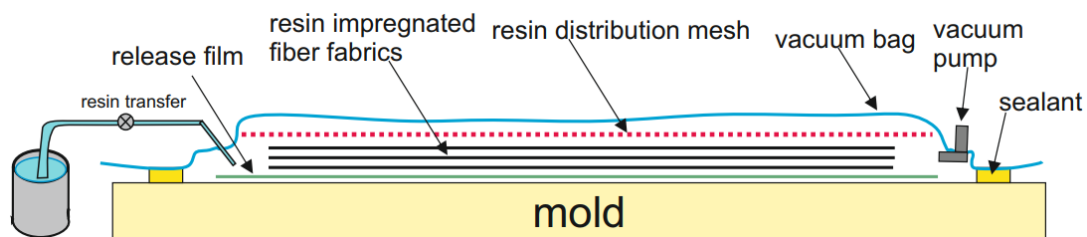
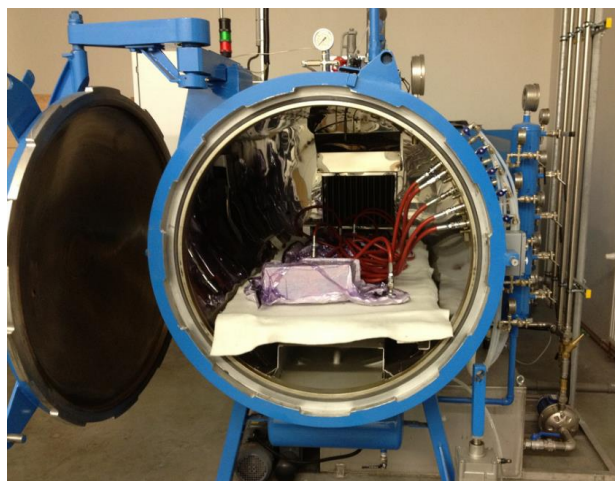


Figure 4. Schematic View of the VARTM Method

### Autoclave Process

An autoclave manufacturing method can be applied where excellent quality is needed such as in aerospace industries. Because in this method, an increased fiber volume ratio is obtained with minimum void content in the matrix. The curing is carried out under pressure and in a heat-generated autoclave as seen in Figure 5. The process parameters of the computer-controlled method depend on the resin system used for lamination. Kermani et al. (2020) produced a honeycomb core sandwich structure with an autoclave oven by controlling the process parameters of autoclave pressure, vacuum bag pressure, and autoclave temperature. The preparation of the composite materials is similar to the vacuum bagging method. After preparing the composite for curing within the

enclosed heat-resisted vacuum bag, the product is placed inside an autoclave. The external sources of vacuum, pressure, and heat provide to densify and consolidate each lamina to form better lamination by removing air and volatiles with the aid of vacuum. In order to prevent the possibility of any internal fire, nitrogen, or carbon dioxide is used. The process is costly and requires labor-intensive production (Baker et al., 2004; Mallick, 2007; Carlsson and Kardomateas, 2011). Bere et al. (2019) specified the steps of the autoclave process for carbon/epoxy prepreg composite laminates as follows: (1) *Heating of the mold for 30 min. at 60 °C, then (2) heating at a rate of 2 °C/min and increasing temperature to 120 °C in 60 min. (3) dwell for 2 hours at 120 °C, (4) cooling of the composite at a rate of 2 °C/min for 60 min.* On the other hand, Plappert et al. (2020) achieved a 60% fiber volume density with a single ramp of temperature increase. The process was performed as follows: Increasing the temperature from ambient to 120 °C in 30 min. with a pressure of 3-bar, then constant temperature for 120 min., and lastly cooling to ambient temperature in 30 min. Also, the reported void fraction in the literature is below 1% for this kind of manufacturing method (Hassan et al., 2017; Mehdikhani et al., 2019).



**Figure 5.** Representation of Autoclave Process (URL 3)

### ***Filament Winding Process***

In order to produce cylindrical parts such as pipes and tubes, filament winding is used effectively. The process includes wrapped bands of continuous fibers over a mandrel as seen in Figure 6. After the winding, the curing is performed at an increased temperature of a mandrel. The resin impregnation can be made before, during, or after winding operation. The strength and the stiffness of the finished product depend on the compaction of fiber layers. The major factors have been specified as helix angle, winding tension, conditions of strand bandwidth, resin content, and its distribution, winding speed, and curing cycle (McIlhagger et al., 2015). A sufficient fiber tension is required on the mandrels to keep the arranged orientation and to prevent fiber misalignments. Low-viscosity resin types are preferred or the resin bath temperature is increased to control the appropriate resin flow. In other cases, there might be voids within the structure that worsen the mechanical properties. Delamination and fiber wrinkles are other defects that could be encountered. The significant parameters affecting the strength of fiber composites are indicated as winding angle, fiber orientation and its sequence, fiber volume fraction, mechanical and physical properties of fiber and matrix, respectively (Prabhakar et al., 2019). Pressure vessels, pipelines, blades, automotive drive shafts, oxygen tanks, the rocket body, etc. are the common examples of filament winding technique (Mallick, 2007).

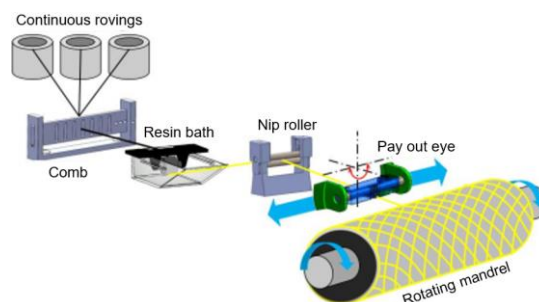


**Figure 6.** Filament Winding Method (Quanjin et al., 2019)

## ADVANCES FOR COMPOSITE MANUFACTURING

As stated by Fan et al. (2010), the further developments for improving the effectiveness of the composite structures strongly depend on the manufacturing methods based on cost-effectiveness, automated with mechanization, and controlling the imperfections. The advanced processes are presented in the following sub-sections.

### *Advances in Lay-up Processes*

When the lay-up process of resin impregnation is applied by handling, it can be messy and may cause health and safety problems due to the hazardous effect of the polymer resins (Baker et al., 2004). Therefore, the hand lay-up process has been automated by using a chopper gun and a spray. As seen in Figure 7, a machine tool that can be used by hand-held or a robot arm. The process can accelerate the manufacturing time with the low-cost operation and reduce the manual work and labor cost. It is possible to mix the resin and its hardener in a reservoir and allow it to distribute chopped fibers and matrix material simultaneously directly onto the mold surface. Although continuous fiber is feeding to chopper guns, the fibers are sprayed as chopped glass fiber which is the main drawback and cannot provide homogeneous mechanical properties for the finished product.

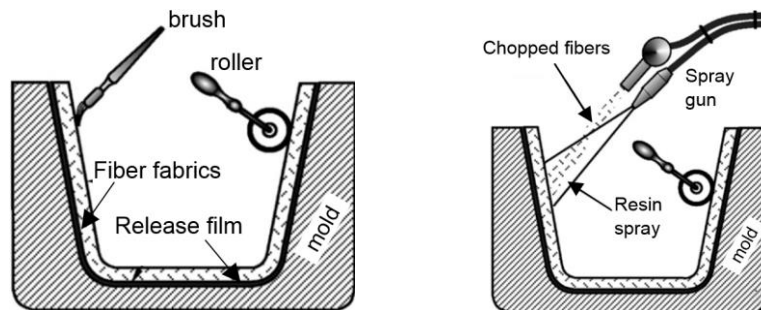


**Figure 7.** Hand Lay-up vs. Spray-up Manufacturing Methods (Swift and Booker, 2013)

Using prepregs is also a better alternative to wet lay-up processes for advanced structures such as sandwich panels for obtaining well-impregnated resin, and increased mechanical properties for the final product. Low void contents are obtained in composite face sheets laminated by prepregs (Karlsson and TomasAström, 1997). For aircraft structures such as wing skins and fuselages, the production and mechanical properties must be excellent. Therefore, prepreg materials with autoclave curing are the best process combination for that kind of application fields. In order to increase production rates, improved shape tolerances, and dimensional accuracy, automated processes have been developed such as automated fiber placement (AFP) and automated tape layup (ATL). AFP process was developed to overcome the drawbacks of ATL (Crosky et al., 2015) that lays up the prepregs either onto a flat or a cylindrical mandrel by using multi-head robot machinery (Carlsson and Kardomateas, 2011) as represented in Figure 8. It was reported that the significant gain for the cost-effectiveness of AFP is low material scrap rate besides reduced labor cost (Crosky et al., 2015).

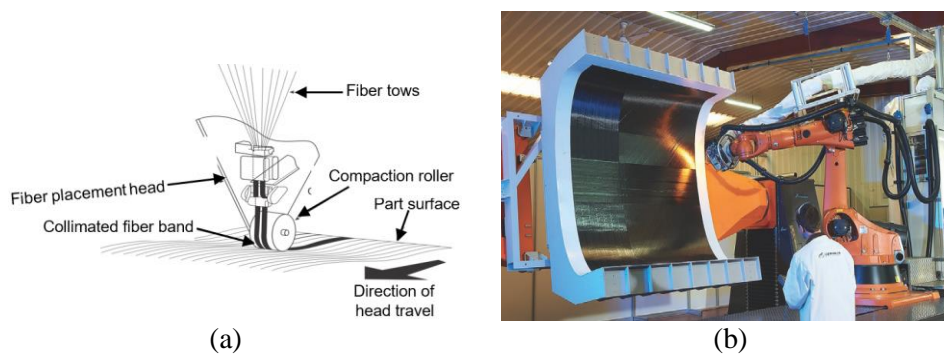


**Figure 8.** a) AFP process (McIlhagger et al., 2015), b) Image of the AFP (Crosky et al., 2015)

**Advances in Pultrusion Method**

The term “pultrusion” is used to define a continuous process for manufacture where the combination of pull and extrusion is applied. The continuous fibers are taken in a polymer matrix resin bath then pulled via heated dies and extruded (Hota et al., 2009). It is a cost-effectively used and automated manufacturing process for continuous and constant cross-sectional composite profiles. This technique is essentially suitable for the fabrication of long and straight structural parts such as cylindrical rods and tubes, beams, shells, etc. (Mazumdar, 2009). It was also reported that a pultrusion process was patented with a new concept. The new technique allowed to produce nonlinear profiles with the aid of curved moving dies (Vedernikov et al., 2020). As presented from Figure 9, continuous fibers are drawn through a resin tank and moved to a heated die having a final shape of the product. As the resin-impregnated fibers pass through the die, the composite material is assumed to form to final shape and cured. After curing and leaving the die, the product is cut properly. Utmost attention must be given to the fiber wet-out to control the mechanical effectiveness of the pultruded part. Because, the amount of resin in the resin bath, its viscosity, bath temperature, the time allowed for resin impregnation of the fibers, and the workability of the mechanical system are the major factors to be considered (URL 3).

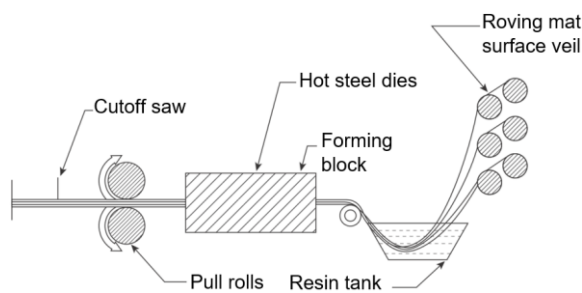


**Figure 9.** Schematic View of Pultrusion Method (McIlhagger et al., 2015)

**Advances in Stitching Machines**

Santhanakrishnan et al. (2018) designed a stitching machine for the sandwich core materials as shown in Figure 10. The machine also provided to make different pile orientations in the stitching process, which allows to find out optimal mechanical properties. Table 1 shows the shear properties of the glass fiber reinforced PVC foam core sandwich. The stitching was performed to the core material with various orientations by using glass fiber yarns.

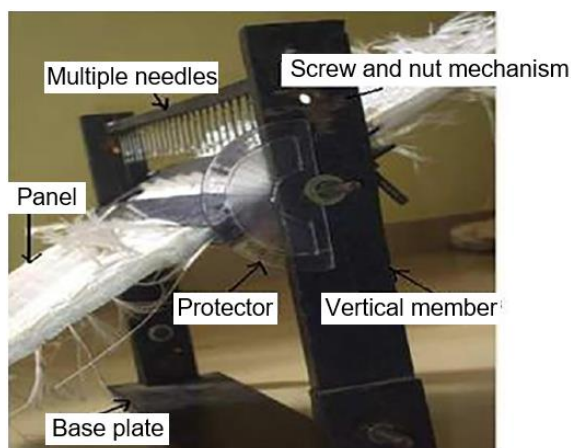


**Figure 10.** Image of Stitching Machine (Santhanakrishnan et al., 2018)

**Table 1.** Shear properties of stitched and unstitched foam core sandwiches (Santhanakrishnan et al., 2018)

Sandwich Panel	Ult. Shear Strength (kPa)	Shear Modulus (MPa)
Unstitched	420	1.75
Stitched- 45°	1686	11.24
Stitched- 90°	963	8.78
Stitched- 90°/45°	2443	13.75
Stitched- 90°/45°/90°	2844	16.32

Stitching of the core materials also enhanced the tensile and compressive strength of the polymer foam core sandwich structures compared to as-received core materials (Yalkin et al., 2017).

### Advances in Hot Press Molding Method

Mei et al. (2017) developed a novel manufacturing method by hot press molding for fabricating carbon fiber reinforced tetrahedral truss core sandwich panels. The process is illustrated in Figure 11.

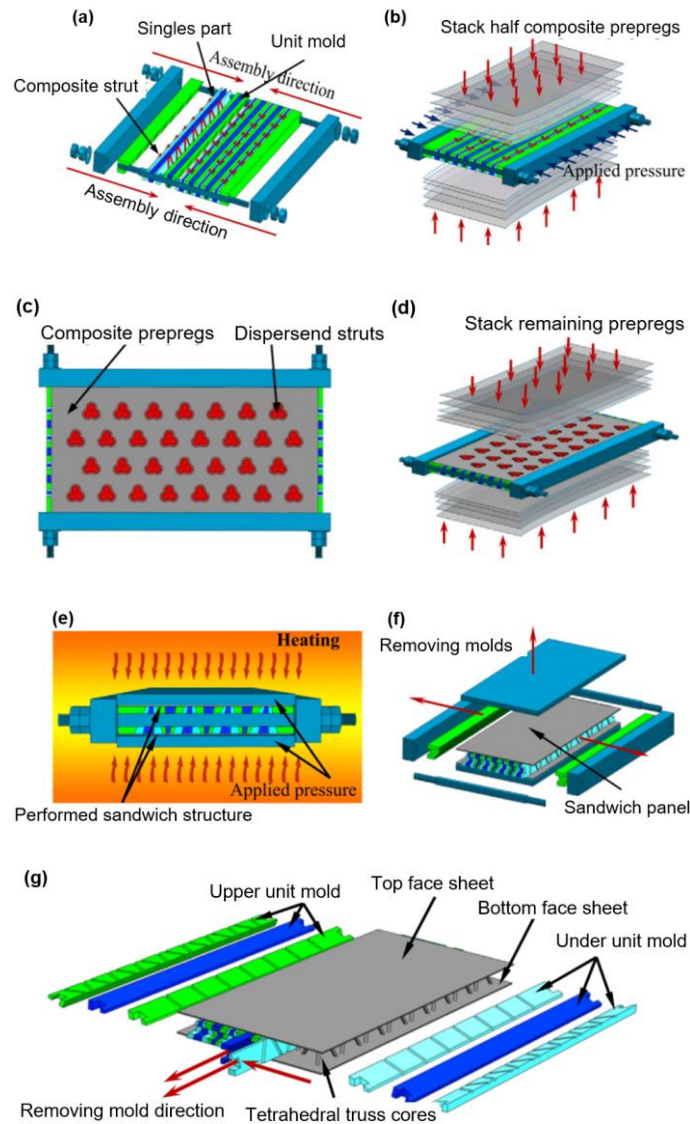


**Figure 11.** Manufacturing process with developed hot press molding; a) placing the prepared composite strut into corresponding position, b) lay-up of five layers of carbon/epoxy prepregs on the mold, c) dispersing end of the struts by penetrating them into prepreg, d) lay-up of another 5-layer of prepregs, e) curing of preformed structure, f, and g) demolding and removal of the composite structure (Mei et al., 2017)

### Same Qualified Resin Transfer Molding (SQRTM)

SQRTM is a newly developed composite manufacturing method consists of the prepreg lay-up and liquid resin transfer molding. The method was first developed and commercialized by Radius Engineering (2020) in order to provide net shape composite products. Figure 12 presents the difference between traditional and net shape productions.



**Figure 12.** a) traditional production of composite parts, b) net shape, single part composite production (URL 4)

SQRTM is also known as the out-of-autoclave process and it has several advantages over the autoclave process. With the aid of SQRTM, large and complex parts can be produced with final shapes with reduced cost. The method differs from the RTM method with prepreg lay-up and the injected resin to the RTM system is the same as that existed in prepreg as shown in Figure 13. This allows using of high qualified toughened materials such as tough resins and toughened agents. The injected resin creates hydrostatic pressure to composite laminate and eliminates the formation of void contents, which improves both quality of the final product and its mechanical properties. By the way, control of the composite quality is easier than the autoclave process due to its complex dependent variables. In addition, the curing in the SQRTM method is approximately two hours shorter than in autoclave as seen in Figure 14. On the other hand, the method has advantages over the RTM technique. Thickness variations in the final part, dimensional accuracy, and surface quality are improved with the aid of SQRTM. The process is currently under the commercialization process by Radius Engineering Inc. (2020). The main difference between the RTM and SQRTM is the used fiber fabrics. While the RTM technique uses dry fabrics, the SQRTM method uses prepreps. The resin material used for the impregnation of prepreps is also used for resin injection of the SQRTM process. Therefore, the SQRTM process has been most suitable and preferable for aerospace industries to produce structural members (URL 2, URL 4).

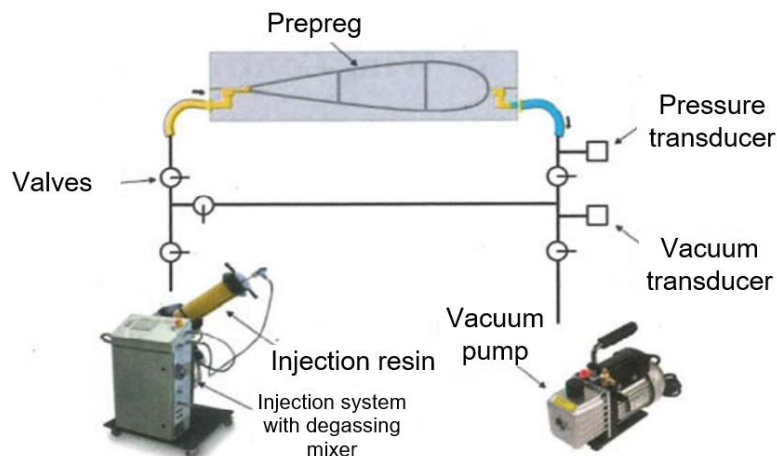


**Figure 13.** Schematic Presentation of SQRTM Process (Gueuning and Mathieu, 2016)

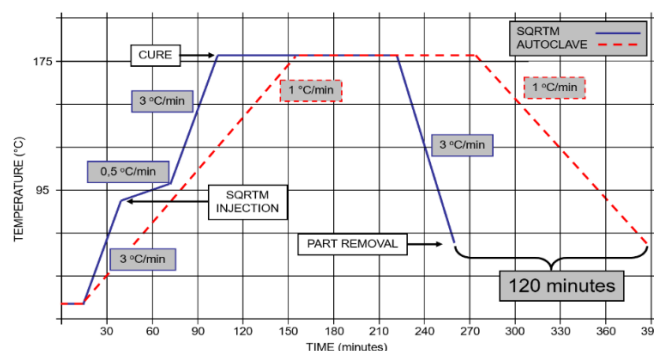


**Figure 14.** Comparative demonstration of curing cycles both in SQRTM and autoclave (URL 4)

## DISCUSSION

The most limiting factor to the use of fiber-reinforced polymer composites and the hybrid materials systems is the cost of constituents. Although the aerospace industry uses composite structures in high volumes, cost reduction is still a challenging task (Mallick, 2007). For instance, honeycomb core sandwich panels with carbon/epoxy face sheets are used for indoor applications, but, due to sudden thermal changes during the operations, honeycomb cells may be filled with water in certain conditions, and it may freeze under cold temperatures. This can cause significant

damage which leads to repair costs (Herbeck et al., 2002). Therefore, the closed-cell rigid polymer foams can be offered for indoor sandwich panel applications to reduce both maintenance and materials costs. Contrary to the aerospace industry, there is an obligation to consider the cost of both materials and manufacturing processes in the automotive sector in order to produce large quantities of vehicles with reduced costs. This is why, the use of carbon fiber technology is restricted and glass fiber and polyester, and/or vinyl ester are preferred as the reinforcement and the polymer matrix, respectively.

The advantages and limitations of the manufacturing methods are evaluated and summarized in Table 2 based on the literature review.

**Table 2.** The Advantages and Limitations of the Manufacturing Methods

Methods	Advantages	Limitations
Hand lay-up	Simple, cheap, versatile, suitable for mechanization	Oldest, labor-intensive, low-volume productions, poor surface finish and dimensional accuracy, low mechanical properties
Vacuum bag	Moderate cost, good mechanical properties, better interface adhesion	High labor skill, low-volume production
RTM	moderate and high-volume productions, complex shapes, good surface finish	Tooling cost, dimensional accuracy of the tool, possibility of insufficient resin impregnation
VARTM	Elimination of void contents, low tooling cost, fast resin wet-out, relatively resin-rich	Additional cost of consumable materials for vacuum process, moderate surface finish compared to RTM
Autoclave	High mechanical properties,	Costly, complex process, require computer control, relatively simple shapes, requires secondary finishing operation
Filament winding	Better mechanical properties, fast, suitable to automation, high volume production, less labor dependent	Simple shapes and profiles, machine and process cost, proper selection of the resin,
Pultrusion	Automated, fast, suitable for nonlinear profiles, long and straight parts, less labor dependent	simple and moderate shapes, costly,
SQRTM	Net-shape, no need for secondary operation, better surface finish and dimensional accuracy, improved product quality, better mechanical properties, large and complex parts, relatively easy to control, and shorter process compared to autoclave	Complex process, high cost, tooling, accuracy of mold

The manufacturing methods are still not completely suitable for mass production, e.g., the parts in the automotive field. Generally, the methods are applied manually, they take hours dependent upon the shape and dimensions of the product, and well-skilled laborers are needed. However, with the advances in the fabrication process, reductions in application time and labor cost are possible. For instance, the prepreg fabrics can be cut with computer-controlled machines to shorten the processing time. Also, the tape lay-up machine eliminates the labor work of hand lay-up. Besides these, the quality of the final product is affected by the manufacturing techniques. Obata et al. (2020) confirmed that the autoclave process almost removes the entrapped resin within the composite laminate and thus higher load capacities can be obtained. However, Haluza et al. (2020) reported that the process of out of



autoclave, i.e. SQRTM, is emerging as an alternative to autoclave which requires higher capital expenses. Pultrusion and filament winding techniques are relatively less labor-dependent, automated and a large number of parts can be produced. The most important drawback in pultrusion, only the production of simple shapes, has now been overcome with the fabrication of nonlinear profiles thanks to the curved dies (Vedernikov, 2020). Quainjin et al. (2019) determined the favorable and restricted features together with the current problems of the filament winding technique. Then they addressed the industrial fields where the technique can be used for particular applications. Although the RTM method is more suitable for relatively complex shapes, the tooling cost is another concern. Robust molds considering the molding materials, design of the molds, determined tolerances, assembly, and demolding, and handling of the parts are required to achieve high production rates.

## CONCLUSION

In this study, the conventionally used composite production methods, and the advances in composite manufacturing technology based on the particular techniques were presented and discussed comparatively. It can be concluded that conventional methods such as hand lay-up, vacuum bag, vacuum-assisted resin infusion, or resin transfer molding techniques are more suitable for laboratory applications, prototype productions, and other purposes where low batch products are demanded or perfect surface quality is not desired. On the other hand, methods such as filament winding, pultrusion, RTM, and SQRTM are more appropriate for commercial purposes since such methods are open to automation and mechanization developments particularly for both flexible and mass productions.

## REFERENCES

- Baker, A., Dutton, S., & Kelly, D. (2004). Composite materials for aircraft structures. *American Institute of Aeronautics and Astronautics*, 2<sup>nd</sup> Edition, USA, 599.
- Bere, P., Sabău, E., Dudescu, C., Neamtu, C. & Fărtan, M. (2019). Experimental research regarding carbon fiber/epoxy material manufactured by autoclave process. *MATEC Web of Conferences*, 299, 1-6.
- Carlsson, L.A., & Kardomateas G.A. (2011). Structural and failure mechanics of sandwich composites, Springer, USA, 386.
- Crosky, A., Grant, C., Kelly, D., Legrand, X. & Pearce, G. (2015). Fibre placement processes for composites manufacture. Edited by Boisse, P., *Advances in Composites Manufacturing and Process Design*, Elsevier, UK, 79-92.
- Durgun, İ., Onur, V., Rukiye, E. & Nurettin, Y. (2014). The Effect of production technique on mechanical properties of polymer based fiber reinforced composite materials. *Otekon'14, 7th Automotive Technologies Congress*, 1-4.
- Fan, H.L., Zeng, T., Fang, D.N. & Yang, W. (2010). Mechanics of advanced fiber reinforced lattice composites. *Acta Mech Sin*, 26, 825-835.
- Genç, Ç. (2006). Experimental Comparison of production methods regarding fiberglass reinforced plastic, MSc Thesis, Kocaeli, Turkey.
- Gibson, L.J. (2000). Mechanical Behaviour of metallic foams. *Ann Rev Mater Sci.*, 30, 191-227.
- Gueuning, D., & Mathieu, F. (2016). Evolution in composite injection moulding processes for wing control surfaces. *Sampe (Society for the Advancement of Material and Process Engineering) Journal*, 52(1), 7-12.
- Haluza, R.T., Bakis, C.E., & Koudela, K.L. (2020). Comparison of woven and stitched out-of-autoclave E-glass/epoxy composites subjected to quasi-static and cyclic tensile loads. *Journal of Reinforced Plastics and Composites*. (First published September 20, 2020).
- Hassan, M., Othman, A., & Kamaruddin, S. (2017). A review on the manufacturing defects of complex-shaped

laminates in aircraft composite structures. *Int J Adv Manuf Technol*, 91, 4081–4094.

Herbeck, L., Kleineberg, M., & Schöppinger, C., (2002). Foam Cores in RTM Structures, Manufacturing Aid of High-Performance Sandwich? *23rd International SAMPE Europe Conference and Tutorials/JEC*, France, 1-11.

Hota, VS., GangaRao, PVV. & Taly, N. (2009). Manufacturing of composite components. *In Reinforced Concrete Design with FRP Composites*, Taylor & Francis Group, LLC, CRC Press, USA, 63–77.

Kar, K.K., 2017. *Composite Materials Processing, Applications, Characterizations*. Springer, Germany, 686.

Karlsson, KF., & TomasAström, B. (1997). Manufacturing and applications of structural sandwich components. *Composites Part A: Applied Science and Manufacturing*, 28(2), 97-111.

Kermani, NN., Simacek, P. & Advani SG. (2020). A bond-line porosity model that integrates fillet shape and prepreg facesheet consolidation during equilibrated co-cure of sandwich composite structures, *Composites Part A: Applied Science and Manufacturing*, 139, 106071.

Kim, JH., Kim, HJ., Chyun, I.B., An, JJ. & Kim, JH. (2014). Characteristic analysis of carbon FRP tube changed cross-sectional shape by bending load. *Materials Research Innovations*, 18, 328-331.

Lumley, T., Mathieu, F., Cornet, D., Gueuning, D., & Hille, N.V. (2020). Out-of-autoclave process and automation: a successful path to highly integrated and cost efficient composite wing moveables. *SAMPE Journal*, 6-17.

Mallick, P.K. (2007) *Fiber-reinforced composites: Materials, manufacturing, and design*. CRC Press, 3<sup>rd</sup> Edition, USA, 638.

Mazumdar S.K. (2009). *Manufacturing techniques in composites manufacturing: Materials, product, and process engineering*, CRC Press, USA, Chapter 6, 1–135.

McIlhagger, A., Archer, E., & McIlhagger, R. (2015). Manufacturing processes for composite materials and components for aerospace applications. Edited by Irving P.E., and Soutis C. *Polymer composites in the aerospace industry*, Woodhead Publishing Series in Composites Science and Engineering, Elsevier, UK, 50, 53-75.

Mehdikhani, M, Gorbatiikh, L, Verpoest, I, & Lomov, SV. (2019). Voids in fiber-reinforced polymer composites: A review on their formation, characteristics, and effects on mechanical performance. *Journal of Composite Materials*, 53 (12), 1579-1669.

Mei, J., Liu, J. & Liu, J. (2017). A novel fabrication method and mechanical behavior of all-composite tetrahedral truss core sandwich panel. *Composites Part A: Applied Science and Manufacturing*, 102, 28-39.

Obata, S., Takahashi, K. & Inaba, K. (2020). Laminate design for a tapered FRP structure with ply drop-off based on yielding of resin pockets, *Composite Structures*, 253, 112787.

Plappert, D., Ganzenmüller, GC., May, M., & Beisel, S. (2020). Mechanical Properties of a Unidirectional Basalt Fiber/Epoxy Composite. *J. Compos. Sci.* 4, 101, 1-12.

Prabhakar, MN., Rajini, N., Ayrilmis, N., Mayandi, K., Siengchin, S., Senthilkumar, K., Karthikeyan, S., & Ismail, SO. (2019). An overview of burst, buckling, durability and corrosion analysis of lightweight FRP composite pipes and their applicability, *Composite Structures*, 230, 111419.

Quanjin, M., Rejab, MRM, Idris, MS., Zhang, B., & Kumar, NM. (2019). Filament winding technique: SWOT analysis and applied favorable factors. *SCIREA Journal of Mechanical Engineering*, 3(1), 1-25.

Santhanakrishnana, R., Kavithaa, N., Sundarama, M. & Venkatanarayananana, PS. (2018). Effect of pile orientation on the shear strength of stitched foam sandwich panel. *Materials Research*, 21(6), 1-6.

Sevkat, E., Brahimi, M., & Berri, S. (2012). The bearing strength of pin loaded woven composites manufactured by

vacuum assisted resin transfer moulding and hand lay-up techniques. *Polymers and Polymer Composites*, 20(3), 321-332.

Swift, K.G., & Booker, J.D. (2013). *Manufacturing process selection handbook*, chapter 5: Plastics and Composites Processing. Elsevier, 1<sup>st</sup> Edition, UK, 141-174.

Torres, M. (2019). Parameters' monitoring and in-situ instrumentation for resin transfer moulding: A review. *Composites Part A: Applied Science and Manufacturing*, 124, 105500.

Uzay, Ç., Acer, D.C., & Geren, N. (2019). Impact strength of interply and intraply hybrid laminates based on carbon-aramid/epoxy composites. *European Mechanical Science*, 3(1), 1-5.

Uzay, Ç. (2020). Developing and testing of polymer foam core sandwich structures with hybrid carbon fiber/wire mesh sheet facings, PhD thesis, Çukurova University, Adana, Turkey.

Uzay, Ç., & Geren, N. (2020). Effect of stainless-steel wire mesh embedded into fibre-reinforced polymer facings on flexural characteristics of sandwich structures. *Journal of Reinforced Plastics and Composites*, 39(15-16), 613-633.

Vedernikov, A., Safonov, A., Tucci, F., Carlone, P. & Akhatov, I. (2020). Pultruded materials and structures: A review. *Journal of Composite Materials*, 54(26), 4081-4117.

URL 1: Radius engineering, <https://www.radiuseng.com/>

URL 2: <https://www.compositesworld.com/articles/sqrm-enables-net-shape-parts>. Accessed: 10/07/2019.

URL 3: <https://www.flickr.com/photos/bcomposite/8938412979/in/photostream/>. Accessed: 15/03/2019.

URL 4: [http://www.radiuseng.com/net\\_shape\\_composites](http://www.radiuseng.com/net_shape_composites). Accessed: 10/07/2019.

Yalkin, H.E., Icten, B.M., & Alpyildiz, T. (2017). Tensile and compressive performances of foam core sandwich composites with various core modifications. *Journal of Sandwich Structures and Materials*, 19(1), 49-65.